SPACE-TIME CODING FOR MIMO RAYLEIGH FADING SYSTEMS

MAO TIANYU

(M. Eng.)

A THESIS SUBMITTED

FOR THE DEGREE OF DOCTOR OF PHILOSOPHY

DEPARTMENT OF ELECTRICAL AND COMPUTER ENGINEERING

NATIONAL UNIVERSITY OF SINGAPORE

2005

Acknowledgements

I would like to thank my advisors, Professor Ko Chi Chung and Assistant Professor Mehul Motani, for their vision and encouragement throughout the years, for their invaluable advice, guidance and tolerance. Thank Dr. Francois Chin, for all the support, understanding and perspectives throughout my graduate study.

My appreciation also goes to my friends in DSA Lab, Dong Liang, Xiang Xu, Zhang Jinbin, Liu Wei, Shi Miao, . . . , for their kindness, friendship and humor.

Finally, I would like to thank my husband, Yang Rui. Without his love and support under circumstances sometimes difficult, the completion of this thesis would not have been possible.

Mao Tianyu

July 2005

Contents

Summary

In this thesis, space-time coding schemes for multiuser and single user systems are discussed. Based on the performance analysis, the code design criteria for multiuser composite fading systems are obtained first. It is shown that the minimum rank and product of the non-zero eigenvalues of codeword distance matrices for the quasi-static fading as well as the rapid fading, of each user's code set, should be maximized. When all the users have the same number of transmit antennas, the code design can be simplified. Optimal 4-state and 8-state STTCs are obtained based on the code design criteria, which outperform the existing space-time codes (STCs).

The code design for generally correlated multiuser fading systems is discussed where three fading cases are investigated: temporally correlated fading, spatially correlated fading, and spatio-temporally correlated fading. It is observed that all the users should use the same code set and the code design for multiuser systems is equivalent to the code design for single user systems. Without any assumption on the dimension of the codeword matrix and the rank of the channel correlation matrix, it is proved that the STC achieving full diversity in a quasi-static fading system can achieve full diversity in a temporally correlated system. The coding gain can be improved by increasing the minimum product of the norms of codeword difference matrices' column vectors and the minimum product of the nonzero eigenvalues of codeword distance matrices. The performance analysis of the spatially and spatio-temporally correlated fading channels demonstrates that the code design for these two fading cases is reduced to the code design for rapid fading channels. Based on these observations, the general code design criteria are further achieved for an arbitrarily correlated fading.

Aiming at obtaining a good performance as well as a high data rate, a new STBC-VBLAST scheme has been proposed, which applies G orthogonal STBCs into the lower layers of vertical Bell Laboratories layered space-time (VBLAST) architecture. At the receiver, low-complexity QR decomposition (QRD) and successive interference cancellation (SIC) are used. The error propagation is combated effectively by improving the system diversity gain significantly though accompanied by a spectral efficiency loss. To get a good tradeoff between the diversity gain and spectral efficiency, G should be chosen to be less than or equal to a threshold G_{th}. We derive G_{th} theoretically, which is determined by the number of antennas and the dimension of the STBC. With appropriately selected G and a higher-order modulation, the STBC-VBLAST system can have a larger spectral efficiency as well as a better performance than other VBLAST schemes. Provided with the high diversity gain, the STBC-VBLAST performs more robustly in the presence of the channel estimation errors. The ordered STBC-VBLAST is also proposed, which uses the modified sorted QRD (SQRD). It is expected that the ordered STBC-VBLAST has a better performance than the STBC-VBLAST as shown in simulations. G_{th} derived for the STBC-VBLAST is also valid for the ordered STBC-VBLAST.

List of Acronyms

ATM	Asynchronous Transfer Mode (ATM)
BER	bit error rate
BLAST	Bell Laboratories layered space-time
CDMA	code division multiple access
CSI	channel state information
DLAST	diagonally layered space-time code
GSM	Global System for Mobile Communication
HLST	horizontally layered space-time
IC	interference cancellation
IS	interference suppression
LMDS	Local Multipoint Distribution System
MIMO	multi-input multi-output
ML	maximum likelihood
MMSE	minimum mean square error
MGF	moment generating function
MUD	multiuser detection

OSTBC	orthogonal space-time block code
p.d.f.	probability density function
PEP	pairwise error probability
PSEP	pairwise symbol error probability
PSK	phase shift keying
QPSK	quadrature phase shift keying
QRD	QR decomposition
SIC	successive interference cancellation
SNR	signal-to-noise ratio
SQRD	sorted QRD
ST	space-time
STC	space-time code
STTC	space-time trellis code
STBC	space-time block code
TCM	trellis coded modulation
UMTS	Universal Mobile Telecommunication System
VBLAST	vertical BLAST
WCDMA	wideband CDMA
WiMax	Worldwide Interoperability for Microwave Access
WLAN	Wireless Local Area Network
ZF	zero forcing

List of Tables

List of Figures

Chapter 1

Introduction

1.1 A Brief History of Wireless Communications

Since 1895, when the first radio transmission took place, wireless communication methods and services have been enthusiastically adopted by people. In 1940's, the public mobile telephone system was introduced. Combined with the cellular concept, it was later improved to be the first generation of cellular system (1G system), which employs the analog transmission. Currently, 2G systems have been deployed widely in the world, of which Global System for Mobile Communication (GSM) and Interim Standard 95 (IS-95) are two typical commercial systems. They use digital transmission techniques and support data traffic with lower to medium throughput. Along with the evolution of the cellular systems, other wireless services are also gaining great popularity, including wireless data systems (e.g., Wireless Local Area Network (WLAN) and wireless Asynchronous Transfer Mode (ATM)) and fixed wireless access(e.g., Local Multipoint Distribution System (LMDS)). They supply a wide range of services with high data rates for different circumstances. Concerning the increased requirements of future mobile data applications such as video conferencing, web browsing and reading emails, 3G system was proposed and have been in commercial use in recent years. Although there are several standards for it, all of them aim to providing at least 144 kbps for full mobility applications, 384 kbps for limited mobility applications and 2 Mbps for low mobility applications. It is expected that in the near future, the 4G systems with data rate at least 50 Mbps will be in use. In general, the development of the wireless systems will go for unification of various mobile applications, wireless services and internet services, with high data rates and good quality, anywhere, anytime, for anyone.

1.2 Motivation

Modern wireless communications request a high data rate and certain quality of service. However, the wireless medium is highly unreliable, compared to the wired channel, due to the path loss and fading, which makes the signals be subject to significant attenuation and distortion in a random way. Moreover, the spectrum for wireless systems is a scare resource and expensive. The physical limitation of wireless channels presents a challenge to the high data rate reliable communications. However, it is shown recently that the capacity of wireless multi-input multi-output (MIMO) communication systems , i.e., systems with multiple transmit and multiple receive antennas, is a linear function of the number of antennas [1], [2]. This highlights the potential of a reliable communication with the high spectral efficiency. Consequently, to use the potential, two main types of schemes were introduced, the space-time code (STC) [3–5] and the Bell Laboratories space-time (BLAST) architecture [6–8]. STC, including the space-time trellis code (STTC) and the space-time block code (STBC), is targeted at the performance improvement by increasing the diversity. On the other hand, BLAST systems try to make the high data rate transmission [9] possible, which are also referred to as the layered STCs.

Diversity techniques have been studied for many years to improve the performance of the communication in fading environments [10]. Unlike, e.g., the time diversity and frequency diversity, which can be employed in single antenna systems, space/antenna diversity is particularly used in MIMO systems and more manageable. It is implemented by separating receive/transmit antennas far enough to create independent fading channels. The receive diversity was paid more attention and a number of signal processing methods for it have been proposed. In fact, receive diversity schemes are already used in current cellular applications. On the other hand, the transmit diversity received less attention. However, the employment of the transmit diversity is also important due to the fact that the mobile station is of small size such that multiple antennas are not available or separated far enough. STC is a two-dimensional design. It brings both temporal and spatial correlations to the transmitted signals to obtain the diversity gain as well as the coding gain, without sacrificing the bandwidth.

The standard code design criteria were derived in [3] for quasi-static fading and rapid fading MIMO channels. It was shown that the pairwise diversity gains and coding gains measure the performance of STCs. Specifically, for quasi-static fading, pairwise diversity gain is equal to the product of the rank of the codeword difference matrices and number of receive antennas. The pairwise coding gains are determined by the product of the nonzero eigenvalues of codeword difference matrices. On the other hand, the pairwise diversity gain and coding gain are determined by the nonzero columns of the codeword difference matrices in a rapid fading environment. Later, other improved code design criteria were proposed for the different circumstances such as, the trace criteria for a system with a large number of transmit antennas and the design criteria for the medium and high signal-to-noise ratios (SNRs) [11], [12]. All these are concerned with the system for single user communication.

However, the code design for multiuser systems has received less attention. Based on existing single-user STTCs, Ng et al. proposed an interference-resistant modulation, by rotating the space-time codes for single user systems before they are transmitted [13]. Nevertheless, this study only considers a single type of fading, assuming that all the users have the quasi-static fading channels. This is not true for many realistic multiuser systems, where different users may operate in different fading environments, i.e., some users may undergo quasi-static fading while the others may undergo rapid fading. This motivates us to study the code design in composite fading channels, in which some users have quasi-static fading channels and the others have rapid fading channels. Our discussion in Chapter 3 gives the code design criteria for composite fading channels, according to which optimal codes are obtained by computer search.

As stated above, with the size limitation of the transmit and/or receive device, the antennas may not locate as far as needed. This causes the correlation between the channels of MIMO systems, which is categorized as the spatial correlation. Even without the spatial correlation, the channel between any transmit-receive antenna pair may not be so low to be quasi-static fading or not so fast to be rapid fading. The channel changes with time but the channel coefficients of different symbol instances are correlated. This type of channel is referred to as the temporally correlated channel. More complicated scenario is that MIMO channels are spatially correlated as well temporally correlated. The early research demonstrates that the optimal code design for correlated fading channels is dependent on the channel correlation matrices [14]. However, in general, the transmitter does not know the channel unless a feedback of the channel state information (CSI) is performed, which is bandwidth-consuming and may not be useful. Robust code designs are required to achieve a good performance in a wide range of correlation situations [15]. Some robust code designs were proposed for different correlation cases [16], [17]. However, assumptions are made on the channel correlation matrices, (e.g., correlation matrix is positive definite) or on the structure of STC (e.g., square codeword matrix). Therefore, it will be of importance to investigate the robust code design for more general cases without such assumptions. The code design for multiuser systems, in which different users undergo different correlated fading situations, is also of great interest. We thus study the code design for multiuser generally correlated fading systems in Chapter 4.

As another dominant category of ST schemes, BLAST architectures are targeted at maximizing the data rate other than the diversity as STTC/STBC does. For example, uncoded VBLAST transmits independent data streams, namely layers, on different transmit antennas, which achieves multiple data rate than that of single transmit antenna systems. Obviously, the performance will be degraded. That is why the appropriate coding/decoding and detection methods are employed to ensure this system to have a high data rate as well as a performance good enough [18]. From the fact that the signals transmitted on different antennas interfere with each other, multiuser detection (MUD) algorithms are naturally applied at the receiver [19], among which the interference suppression (IS) and successive interference cancellation (SIC) are more favorable from aspects of complexity and quality of performance [20]. On the other hand, the deficiency inherent of the successive detection is the error propagation, which makes the performance of the lowest layer dominate the performance of the whole system [21]. It is also shown that the lowest layer has the smallest diversity gain among all the layers [22]. Thus to embed a group of STCs into a BLAST system is an effective way to have good tradeoff between the transmission rate and the performance [23]. Despite the research work being done, it is still desirable to find a scheme with appropriately chosen and combined STC and BLAST. New low-complexity STBC-VBLAST schemes are then proposed in this thesis, which obtain much higher diversity gain than VBLAST, thus the improved performance. A theorem is derived on how to integrate the STBC with the VBLAST to achieve a good tradeoff between the diversity gain and the spectral efficiency.

1.3 Literature Review

With rapid growth in mobile computing and other wireless data applications, services with higher and higher data rate will be required for future communications. On the other hand, band-limited and severely conditioned wireless channels are the narrow pipes that challenge the transmission of rapid flow of data. Nevertheless, the recent information-theoretic analysis of the capacity of MIMO systems suggests us a potential way to widen this pipe. Both Foschini and Telatar demonstrated that the capacity of MIMO channels grows linearly with the minimum number of transmit and receive antennas [1], [2]. However, the capacity only provides an upper bound realized by coding, modulation, detection and decoding with boundless complexity or latency [24]. In practice, the development of efficient coding, modulation and signal processing techniques is required to achieve the spectral efficiency as large as implied by the channel capacity.

Diversity techniques are widely used approaches to effectively use the wireless channels. They reduce the effects of multipath fading and improve the reliability of transmission [10], [25], [26]. The diversity method requires that a number of transmission paths are available, all carrying the same message but not having the fully correlated fading statistics. An intuitive explanation of the diversity concept is that if one path undergoes a deep fading, another independent path may have a strong signal. According to the domain where the diversity is introduced, diversity techniques are classified into *time, frequency* and *space/antenna diversity.*

A time diversity technique exploits the time variation of the fading channel. It is shown that sequential amplitude samples of a fading signal, if separated more than the coherence time, will be uncorrelated [27], [28]. Multiple diversity branches can be provided by transmitting the replicas of a symbol in time slots separated at least by coherent time. In practice, channel coding and interleaving are combined to employ the time diversity. However, when fading is slow, this will result in a large delay. The fact that the signals transmitted over distinct frequencies separated by coherence bandwidth induce independent fading is exploited to provide the frequency diversity [28]. Time diversity and frequency diversity normally introduce redundancy in time and/or frequency domain, and therefore result in a loss of bandwidth efficiency.

In fact, space diversity is the earliest diversity technique employed. This historical technique has found many applications over the years and is in wide use in a variety of present microwave systems. Space diversity is obtained typically by using multiple antennas for transmission and/or reception. The distance between them should be a few wavelengths to ensure independent fading [10]. Polarization diversity and angle diversity are another two examples of space diversity [29], [30]. They use diversity branches provided by the antenna polarizations and angles of arrival. Unlike time diversity and frequency diversity, space diversity does not induce any loss in bandwidth efficiency.

Depending on whether multiple antennas are used for transmission or reception, two types of space diversity can be used: *receive diversity* and *transmit diversity*. In receive diversity schemes, multiple antennas are deployed at the receiver to acquire separate copies of the transmitted signals which are then properly combined to mitigate channel fading [26], [31]. It has been studied for decades and used in current cellular systems. For example, in GSM and IS-136, multiple antennas are used at the base station to create uplink receive diversity. However, due to, e.g., the size and power limitations at the mobile units, receive antenna diversity appears less practical for the downlink transmissions. Transmit diversity relies on multiple antennas at the transmitter and is suitable for downlink transmissions because having multiple antennas at the base station is certainly feasible. This has inspired growing research work on transmit antenna diversity. Many transmit diversity schemes have been proposed, and can be classified as open-loop [32–34] and closed-loop schemes [35–37]. Compared to the closed-loop schemes, open-loop schemes do not require channel knowledge at the transmitter. On the other hand, the closed loop schemes reply on some channel information at the transmitter that is acquired through feedback channels. Although feedback channels are present in most wireless systems (for power control purposes), mobility may cause fast channel variations. As a result, the transmitter may not be capable of capturing the channel variations in time. Thus, the usage of open-loop transmit diversity schemes is well motivated for future wireless systems which are characterized by the high mobility.

In contrast with receive diversity, transmit diversity has a dominant implementation difficulty: the transmitted signals interfere each other at the receiver. Thus a special arrangement of the transmitted signals and/or the dedicated signal processing at the receiver are needed to separate the signals and exploit diversity. Typical examples are the delay diversity scheme by Seshadri [38] and the linear processing techniques in [39], [40]. Recently, a scheme of STC [3] was proposed, which is essentially a generalization of these transmit diversity schemes. STC is a joint design of the two-dimensional coding and modulation that introduces temporal and spatial correlation into signals transmitted on different antennas, in order to provide the diversity and coding gain without sacrificing the bandwidth [5].

To take into account the temporal and spatial relations of the signals, the transmitted signals are usually expressed in a two-dimensional matrix form, called codeword matrix, instead of a vector form for traditional channel codings. For an (n_T, n_R)

Rayleigh quasi-static flat fading MIMO system where n_T and n_R are the number of transmit and receive antennas respectively, the work in [3] reveals that the maximum available diversity is equal to $n_R n_T$. This is because that the *codeword difference matrix* or *codeword distance matrix* can at most provide $n_R n_T$ virtual diversity branches. By contrast, when channels are independent from symbol to symbol, the diversity gain only relies on the temporal arrangement of the codeword matrix and the number of receive antennas. These results in the code design criteria for flat Rayleigh fading systems, which are famous *determinant criterion* and *rank criterion* for quasi-static fading, and *product criterion* and *distance criterion* for rapid fading.

Some handcrafted STTCs with $4 \sim 32$ states were designed in [3] with different spectral efficiencies. All of them obey the rules that transitions departing from the same state have the second symbol in common, and transitions arriving at the same state have the same first symbol. These are required to ensure the codeword difference matrix always has a rank equal to the number of transmit antenna. However, these codes do not have the optimal coding gain. Based on the code design criteria, Baro and Grimm et al. established the generalized ST trellis encoder model and carried on the computer searches to get STTC with improved coding gain [41], [42]. To perform the computer searches effectively, Blum proposed a design procedure which calculates some typical lower and upper bounds for coding gain as well as the necessary and sufficient conditions on the diversity gain [43].

A number of optimal STTCs that provide maximum diversity and coding gain were presented in [44–47]. In [48], the design of M-ary PSK STTC is transformed into the binary domain where general binary design criteria of the unmodulated codeword matrix were derived for full diversity PSK-modulated STTCs. Later, Safar proposed a systematic code construction method that jointly considers diversity gain and coding gain for an arbitrary number of transmit antennas and any memoryless modulation [49].

Noticing the code design criteria mentioned above is based on the assumption that SNR is high, Tao et al. proposed modifications of the design criteria for different ranges of SNR [12]. It is shown that for a medium SNR, the effect of the identity matrix can not be neglected. Furthermore, when SNR is low, the trace instead of the determinant of the codeword distance matrix should be maximized. The STTCs based on these modified criteria were designed and presented better performance at low and medium SNRs. Meanwhile, Yuan found that when the diversity gain is larger than or equal to four, the performance of STTC is dominated by the minimum squared Euclidean distance, i.e, the trace of codeword distance matrix [11], [50]. The codes designed under the so called trace criterion outperform those designed according to determinant criterion when the diversity gain is greater than 3 [51], [52].

However, when the number of antennas is fixed, the decoding complexity of STTC increases exponentially as a function of the diversity gain and transmission rate [3]. In 1998, Alamouti proposed a simple STC scheme for systems with two transmit antennas [53]. This STC is later referred to as Alamouti's code that enables the linear maximum likelihood (ML) detection and decoding. In addition, Alamouti's code can get full diversity. These attractive characteristics make this scheme used in realistic communication systems such as UMTS (Universal Mobile Telecommunication System) and Worldwide Interoperability for Microwave Access (WiMax). Tarokh later generalized Alamouti's transmit diversity scheme to STBCs for an arbitrary number of transmit antennas [4], [54]. The orthogonal structure of STBC enable the linear ML decoding at the receiver. It is also shown in [4] that, for real signal constellations, that rate one *generalized real orthogonal* STBC can be constructed for any number of transmit antennas. However, rate one *generalized complex orthogonal* STBC only exists for $n_T = 2$. The extension of the above STBC was studied in [55–58], where different quasi-orthogonal STBCs were proposed to get different tradeoffs between transmission rate, error performance and decoding complexity. Another family of STBC, algebraic STBC, also get attention recently (e.g., [59], [60]), which will not be treated in this thesis.

In addition to the flat fading, other fading situations, such as time-selective and frequency-selective fading, were also discussed in some researches to address communications with the wide band and high mobility [61–65]. All these are under the assumption that the fading channels between antennas are independent. However, it is usually difficult to satisfy such a ideal condition in practice. The degree of the correlation between channel transmission paths from a transmit antenna to a receive antenna depends significantly on the scattering environment and on the antenna separation at the transmitter and receiver [10], [66], [67]. It has been demonstrated that if majority of the channel scatters are located closely to the mobile station, the paths will be highly spatially correlated unless the antennas are sufficiently separated in space. Sometimes the quasi-static fading or rapid fading is hardly the accurate description of the fading environment. The block fading, such as the one considered in [63], is also hard to be justified some time. More general time-varying channel situation is needed to be considered in many circumstances.

In an information-theoretic aspect, Shiu showed that in quasi-static fading, the capacity and performance degrades as a function of the channel spatial correlation [68]. The performance analysis of the correlated MIMO Rayleigh fading system was done in [14], [69–71]. The performances of existing STCs under different fading correlations were also investigated to see how the correlation affects the performance [72]. It is shown that the performance depends on a matrix which is associated with the transmit codeword matrix as well as the channel correlation matrix. However, in general, the transmitter does not know the CSI nor the statistics unless they are fed back. This is bandwidth cost and may not be useful. Under this circumstance, robust STCs are designed to achieve a good performance in a wide range of correlation situations [15], [16], [73] where the code design criteria that are independent of the channel correlation matrix are formulated. There, the robustness of the STCs was investigated either by analysis and experimental observation. The smart-greedy codes of [3] were shown to yield worse performance in certain spatio-temporally correlated channels. Particularly, the channel with only temporal correlation was studied. In [74], a bit-interleaved STBC scheme was proposed to show better performance than those in [16]. Su et al. derived the code design criteria and presented square STBCs for arbitrary time-correlated fading MIMO systems [17], [75].

The code design we have discussed is usually under the assumption that the receiver knows or estimates the CSI perfectly. In addressing the case that channel is not known both at the transmitter and receiver, unitary STC was introduced [76], [77].

The differential schemes that are naturally extended from the concept of DPSK were also proposed [78–80]. It is expected that the performance of the differential coding is 3 dB worse than that of the codes with the ideal CSI at the receiver. When imperfect channel estimation is performed at the receiver, studies in [65], [81] investigated the impact of estimation errors. It is demonstrated that the channel estimation error adds a fixed portion to the noise power and leads to an error floor in the performance curve.

Compared to the code design for single user systems, the code design for multiuser narrow band systems receives little attention. Most researches focus on the decoding and detection at the receiver [82–84]. The transmitter either simply combines STCs together with CDMA or uses ST spreading [85–88]. In [13], the STC design for multiuser systems is addressed comprehensively by Ng et al. The authors applied linear precoded STTC, i.e., rotating STTC by a unitary matrix similar to [89]. The rotation angles were optimized for different users to get a good performance. However, the study is constrained to the condition that all the users have the quasi-static fading.

As stated previously, MIMO systems have the potential to achieve a much higher bandwidth efficiency than single antenna systems in fading environment. STTC and STBC improve error performance through maximizing diversity and coding gain, thus improving the spectral efficiency under a certain requirement on the error probability [9]. A more intuitive way is to perform spatial multiplexing under a certain error probability or outage capacity [8]. Many BLAST architectures have been proposed to exploit this potential. The first BLAST structure is the DLST architecture proposed by Foschini [6], which distributes the code blocks along the diagonals, called layers, of the transmit codeword matrix. Consequently, VBLAST was introduced [7], [90], [20]. In VBLAST, each layer is either uncoded or coded independently and associated with a certain transmit antenna. Unlike DLST, the vertical arrangement of the layers enables detection and coding with lower complexity, but with different performances for different layers. With each layered coded independently, coded VBLAST is also called HLST [68], [91]. In some papers, HLST is generalized to be referred to as the horizontally coded BLAST with dependently coded layers [18].

Treating a BLAST system as a multiuser system makes it easy to understand that interference suppression (IS) and ordered SIC [19], [6], [92] can be used in the detection for BLAST systems. In [7], Golden et al. proposed a zero forcing (ZF) SIC algorithm with the optimum ordering, referred to as the ZF-VBLAST algorithm. Another algorithm, which uses minimum mean square error (MMSE) criterion and SIC was referred to as MMSE-VBLAST [90], [20]. However, both algorithms involve the computation of pseudo-inverses of matrices, which greatly increases the computational complexity. In [68], Shiu applies QR decomposition (QRD) to the detection. Although the performance is degraded (when the ordering is not optimized), the computational effort at the receiver is reduced enormously. To take advantage of the simplicity of QRD as well as ordering, Wübben proposed an efficient detection algorithm [93], which employs sorted QRD (SQRD). It has been shown that the performance of the VBLAST with SQRD is very close to that of ZF-VBLAST. However, similar to the situation of SIC in MUD, the error propagation inherent in SIC considerably degrades the performance of BLAST systems using SIC [21]. This error propagation also affects the performance of the channel decoder when the coded transmission is used.

To improve the performance, the turbo processing principle can be applied, so that the detection block and decoding block share information in an iterative fashion to do joint detection and decoding [94–96]. Iterative detection and decoding have their own challenges, such as high complexity, convergence and decoding delay. Power allocation was also considered to combat the error propagation problem in VBLAST systems [97]. The limitation is that the CSI is required at both transmitter and receiver.

Now, the challenge of BLAST systems is to design a coding scheme and low-complexity detector, which can get a high spectral efficiency as well as a good performance. In fact, it is natural to combine or concatenate the coding schemes to take advantage of all. For example, in [98] and [99], STBC was concatenated with recursive code and turbo trellis coded modulation (TCM) respectively. Likewise, HLST can be seen as an example of combining VBLAST and channel coding. Based on the fact that the STC has a high diversity gain and the BLAST has a high transmission rate but worse performance, combining the STC and BLAST is a reasonable choice to achieve a good tradeoff between the data rate and error performance [21], [23].

1.4 Main Contributions of the Thesis

Noticing the lack of research on the code design for narrowband multiuser MIMO systems, we first investigate the code design for multiuser composite fading channels, in which some users have quasi-static fading channels while the others have rapid fading channels.

- A multiuser composite fading system is considered. It is shown that the performance is determined by the rank and nonzero eigenvalues of a matrix **A**, which is the sum of two special matrices, one is characterizing quasi-static fading, the other is characterizing rapid fading.

- The code design criteria are achieved, which require the minimum rank of codeword distance matrices as well as the minimum product of the nonzero eigenvalues of codeword distance matrices for both quasi-static and rapid fading from each user's code set to be maximized.

- The optimal 4-state and 8-state STTCs for composite fading are obtained by computer search, which outperform the existing STCs by 3 dB and 5 dB at a bit error rate (BER) of 10^{-3} respectively.

Our discussion is then extended to the code design for multiuser generally correlated fading systems. Without any assumption on, such as the rank of channel correlation matrix and the dimension of the codeword matrix, we mainly achieve the following results:

- All users should use the same code set and the code design for multiuser systems can be reduced to the code design for single user systems.

- When channels are only temporally correlated, the minimum rank and number of the nonzero columns of codeword difference matrices should be maximized in order to get the maximum diversity gain. The upper bound of the coding gain is determined by the product of the norms of codeword difference matrices' nonzero column vectors. When the minimum number of nonzero columns of codeword difference matrices is equal to the minimum rank of codeword distance matrices, the coding gain is lower bounded by the minimum product of the nonzero eigenvalues of codeword distance matrices.

- For spatially and spatio-temporally correlated fading systems, the code design criteria are the same as those for rapid fading systems: the minimum number and the minimum product of the norms of codeword difference matrices' nonzero column vectors needed to be maximized.

- Based on above results, a set of code design criteria for arbitrarily correlated fading systems are obtained.

With the purpose of getting a good performance as well as a high data rate, we have the following contributions:

- The STBC-VBLAST and ordered STBC-VBLAST are proposed. For an (n_T, n_R) system, the (n, m, G) STBC-VBLAST integrates G $n \times m$ STBC into the VBLAST.

- The diversity gain of an (n, m, G) STBC-VBLAST is the minimum of $n(n_R - n_T) + n^2$ and $n_R - n_T + Gn + 1$. The ordered STBC-VBLAST has a better performance than the STBC-VBLAST.

- In order to get a good tradeoff between the diversity gain and spectral efficiency, G should be chosen such that $G \leq G_{th}$, where $G_{th} = n + (n_R - n_T) - \lfloor \frac{n_R - n_T + 1}{n} \rfloor$ for both STBC-VBLAST and ordered STBC-VBLAST.

- When channel estimation errors present, the error probability and error floor are the decreasing functions of the diversity gain. Thus the (ordered) STBC-VBLAST performs more robust than VBLAST schemes, such as ZF-VBLAST, when perfect channel estimation is absent.

- The computational complexity of the (ordered) STBC-VBLAST is of order $O(n_R n_T^2)$, compared to $O(n_T^4)$ for ZF-VBLAST.

1.5 Organization of the Thesis

In Chapter 2, a frequency nonselective MIMO fading channel model is introduced. The basic concepts of STTC and STBC are presented. Two important factors of STC systems, diversity gain and coding gain, are explained. The structures of BLAST systems and typical detection algorithms are presented for further discussions.

In Chapter 3, code design criteria are derived for narrowband multiuser composite fading systems. Different users may have different number of transmit antennas. The code design criteria require the minimum rank and product of the nonzero eigenvalues of codeword distance matrices from each user's code set to be maximized. Specifically, if all the users have the same number of antennas, they will share the common code set and the code design is simplified. Based on the criteria, we obtain the optimal 4-state and 8-state space-time trellis codes for a two-user QPSK system through exhaustive search. We also show by simulation that the new codes have better performance than existing STCs in composite fading channels.

In Chapter 4, we extended our discussion of code design for multiuser composite fading systems to the code design for multiuser generally correlated fading channels. The joint pairwise error probabilities for three different channel correlation situations are analyzed: temporally correlated fading, spatially correlated fading, and spatio-temporally correlated fading. It is demonstrated that the diversity gain and coding gain are determined by the STC and channel correlation of individual user. This suggests that all users should use the same code set and the code design for multiuser systems can be reduced to code design for single user systems.

The specific code design criteria are also obtained for these three fading cases individually. Based on all these results, we further get a set of general code design criteria suitable for all three fading situations. It is shown that the STTCs obtained based on the general code design criteria perform more robust than other STTCs.

In chapter 5, the STBC-VBLAST and ordered STBC-VBLAST are proposed. The improved diversity gain allows the new schemes to suppress error propagation very efficiently and to outperform other VBLAST systems.

The higher diversity gain also means that STBC-VBLAST systems have better performance in the presence of channel estimation error. How to choose the number of STBC layers is discussed in the sense of getting a good tradeoff between the diversity gain and spectral efficiency. Benefitting from the simplicity of the decoding of STBC and QRD/SQRD, the detection process has much lower complexity than existing BLAST schemes such as ZF-VBLAST.

Finally, the conclusions are given in Chapter 6.

Chapter 2

Fundamentals

2.1 MIMO Rayleigh Fading Channel Modeling

A MIMO channel is realized with multiple antennas at both transmitter and receiver. For an (n_T, n_R) system, there are $n_T n_R$ channels between given pairs of transmit and receive antennas. The individual channels can be characterized as flat, time selective, or frequency selective fading with key modeling parameters, such as Doppler spread, delay spread, coherent time, and coherent bandwidth [27]. In addition, unlike the single-antenna system, another important factor for MIMO channel is the correlations between these individual channels.

Originated from the traditional Jakes and Clarke model, some researches have been done on modeling the MIMO channel, see [67], [100], [101], for example. All these models characterize the fading environment as the mobile/base station (MS/BS) surrounded by many local scatters. The received signal is the superposition of the reflected versions of the transmitted signal that are affected by the movement of

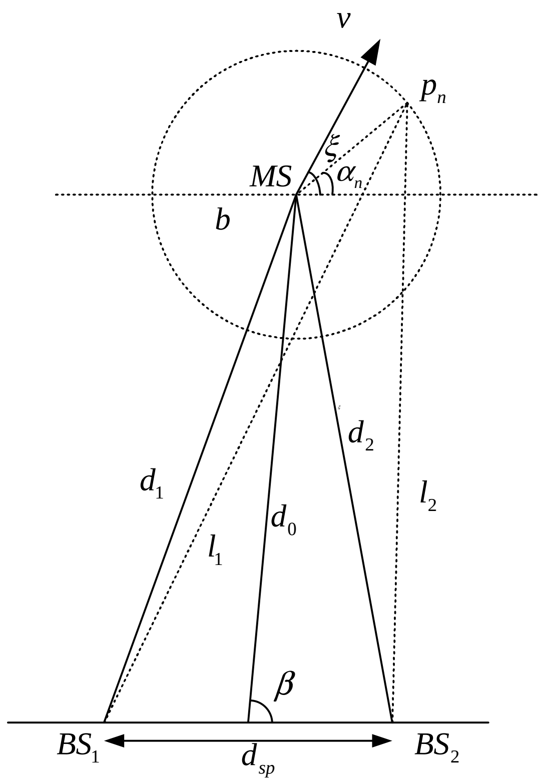

Figure 2.1: The transmission model between a mobile and base station.

MS and the locations of the scatters.

Here, we give a brief review of a frequency nonselective MIMO Rayleigh fading channel model using "circular ring" geometry, which is introduced in [67] and will be used for the simulations in later chapters. A typical geometrical configuration for a $(2,1)$ system is shown in Fig. 2.1. The channel responses between transmit antennas BS_1, BS_2 and MS are

$$h_1(t) = \sqrt{\frac{\sigma^2}{N}} \sum_{n=1}^{N} \exp\{j2\pi f_D t \cos(\xi - \alpha_n) + j\phi_n\} \tag{2.1}$$

and

$$h_2(t) = \sqrt{\frac{\sigma^2}{N}} \sum_{n=1}^{N} \exp\{j2\pi f_D t \cos(\xi - \alpha_n) + j\phi_n + j\Delta\phi_n\} \tag{2.2}$$

respectively, where N is the number of scatters. σ^2 is the variance of the channel; f_D is the Doppler spread caused by the vehicle movement; $\alpha_n = 2\pi n/N$, is the angle of the nth scatter on the scatter ring. ϕ_n is the initial phase shift introduced by the nth scatter where $\{\phi_n\}_{n=1}^{N}$ are usually assumed to be i.i.d random variables with uniform distributions over $[0, 2\pi)$. $\Delta\phi_n$ is the phase difference caused by the different path lengths from the scatter n to the two transmit antennas. Furthermore, as shown in Fig. 2.1, b is the scatter ring radius; d_0 is the mobile distance to the center of the BS antenna pair; β is the mobile position angle with respect to the end-fire of the antennas; ξ is the mobile moving direction with respect to the end-fire of the BS antennas. Thus we have, as shown in [67],

$$\begin{aligned} \Delta\phi_n &= \frac{2\pi(l_1 - l_2)}{\lambda} \\ &\approx d_{sp} \cos\beta + z_c \cos\alpha_n - z_s \sin\alpha_n, \end{aligned} \tag{2.3}$$

where l_1 and l_2 are defined as in Fig. 2.1, and

$$\begin{aligned} z_c &= \frac{2b}{d_1 + d_2}[d_{sp} - (d_1 - d_2)\cos\theta\cos\beta] \\ &\approx \frac{b}{d} d_{sp} \sin^2\beta, \end{aligned} \tag{2.4}$$

and

$$\begin{aligned} z_s &= \frac{2b}{d_1+d_2}(d_1-d_2)\cos\theta\sin\beta \\ &\approx \frac{b}{d}d_{sp}\sin\beta\cos\beta. \end{aligned} \tag{2.5}$$

The generalized space-time cross-correlation function is therefore

$$\begin{aligned} \rho &= R_{h_1,h_2}(\tau, d_{sp}) \\ &= \sigma^2 \exp[j\frac{2\pi}{\lambda}(d_1-d_2)] \times J_0\left[2\pi\sqrt{\left(f_D\tau\cos\xi+\frac{z_c}{\lambda}\right)^2+\left(f_D\tau\sin\xi-\frac{z_c}{\lambda}\right)^2}\right]. \end{aligned} \tag{2.6}$$

From Eq. (2.6), we can see that the temporal correlation is exclusively a function of f_D while the spatial correlation is the function of geometry model and wavelength. Specifically, when $d_{sp}=0$, the space-time cross-correlation reduces to the temporal correlation as $\sigma^2 J_0(2\pi f_D\tau)$ [10]. Using the same geometry model, the channel correlation model for a system with more transmit and/or receive antennas can be obtained in the same way.

The channel responses shown in Eq. (2.1) and Eq. (2.2) will be used to simulate the CSI for the following chapters.

2.2 Space-time Codes

In this section, we will give an overview of STCs and briefly explain its principle.

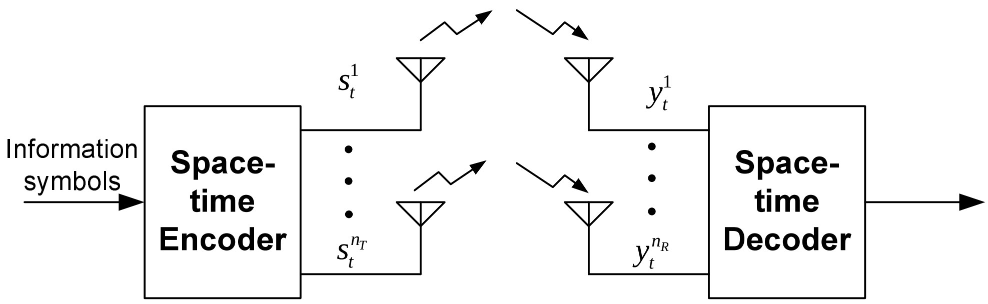

Figure 2.2: Space-time system block diagram.

2.2.1 Signal Model

Consider an (n_T, n_R) system as shown in Fig. 2.2. At each time slot t, symbols $s_t^i, i = 1, 2, \ldots, n_T$, are transmitted simultaneously from the n_T transmit antennas. The received signal at each receive antenna is a noisy superposition of the n_T transmitted signals corrupted by the fading channel. Assuming the channel is flat fading and the noise in the channel is white Gaussian, the signal y_t^j received by antenna j at time t is given by

$$y_t^j = \sqrt{E_s} \sum_{i=1}^{n_T} h_{i,j}^t s_t^i + n_t^j, \tag{2.7}$$

where the noise n_t^j at time t is modeled as independent samples of a zero-mean complex Gaussian random variable with variance $N_0/2$ per real dimension. The coefficient h_{ij}^t is the channel gain from transmit antenna i to receive antenna j at time t. Generally, the transmission and detection are considered in a block with L symbols. It will be convenient to denote the normalized transmitted signal in matrix form as, for further discussion,

$$\mathbf{S} = \begin{bmatrix} s_1^1 & s_2^1 & \cdots & s_L^1 \\ \vdots & \vdots & \ddots & \vdots \\ s_1^{n_T} & s_2^{n_T} & \cdots & s_L^{n_T} \end{bmatrix}. \tag{2.8}$$

2.2.2 Performance Analysis and Design of STC

It is assumed that the channel is known at the receiver and ML decoding is used, where the decision metric is [3]

$$\sum_{t=1}^{L} \sum_{j=1}^{n_R} \left| y_t^j - \sqrt{E_s} \sum_{i=1}^{n_T} h_{i,j}^t s_t^i \right|^2. \tag{2.9}$$

The receiver will calculate the decision metric and decide in favor of the transmitted signals $\{s_t^i\}, i = 1, 2, \ldots, n_T; t = 1, 2, \ldots, L$, with the minimum Δ^2. To analyze the error performance of the STC, we usually consider the pair-wise error probability (PEP) which decides the union bound of the former. The PEP between $\mathbf{S}$ and $\hat{\mathbf{S}}$, $P(\mathbf{S}, \hat{\mathbf{S}})$, is the error probability that the receiver decides erroneously in favor of a signal $\hat{\mathbf{S}}$ when $\mathbf{S}$ is transmitted. The PEP conditioned on CSI can be expressed as

$$\begin{aligned} P(\mathbf{S}, \hat{\mathbf{S}} | h_{i,j}^t) &= P\left(\sum_{t=1}^{L} \sum_{j=1}^{n_R} \left| y_t^j - \sqrt{E_s} \sum_{i=1}^{n_T} h_{i,j}^t s_t^i \right|^2 > \sum_{t=1}^{L} \sum_{j=1}^{n_R} \left| y_t^j - \sqrt{E_s} \sum_{i=1}^{n_T} h_{i,j}^t \hat{s}_t^i \right|^2 \right) \\ &= Q\left(\sqrt{\frac{E_s}{2N_0} \Delta^2} \right), \end{aligned} \tag{2.10}$$

where

$$\Delta^2 = \sum_{t=1}^{L} \sum_{j=1}^{n_R} \left| \sum_{i=1}^{n_T} h_{i,j}^t s_t^i - \sum_{i=1}^{n_T} h_{i,j}^t \hat{s}_t^i \right|^2. \tag{2.11}$$

The PEP between $\mathbf{S}$ and $\hat{\mathbf{S}}$ is thus the expectation of conditional PEP on $h_{i,j}$'s, which can be written as

$$P(\mathbf{S}, \hat{\mathbf{S}}) = E\left[Q\left(\sqrt{\frac{E_s}{2N_0}\Delta^2}\right)\right]. \tag{2.12}$$

Since the Q function is an integral, it may be more useful to use its Chernoff bound to analyze the PEP:

$$P(\mathbf{S}, \hat{\mathbf{S}}) \leq E\left[\exp\left(-\frac{E_s}{4N_0}\Delta^2\right)\right] = \phi_{\Delta^2}(s)|_{s=-\frac{E_s}{4N_0}}. \tag{2.13}$$

where $\phi_{\Delta^2}(s)$ is the moment generating function (MGF) of Δ^2. In the following sections, the performances of STCs will be discussed based on Eq. (2.13). We will show that the performance of a specific STC is dependent on the channel fading situations. This implies that the code design for different channels will base on different criteria.

Performance and code design of STC under Quasi-static Rayleigh Fading

Recall that the channels do not change within one code block with L symbols under the assumption of quasi-static fading. The received signal in one block can be equivalently denoted in the matrix form as, based on Eq. (2.7),

$$\mathbf{Y} = \sqrt{E_s}\mathbf{H}\mathbf{S} + \mathbf{N}, \tag{2.14}$$

where

$$\mathbf{Y} = \begin{bmatrix} y_1^1 & y_2^1 & \cdots & y_L^1 \\ \vdots & \vdots & \ddots & \vdots \\ y_1^{n_R} & y_2^{n_R} & \cdots & y_L^{n_R} \end{bmatrix} \tag{2.15}$$

and

$$\mathbf{H} = \begin{bmatrix} h_{1,1} & h_{1,2} & \cdots & h_{1,n_T} \\ \vdots & \vdots & \ddots & \vdots \\ h_{n_R,1} & h_{n_R,2} & \cdots & h_{n_R,n_T} \end{bmatrix}. \tag{2.16}$$

$\mathbf{S}$ is defined in Eq. (2.8). It can be seen that

$$\Delta^2 = tr\left(\mathbf{H}(\mathbf{S}-\hat{\mathbf{S}})(\mathbf{S}-\hat{\mathbf{S}})^H\mathbf{H}^H\right), \tag{2.17}$$

where $tr(\cdot)$ indicates the trace of $(\cdot)$. Since $\mathbf{D} = (\mathbf{S}-\hat{\mathbf{S}})(\mathbf{S}-\hat{\mathbf{S}})^H$ is a Hermitian matrix, we have

$$\mathbf{D} = \mathbf{U}\Lambda\mathbf{U}^H, \tag{2.18}$$

where $\mathbf{U} \in \mathcal{C}^{n_T \times n_T}$ is an unitary matrix and $\Lambda \in \mathcal{C}^{n_T \times n_T}$ is a diagonal matrix with eigenvalues of $\mathbf{D}$ at the diagonal. With $rank(\mathbf{D}) = r$,

$$\Lambda = diag(\lambda_1, \lambda_2, \ldots, \lambda_r, 0, \ldots, 0).$$

Further define a new vector, $\mathbf{v}_i \in \mathcal{C}^{n_R \times 1}$, as

$$\mathbf{v}_i = \mathbf{H}\mathbf{u}_i, i = 1, 2, \ldots, r, \tag{2.19}$$

where $\mathbf{u}_i$ is the ith column of $\mathbf{U}$. Then

$$\Delta^2 = \sum_{i=1}^{r} \lambda_i \|\mathbf{v}_i\|^2 = \sum_{i=1}^{r} \lambda_i \beta_i = \sum_{i=1}^{r} \xi_i. \tag{2.20}$$

Note that all the elements of $\mathbf{H}$ are i.i.d. complex Gaussian random variables and each entry of $\mathbf{v}_i$ is also i.i.d. complex Gaussian. Therefore, ξ_i is $\mathcal{X}^2_{2n_R}$ distributed with mean $\lambda_i n_R$. In addition, since the columns of $\mathbf{U}$ are orthonormal, elements of $\mathbf{v}_i$ and $\mathbf{v}_j$ are uncorrelated, hence independent, for $i \neq j$. As a result, ξ_i and ξ_j are independent for $i \neq j$. Thus

$$\phi_{\Delta^2}(s) = \prod_{i=1}^{r} \phi_{\xi_i}(s) = \prod_{i=1}^{r} \left(\frac{1}{1 - \lambda_i s} \right)^{n_R}. \tag{2.21}$$

The PEP is upper bounded as, when SNR$= E_s/N_0$ is large,

$$P(\mathbf{S}, \hat{\mathbf{S}}) \leq \prod_{i=1}^{r} \left(\frac{1}{1 + \frac{E_s}{4N_0}\lambda_i} \right)^{n_R} \approx \left(\frac{E_s}{4N_0} \right)^{-rn_R} \prod_{i=1}^{r} \lambda_i{}^{-n_R}. \tag{2.22}$$

Based on Eq. (2.22), the pairwise diversity gain and gain coding gain are defined as $\eta'_d = rn_R$ and $\eta'_c = (\prod_{i=1}^{r} \lambda_i)^{1/r}$ respectively. The diversity gain indicates the slope of the PEP versus SNR curve, and the increment of the coding gain will shift the curve left. Thus the code design should maximize η'_d and η'_c over all pairs of distinct code matrices $(\mathbf{S}, \hat{\mathbf{S}})$. Note that the minimum pairwise diversity gain and coding gain have the dominant effect on the performance. According to [3], the diversity gain of a STC is defined as the minimum pairwise diversity gain; and the coding gain is defined as the minimum pairwise coding gain of the distinct pairs of code matrices with pairwise diversity gain η_d, by the following equations:

$$\eta_d = \arg\min_{(\mathbf{S},\hat{\mathbf{S}})} rn_R \tag{2.23}$$

and

$$\eta_c = \arg\min_{\substack{(\mathbf{S},\hat{\mathbf{S}}) \\ rn_R=\eta_d}} \left(\prod_{i=1}^{r} \lambda_i\right)^{1/r}. \tag{2.24}$$

It can be seen that the performance of the STC depends on the properties of $\mathbf{S}-\hat{\mathbf{S}}$ and $(\mathbf{S}-\hat{\mathbf{S}})(\mathbf{S}-\hat{\mathbf{S}})^H$, which are referred to as the *codeword difference matrix* and the *codeword distance matrix* in some papers. However, to be consistent with the derivation in later chapters, we define the codeword difference matrix and the codeword distance matrix as $\mathbf{S}-\hat{\mathbf{S}}$ and $(\mathbf{S}-\hat{\mathbf{S}})^H(\mathbf{S}-\hat{\mathbf{S}})$ respectively in this thesis. This will not cause misunderstandings in the statements and results, since what we are concerned about is just the rank and nonzero eigenvalues of the codeword distance matrix, which are the same for $(\mathbf{S}-\hat{\mathbf{S}})^H(\mathbf{S}-\hat{\mathbf{S}})$ and $(\mathbf{S}-\hat{\mathbf{S}})(\mathbf{S}-\hat{\mathbf{S}})^H$. Based on Eq. (2.22), two code design criteria have been obtained in [3]:

1. *Rank criterion*: In order to achieve the maximum diversity gain, the codeword distance matrix $\mathbf{D}$ or equivalently the codeword difference matrix $\mathbf{S}-\hat{\mathbf{S}}$ has to be full rank taken over all possible pairs of distinct $\mathbf{S}$ and $\hat{\mathbf{S}}$.

2. *Determinant criterion*: In order to achieve the maximum coding gain, the minimum product of nonzero eigenvalues of $\mathbf{D}$ taken over all pairs of distinct $\mathbf{S}$ and $\hat{\mathbf{S}}$ should be maximized.

Performance and design of STC under Rapid Rayleigh Fading

The same method is used for the performance analysis of STC under rapid fading channels. For a rapid fading system, the channels at different symbol intervals are independent. The received signal vector at time t is

$$\mathbf{y}_t = \mathbf{H}_t\mathbf{s}_t + \mathbf{n}_t, \tag{2.25}$$

where $\mathbf{H}_t = [h_{i,j}^t] \in \mathcal{C}^{n_R \times n_T}$ is the channel matrix at time t, $\mathbf{s}_t$ is the tth column of $\mathbf{S}$ and $\mathbf{n}_t$ is the noise vector at time t. Then

$$\begin{aligned}\Delta^2 &= \sum_{t=1}^{L} \|\mathbf{H}_t(\mathbf{s}_t - \hat{\mathbf{s}}_t)\|^2 \\ &= \sum_{t=1}^{L} tr\left(\mathbf{H}_t(\mathbf{s}_t - \hat{\mathbf{s}}_t)(\mathbf{s}_t - \hat{\mathbf{s}}_t)^H\mathbf{H}_t^H\right) = \sum_{t=1}^{L} \xi_t.\end{aligned} \tag{2.26}$$

Since $\mathbf{D}_t = \mathbf{H}_t(\mathbf{s}_t - \hat{\mathbf{s}}_t)(\mathbf{s}_t - \hat{\mathbf{s}}_t)^H\mathbf{H}_t^H$ has the rank of at most one, and the corresponding eigenvalue is $\|\mathbf{s}_t - \hat{\mathbf{s}}_t\|^2$, ξ_t can be expressed as

$$\xi_t = \|\mathbf{s}_t - \hat{\mathbf{s}}_t\|^2\beta_t, \tag{2.27}$$

where β_t is the chi-square variate with freedom $2n_R$. Consequently,

$$\phi_{\Delta^2}(s) = \prod_{t=1}^{L}\left(\frac{1}{1 - \|\mathbf{s}_t - \hat{\mathbf{s}}_t\|^2 s}\right)^{n_R}. \tag{2.28}$$

Substituting $-E_s/4N_0$ for s, and still with the assumption that SNR is high, we have

$$P(\mathbf{S}, \hat{\mathbf{S}}) \leq \left(\frac{E_s}{4N_0}\right)^{n_R|\Omega|} \prod_{t \in \Omega} \left(\frac{1}{\|\mathbf{s}_t - \hat{\mathbf{s}}_t\|^2}\right)^{n_R}, \tag{2.29}$$

where $\Omega = \{t : \mathbf{s}_t - \hat{\mathbf{s}}_t \neq 0\}$ and $|\Omega|$ is the cardinality of Ω. Similarly, the pairwise diversity gain and coding gain are, for rapid fading system, $\eta'_d = n_R|\Omega|$ and $\eta'_c = \left(\prod_{t \in \Omega} \|\mathbf{s}_t - \hat{\mathbf{s}}_t\|^2\right)^{1/|\Omega|}$ respectively. Note that the situation here is different from that of quasi-static fading systems. The diversity gain of a STC under the rapid fading system is dependent on the nonzero columns of $\mathbf{S} - \hat{\mathbf{S}}$ not the rank of $\mathbf{S} - \hat{\mathbf{S}}$. Similarly, two STC design criteria are obtained for rapid fading channels [3]:

1. *Distance criterion*: In order to achieve the maximum diversity, the minimum number of nonzero columns of codeword difference matrices taken over all possible pairs of distinct $\mathbf{S}$ and $\hat{\mathbf{S}}$ should be maximized.

2. *Product criterion*: In order to achieve the maximum coding gain, the minimum product of the norms of codeword difference matrices' nonzero column vectors taken over all pairs of distinct $\mathbf{S}$ and $\hat{\mathbf{S}}$ should be maximized.

2.2.3 Impact of Channel Correlation on the Performance of STC

In the previous sections, we investigate the performance and STC design in quasi-static fading and rapid fading systems, where we suppose there is no correlation between the transmit and receive antennas. Moreover, either very slow fading where the channel gain is constant over one code block, or very fast fading where the channel gains are independent from symbol to symbol is assumed. In this section a more general case that the channels are arbitrarily spatially and temporally correlated will be reviewed [14]. In order to simplify the illustration, one receive antenna is assumed. Letting

$$\mathbf{C}_i = diag(s_1^i, s_2^i, \ldots, s_L^i) \tag{2.30}$$

and

$$\mathbf{C} = \begin{bmatrix} \mathbf{C}_1 & \mathbf{C}_2 & \cdots & \mathbf{C}_{n_R} \end{bmatrix}^T, \tag{2.31}$$

we have

$$\mathbf{x} = \mathbf{C}\mathbf{g} + \mathbf{w}, \tag{2.32}$$

where

$$\mathbf{x} = \begin{bmatrix} y_1^1 & y_2^1 & \cdots & y_L^1 & y_1^2 & \cdots & y_L^2 & \cdots & y_1^{n_R} & \cdots & y_L^{n_R} \end{bmatrix}^T \tag{2.33}$$

and

$$\mathbf{g} = \begin{bmatrix} \mathbf{g}_1^T & \mathbf{g}_1^T & \cdots & \mathbf{g}_{n_R}^T \end{bmatrix}^T, \tag{2.34}$$

in which

$$\mathbf{g}_i = \begin{bmatrix} h_{1,i}^1 & h_{1,i}^2 & \cdots & h_{1,i}^L & h_{2,i}^1 & \cdots & h_{2,i}^L & \cdots & h_{n_T,i}^L \end{bmatrix}^T. \tag{2.35}$$

The correlation of the channels is specified by the correlation matrix of $\mathbf{g}$ as

$$\mathbf{R}_c = E[\mathbf{g}\mathbf{g}^H]. \tag{2.36}$$

The PEP of transmitting $\mathbf{S}$ but deciding $\hat{\mathbf{S}}$ is

$$P(\mathbf{S}, \hat{\mathbf{S}}) = P(\|\mathbf{x} - \mathbf{C}\mathbf{g}\|^2 > \|\mathbf{x} - \hat{\mathbf{C}}\mathbf{g}\|^2), \tag{2.37}$$

where $\mathbf{C}$ and $\hat{\mathbf{C}}$ are constructed from $\mathbf{S}$ and $\hat{\mathbf{S}}$ respectively. We first consider a loose bound by using standard Chernoff bound. Then

$$P(\mathbf{S}, \hat{\mathbf{S}}) \leq E\left[\exp\left(\frac{E_s}{4N_0}\Delta^2\right)\right], \tag{2.38}$$

where

$$\Delta^2 = \mathbf{g}^H(\mathbf{C} - \hat{\mathbf{C}})^H(\mathbf{C} - \hat{\mathbf{C}})\mathbf{g}. \tag{2.39}$$

Note that Δ^2 is the quadrature form of a sequence of Gaussian random variables with covariance

$$\mathbf{R} = (\mathbf{C} - \hat{\mathbf{C}})\mathbf{R}_c(\mathbf{C} - \hat{\mathbf{C}})^H. \tag{2.40}$$

Similar to the discussion in previous sections, according to the theory on the MGF of multivariate Gaussian variables, we have

$$E\left[\frac{E_s}{4N_0}\Delta^2\right] = \det\left(\mathbf{I}_{n_R L} + \frac{E_s}{4N_0}\mathbf{R}\right)^{-1}. \tag{2.41}$$

Then

$$P(\mathbf{S}, \hat{\mathbf{S}}) \leq \prod_{i=1}^{r}\left(\frac{1}{1 + \frac{E_s}{4N_0}\lambda_i(\mathbf{R})}\right)^{n_R}, \tag{2.42}$$

where $r = rank(\mathbf{R})$ and $\lambda_i(\mathbf{R})$ is the ith nonzero eigenvalue of $\mathbf{R}$.

Another upper bound of PEP is achieved through the MGF of Gaussian random variables as well, but Chernoff bound is not used. It has been shown that the upper bound in [14] is tighter than Chernoff bound and is an asymptotic approximation of the exact PEP. Here we only show some important results in [14]. Based on Eq. (2.37), PEP can be expressed as

$$P(\mathbf{S}, \hat{\mathbf{S}}) = P(z < 0), \tag{2.43}$$

where $z = \|\mathbf{x} - \hat{\mathbf{C}}\mathbf{g}\|^2 - \|\mathbf{x} - \mathbf{C}\mathbf{g}\|^2$. It is proved that the MGF of z is

$$\begin{aligned} \phi_z(j\omega) &= \prod_{i=1}^{r} \frac{1}{N_0 E_s \lambda_i(\mathbf{R})} \left(\omega^2 - \frac{j\omega}{N_0} + \frac{1}{N_0 E_s \lambda_i(\mathbf{R})} \right)^{-1} && (2.44) \\ &= \prod_{i=1}^{r} \left(\frac{-j}{N_0 E_s \lambda_i(\mathbf{R})(t - jp_i^+)} \right) \left(\frac{j}{\omega - jp_i^-} \right), && (2.45) \end{aligned}$$

where

$$p_i^{\pm} = \frac{1}{2N_0} \left(1 \pm \sqrt{1 + \frac{4N_0}{E_s \lambda_i(\mathbf{R})}} \right). \tag{2.46}$$

The residue theory implies that

$$P(\mathbf{S}, \hat{\mathbf{S}}) = \sum_{i=1}^{r} \mathrm{Res} \left[-\frac{1}{\omega} \prod_{k=1}^{r} \frac{1}{(\omega - jp_k^+)(\omega - p_k^-)} \right]_{\omega = jp_i^+} \left(\frac{1}{\prod_{i=1}^{r} N_0 E_s \lambda_i(\mathbf{R})} \right). \tag{2.47}$$

Noticing that if the poles of $\phi_z(j\omega)$ in the upper half plane is repeated, the calculation of Eq. (2.47) is very complicated. However, the fact that the movement of $p_i^{\pm}$ toward the origin will increase the residue, the following upper bound is obtained, which is tighter than Chernoff bound when SNR is high.

$$P(\mathbf{S}, \hat{\mathbf{S}}) \leq \begin{pmatrix} 2r - 1 \\ r - 1 \end{pmatrix} \left(\frac{E_s}{N_0} \right)^{-r} \left(\prod_{i=1}^{r} \lambda_i(\mathbf{R}) \right)^{-1} \leq \left(\frac{E_s}{4N_0} \right)^{-r} \left(\prod_{i=1}^{r} \lambda_i(\mathbf{R}) \right)^{-1}. \tag{2.48}$$

It can be seen that the performance of a STC depends on the rank and eigenvalues of $\mathbf{R}$, which is associated with not only the STC itself but the correlation matrix of the channel. In case that the transmitter knows the channel, the code design should take the channel correlation into account for the optimal performance. In general, channel is assumed to be known or estimated at the receiver and there is no feedback to transmitter. The code design needs to be suitable for different correlation situations. We will discuss this in Chapter 4 in more details.

2.2.4 Space-time Trellis Code and Space-time Block Code

In this section, we will show the principles of the STTC and STBC.

Space-time Trellis Codes

STTC is a two-dimensional extension of the traditional trellis code. For an M-PSK STTC, the encoder is composed of $m = \log_2 M$ shift registers, which is shown in Fig. 2.3. All the input sequences are binary. However, the tap weights and the output symbols are elements of $GF(M)$. Each shift register may have different memory order ν_i. The total memory order of the ST trellis encoder is $\nu = \sum_{i=1}^{m} \nu_i$. The output vector, $\mathbf{s}_t \in \mathcal{C}^{n_T \times 1}$, at each time t can be expressed as

$$\mathbf{s}_t = \sum_{i=1}^{m} \mathbf{b}_t^i \mathbf{G}_i \mod M, \tag{2.49}$$

where

$$\mathbf{b}_t^i = \begin{bmatrix} b_t^i & b_{t-1}^i & \cdots & b_{t-\nu_i}^i \end{bmatrix}^T, \tag{2.50}$$

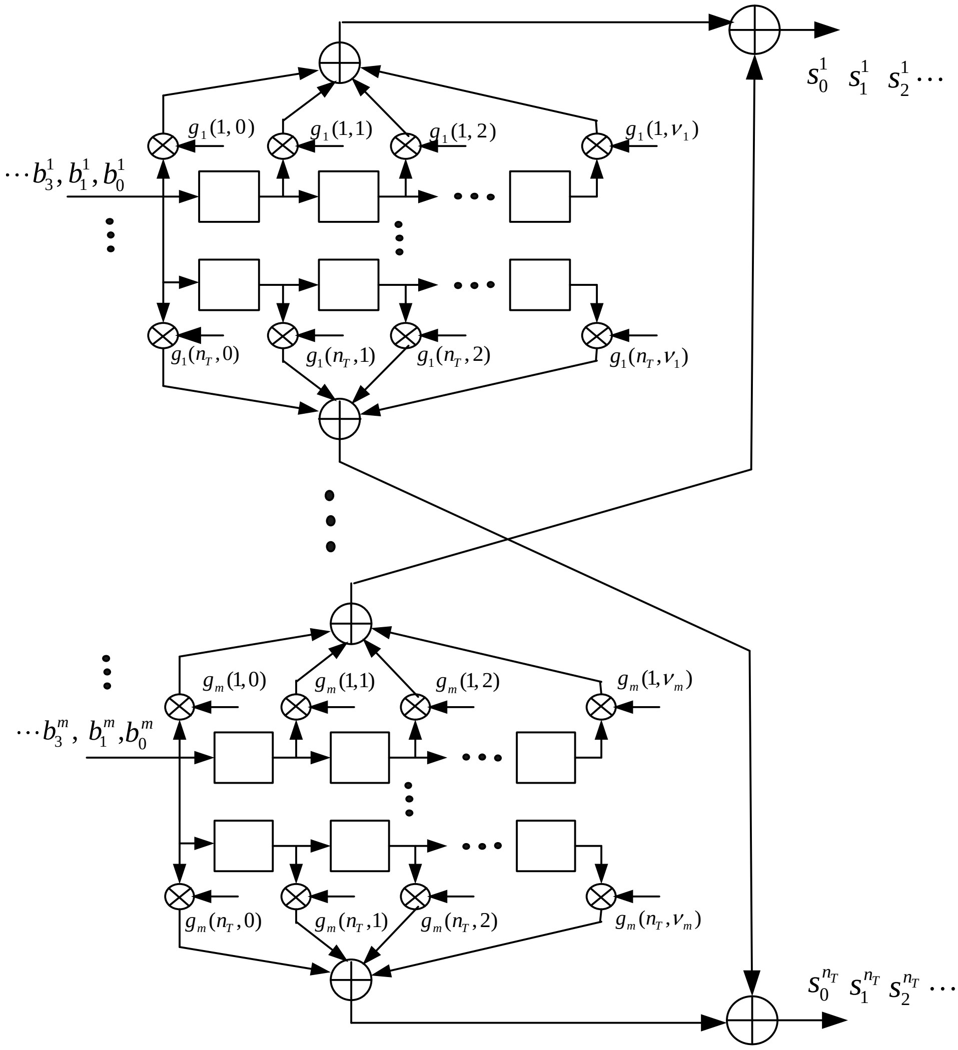

Figure 2.3: The block diagram of a STTC encoder.

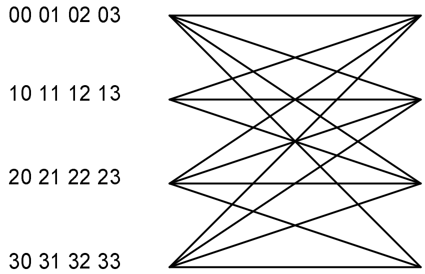

Figure 2.4: An example of the 4-state QPSK STTC.

and

$$\mathbf{G}_i = \begin{bmatrix} g_i(1,0) & g_i(1,1) & \cdots & g_i(1,\nu_i) \\ g_i(2,0) & g_i(2,1) & \cdots & g_i(2,\nu_i) \\ \vdots & \ddots & \ddots & \vdots \\ g_i(n_T,0) & g_i(n_T,1) & \cdots & g_i(n_T,\nu_i) \end{bmatrix}. \tag{2.51}$$

We use the 4-state QPSK STTC designed in [3] as an example to explain how the encoder works. The trellis diagram is shown in Fig. 2.4. The two corresponding generator matrices are

$$\mathbf{G}_1 = \begin{bmatrix} 0 & 2 \\ 2 & 0 \end{bmatrix} \text{ and } \mathbf{G}_2 = \begin{bmatrix} 0 & 1 \\ 1 & 0 \end{bmatrix}. \tag{2.52}$$

From Eq. (2.49), it can be seen that the code design is a process to find the generator matrices according to the criteria we discussed above. Many researches on the code design were done by exhaustively searching of the generator matrices [41], [42]. And the optimal codes for different fading environment, such as quasi-static fading and rapid fading, were obtained. The challenge on the searching is the complexity. For each set of generator matrices, all the possible code matrices have to be examined based on the code design criteria. Moreover, the length of the code block is very long and not specified in general. To solve this problem, some analytic tools [43] are proposed to assist the code searching. Recently, noticing that the number of the possible generator matrices increases rapidly with the number of transmit antennas and the number of states, Abdool-Rassool et.al proposed a faster searching method by employing the good properties of the generator matrices, such as symmetry [102].

Space-time Block Codes

The first STBC was introduced by Alamouti [53] for two-transmit-antenna systems, which was, at that time, referred to as the two-branch transmit diversity scheme. Tarokh later proposed a so-called STBC for the systems with an arbitrary number of transmit antennas, which preserves the orthogonality. Sometimes, these STBCs are denoted as OSTBCs to explicitly indicate that they are orthogonal. Although there are other types of STBC proposed, we only cover the orthogonal STBC in this thesis. Unless otherwise mentioned, all the STBCs referred here are the orthogonal STBCs.

Unlike the STTC, the STBC codeword matrix $\mathcal{G}_{n_T} \in \mathcal{C}^{n_T \times L}$, is obtained by using the linear combinations of the input symbols, $x_1, x_2, \ldots, x_n$, and their conjugates (sometimes 0 is used) as elements in a specific way such that the codeword matrix has the orthogonal structure. n_T is the number of transmit antennas and L is the code block length of a STBC. We call $\mathcal{G}_{n_T}$ a $n_T \times L$ STBC. It should be pointed out that, to be consistent with the denotation in previous sections, the codeword matrix here is the transpose of those in [53]. STBC can be categorized into two groups: one is the *generalized real orthogonal design* (real STBC), for which $x_1, x_2, \ldots, x_n$ are all real when the modulation with real signal constellations is used; the other is the *generalized complex orthogonal design* (complex STBC) for the complex input symbols (e.g., QPSK). Specifically, for a codeword matrix designed with a real input symbol sequence $x_1, x_2, \ldots, x_n$, the entries can be $0, \pm x_1, \pm x_2, \ldots, \pm x_n$. For the complex input symbols, the entries will be selected from $\{0, \pm x_1, \pm x_1^*, \pm x_1, \pm x_2^*, \ldots, \pm x_n, \pm x_n^*\}$, and/or their linear combinations. Generally, we have $n \leq L$, and the code rate of a STBC is $n/L \leq 1$.

Examples of real STBC's for $n_T = 2, 3, 4$ are

$$\mathcal{G}_2^r = \begin{bmatrix} x_1 & x_2 \\ -x_2 & x_1 \end{bmatrix}, \tag{2.53}$$

$$\mathcal{G}_3^r = \begin{bmatrix} x_1 & -x_2 & -x_3 & -x_4 \\ x_2 & x_1 & x_4 & -x_3 \\ x_3 & -x_4 & x_1 & x_2 \end{bmatrix}, \tag{2.54}$$

and

$$\mathcal{G}_4^r = \begin{bmatrix} x_1 & -x_2 & -x_3 & -x_4 \\ x_2 & x_1 & x_4 & -x_3 \\ x_3 & -x_4 & x_1 & x_2 \\ x_4 & x_3 & -x_2 & x_1 \end{bmatrix}. \tag{2.55}$$

where the superscript r indicates the real STBC and the subscript denotes the number of transmit antennas used for STBC. For the complex STBC, Alamouti's code is one example for the system with two transmit antennas:

$$\mathcal{G}_2^c = \begin{bmatrix} x_1 & -x_2^* \\ x_2 & -x_1^* \end{bmatrix}, \tag{2.56}$$

where the superscript c is used to denote that the STBC is complex. For $n_T = 3$, we have

$$\mathcal{G}_3^c = \begin{bmatrix} x_1 & -x_2 & -x_3 & -x_4 & x_1^* & -x_2^* & -x_3^* & -x_4^* \\ x_2 & x_1 & x_4 & -x_3 & x_2^* & x_1^* & x_4^* & -x_3^* \\ x_3 & -x_4 & x_1 & x_2 & x_3^* & -x_4^* & x_1^* & x_2^* \end{bmatrix} \tag{2.57}$$

and

$$\mathcal{H}_3^c = \begin{bmatrix} x_1 & -x_2^* & \frac{x_3^*}{\sqrt{2}} & \frac{x_3^*}{\sqrt{2}} \\ x_2 & x_1^* & \frac{x_3^*}{\sqrt{2}} & -\frac{x_3^*}{\sqrt{2}} \\ \frac{x_3}{\sqrt{2}} & \frac{x_3}{\sqrt{2}} & \frac{-x_1-x_1^*+x_2-x_2^*}{2} & \frac{x_1-x_1^*+x_2+x_2^*}{2} \end{bmatrix}. \tag{2.58}$$

Similarly, for $n_T = 4$, two STBCs can be constructed as

$$\mathcal{G}_4^c = \begin{bmatrix} x_1 & -x_2 & -x_3 & -x_4 & x_1^* & -x_2^* & -x_3^* & -x_4^* \\ x_2 & x_1 & x_4 & -x_3 & x_2^* & x_1^* & x_4^* & -x_3^* \\ x_3 & -x_4 & x_1 & x_2 & x_3^* & -x_4^* & x_1^* & x_2^* \\ x_4 & x_3 & -x_2 & x_1 & x_4^* & x_3^* & -x_2^* & x_1^* \end{bmatrix}, \tag{2.59}$$

and

$$\mathcal{H}_4^c = \begin{bmatrix} x_1 & -x_2^* & \frac{x_3^*}{\sqrt{2}} & \frac{x_3^*}{\sqrt{2}} \\ x_2 & x_1^* & \frac{x_3^*}{\sqrt{2}} & -\frac{x_3^*}{\sqrt{2}} \\ \frac{x_3}{\sqrt{2}} & \frac{x_3}{\sqrt{2}} & \frac{-x_1-x_1^*+x_2-x_2^*}{2} & \frac{x_1-x_1^*+x_2+x_2^*}{2} \\ \frac{x_3}{\sqrt{2}} & -\frac{x_3}{\sqrt{2}} & \frac{x_1-x_1^*-x_2+x_2^*}{2} & -\frac{x_1+x_1^*+x_2-x_2^*}{2} \end{bmatrix}. \tag{2.60}$$

Note that the examples of STBC given above have different code rate. The real STBC presented are all rate one. However, despite the complex 2×2 STBC with rate one, the complex STBC's for $n_T = 3, 4$ are with the rates of $1/2$ or $3/4$. It has been proved theoretically that the rate one real STBC can be constructed for any number of transmit antennas while the square ($n_T = L$) rate one real STBC only exists for $n_T = 2, 4, 8$. However, rate one complex STBC only exists for $n_T = 2$.

According to the performance analysis of previous sections, the orthogonal structure of STBC ensures that it has full diversity when the channel is static during the code block, for $\mathcal{G}_{n_T}\mathcal{G}_{n_T}^T = \mathcal{D}$, where $\mathcal{D}$ is a diagonal matrix. Another attractive property of STBC is that the ML decoding of it at the receiver can be done linearly. For example, assume that $\mathcal{G}_2^c$ is transmitted and there is one receive antenna, the received signal is

$$\mathbf{Y} = \begin{bmatrix} y_1 & y_2 \end{bmatrix} = \begin{bmatrix} h_1 & h_2 \end{bmatrix} \begin{bmatrix} x_1 & -x_2^* \\ x_2 & x_1^* \end{bmatrix} + \begin{bmatrix} n_1 & n_2 \end{bmatrix}. \tag{2.61}$$

Defining $\tilde{\mathbf{y}} = \begin{bmatrix} y_1 \\ y_2^* \end{bmatrix}$, we have

$$\begin{aligned} \tilde{\mathbf{y}} &= \begin{bmatrix} h_1 & h2 \\ h_2^* & -h_1^* \end{bmatrix} \begin{bmatrix} x_1 \\ x_2^* \end{bmatrix} + \begin{bmatrix} n_1 \\ n_2^* \end{bmatrix} \\ &= \tilde{\mathbf{H}}\mathbf{x} + \tilde{\mathbf{n}}. \end{aligned} \tag{2.62}$$

It can be seen that $\tilde{\mathbf{H}}^H\tilde{\mathbf{H}} = (|h_1|^2 + |h_2|^2)\mathbf{I}$, thus the decision statistics is

$$\mathbf{y}' = \tilde{\mathbf{H}}^H\tilde{\mathbf{y}} = (|h_1|^2 + |h_2|^2)\mathbf{c} + \mathbf{n}'. \tag{2.63}$$

The linear processing in Eq. (2.63) demonstrates that the two symbol x_1 and x_2 can be decoded separately, i.e.,

$$\hat{x}_1 = \arg\min_{x_1} |y'_1 - x_1|^2, \tag{2.64}$$

$$\hat{x}_2 = \arg\min_{x_2} |y'_2 - x_2^*|^2. \tag{2.65}$$

This will reduce the decoding complexity to be a linear function, instead of an exponential function, of the constellation size as for general ML decoding. Specifically, for QPSK modulation, the linear processing reduces the number of calculations of decoding metrics from 4^2 to 4×2.

2.3 BLAST Systems

2.3.1 Overview of BLAST Architectures

Unlike STTC and STBC, which aim at improving the diversity, BLAST is targeted at the high data rate. The simplest BLAST architecture is uncoded VBLAST. For a system with n_T transmit antennas, the information symbol sequence is split into n_T streams that are transmitted simultaneously from all the antennas [7]. Its block diagram is shown in Fig. 2.5. The VBLAST with independently coded layers is also called HLST [22]. The name is further used for the more general cases that, e.g.,

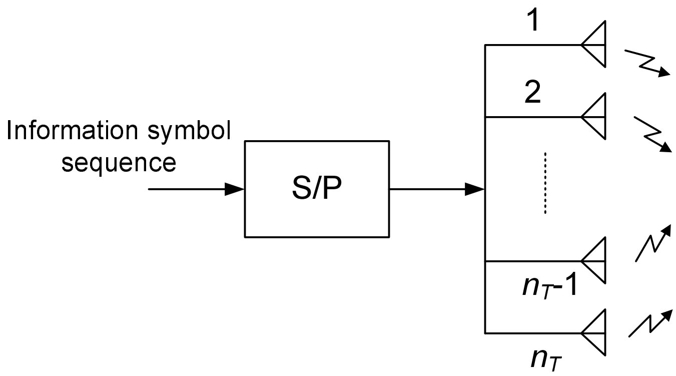

Figure 2.5: The block diagram of an uncoded VBLAST.

the information symbol sequence is encoded before divided into several streams as shown in Fig. 2.6 [46]. Denoting the tth symbol in the ith symbol stream after encoding and splitting as s_t^i, the transmitted signal matrix is

$$\mathbf{S} = \begin{bmatrix} s_1^1 & s_2^1 & \cdots & s_L^1 \\ s_1^2 & s_2^2 & \cdots & s_L^2 \\ \vdots & \vdots & \ddots & \vdots \\ s_1^{n_T} & s_2^{n_T} & \cdots & s_L^{n_T} \end{bmatrix}, \tag{2.66}$$

where L is code block length. Instead of arranging the coded streams horizontally, DLST puts the streams along parallel diagonals of the signal matrix, which can be expressed as, for example, when $n_T = 3$,

$$\mathbf{S} = \begin{bmatrix} s_1^1 & s_1^2 & s_1^3 & s_4^1 & s_4^2 & s_4^3 & \cdots \\ 0 & s_2^1 & s_2^2 & s_2^3 & s_5^1 & s_5^2 & \cdots \\ 0 & 0 & s_3^1 & s_3^2 & s_3^3 & s_6^1 & \cdots \end{bmatrix}. \tag{2.67}$$

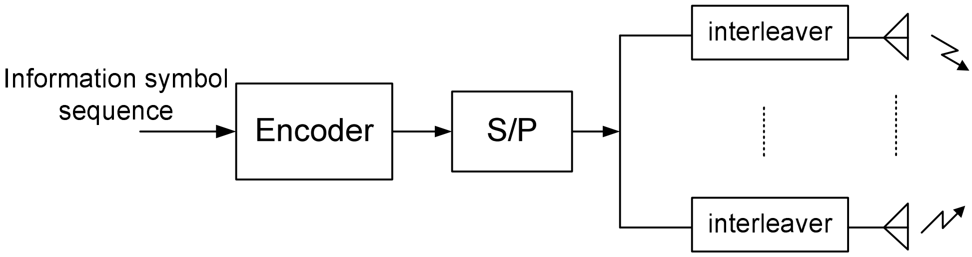

Figure 2.6: The block diagram of an example of the coded VBLAST.

A more recent scheme, threaded layered space-time (TLST) code, maps the streams in cyclicly shifting way. An example codeword matrix is

$$\mathbf{S} = \begin{bmatrix} s_1^1 & s_2^3 & s_3^2 & s_4^1 & \cdots \\ s_1^2 & s_2^1 & s_2^3 & s_4^2 & \cdots \\ s_1^3 & s_2^2 & s_3^1 & s_4^3 & \cdots \end{bmatrix}, \tag{2.68}$$

which can also be seen as a modified DLST with the nonzero elements on the left corner of the signal matrix. Although there are different transmission schemes, the detection methods at the receiver are suitable for all these schemes but with different performances and complexities.

2.3.2 BLAST Receivers

Treating a BLAST system as a multiuser system with single transmit antenna for each user, multiuser detection methods can be used at the BLAST receiver. The symbols on one transmitted antenna are considered as desired and the symbols from other antennas are treated as interferer. Two typical linear methods are usually used for the BLAST systems: one combines ZF with SIC algorithm with optimal ordering (ZF-BLAST), the other combines an MMSE approach with SIC (MMSE-BLAST). In the following part, we will investigate these two methods in detail. For simplicity, the uncoded VBLAST is used for illustration.

ZF-BLAST Receiver

ZF-BLAST was proposed in [7], which is an optimally ordered ZF IS together with SIC. Recall that the received signal at time t is

$$\mathbf{y}_t = \mathbf{H}_t \mathbf{s}_t + \mathbf{n}_t. \tag{2.69}$$

ZF IS for symbol s_t^i of layer i is performed by linearly weighting $\mathbf{y}_t$ to suppress the interference from layers higher than i, i.e.,

$$\mathbf{w}_t^{iH} \mathbf{H}_t(j) = \begin{cases} a_i, & i = j \\ 0, & i < j \end{cases} , \tag{2.70}$$

where a_i is a constant dependent on the norm of $\mathbf{w}_i$.

If no ordering is performed, ZF-BLAST receiver is reduced to the QRD receiver [22], where QRD of the channel matrix, $\mathbf{H}_t = \mathbf{Q}_t \mathbf{F}_t$, is used to do the ZF IS. $\mathbf{Q}_t$ has orthonormal columns and $\mathbf{F}_t$ is an upper triangular matrix. Therefore, the ith column vector of $\mathbf{Q}_t$, $\mathbf{Q}_t(i) = \mathbf{w}_t^i$. ZF IS of all the layers can be done by one step: multiplying $\mathbf{y}_t$ by $\mathbf{Q}_t^H$. Then we have

$$\mathbf{r}_t = \mathbf{Q}^H \mathbf{y}_t = \mathbf{F}_t \mathbf{s}_t + \mathbf{n}'_t, \tag{2.71}$$

where $\mathbf{n}'_t = \mathbf{Q}_t^H \mathbf{n}_t$, which is still a vector of i.i.d. Gaussian variables. Specifically, $\mathbf{F}_t$ can be expressed as

$$\mathbf{F}_t = \begin{bmatrix} F_{1,1}^t & F_{1,2}^t & \cdots & F_{1,n_T}^t \\ & F_{2,2}^t & \cdots & F_{2,n_T}^t \\ & \mathbf{0} & \ddots & \vdots \\ & & & F_{n_T,n_T}^t \end{bmatrix}. \tag{2.72}$$

With $\mathbf{F}_t$ being upper triangular, the ith element of $\mathbf{r}_t$, r_t^i is immune from the interference from the layers higher than i. Therefore, in the first stage, detection of $s_t^{n_T}$ is done by using $r_t^{n_T}$ as the decision statistics. Then $s_t^{n_T}$ is fed back to cancel out its contribution to $\mathbf{r}_t$ so that $s_t^{n_T-1}$ can be detected at second stage. This operation will repeat until all the symbols are detected. The successive multi-stage detection is expressed as

$$\hat{s}_t^i = \arg\min_{s_t^i} \left| \frac{r_t^i - \sum_{k=1}^{i-1} F_{i,k}^t s_t^k}{F_{i,i}^t} \right|^2, \tag{2.73}$$

where $\hat{s}_t^i$ indicates the estimation of s_t^i.

It can be seen that the system performance depends on the diagonal elements of $\mathbf{F}_t$. That means, the order of successive detection of the layers, i.e., the order of the columns of the channel matrix $\mathbf{H}_t$, affects the BER performance. Golden et.al addressed this problem in [7]. Let the ordered set $(k_1, k_2, \ldots, k_{n_T})$ be a permutation of $(1, 2, \ldots, n_T)$. Generally, the weighting vector $\mathbf{w}_t^{k_i}$ is orthogonal to the subspace spanned by the k_{i+1} to k_{n_T} columns of $\mathbf{H}_t$. It is not difficult to show that when $\|\mathbf{w}_t^{k_i}\|^2$ is constrained to 1, $\mathbf{w}_t^{k_i}$ is unique and its hermitian is just the k_ith row of

$\mathbf{H}_t^{k_i\pm}$, where $\mathbf{H}_t^{k_i-}$ denotes the matrix obtained by removing the columns from k_1 to k_i and $(\cdot)^+$ denotes generalized inverse of $(\cdot)$. Furthermore, the error performance of layer k_i depends on $\rho_{k_i} = E_s/N_0\|\mathbf{w}_t^{k_i}\|^2$. Therefore, different ordering leads to different ρ_{k_i} and $\|\mathbf{w}_t^i\|^2$ is desired to be as small as possible. Consequently, the aim of ordering is focused on maximizing ρ_{k_i}'s over all possible detection orderings. It has been proved that simply choosing the maximum ρ_{k_i} at each stage in the successive detection process leads to the global optimal ordering.

The resultant detection algorithm, referred to as Golden algorithm or ZF-VBLAST, is as follows:

Set $\mathbf{H}_{t(1)} = \mathbf{H}_t$, $\mathbf{y}_1 = \mathbf{y}$

For $i = 1, 2, \ldots, n_T$

$\mathbf{G}_t^i = \mathbf{H}_{t(i)}^+$

$k_i = \arg\min_j \|\mathbf{G}_t^i(j)\|^2$

$(\mathbf{w}_t^{k_i})^H = \mathbf{G}_t^i(k_i)$

$r_{k_i} = (\mathbf{w}_t^{k_i})^H \mathbf{y}_i$

$\hat{s}_{k_i} = \text{quantized} \quad r_{k_i}$

$\mathbf{y}_{i+1} = \mathbf{y}_i - \mathbf{H}_{t(i)}(k_i)\hat{s}_{k_i}$

$\mathbf{H}_{t(i+1)} = \mathbf{H}_{t(i)}^{k_i-}$

End

where $\mathbf{G}_t^i(j)$ and $\mathbf{H}_t(k_i)$ are the jth and the k_ith column of $\mathbf{G}_t^i$ and $\mathbf{H}_t$ respectively. It is easy to see that when the horizontal coding is applied, the detection of each layer will be performed in one code block other than in one symbol interval. Then the detected symbols are decoded and encoded again to cancel out the interference they bring into higher layers. Similarly, the detection and decoding of DLST is done layer by layer, though the layer is diagonal. It is generally assumed that the code block is lasting for just a single diagonal. Note that the first layer (diagonal) is free of interference, which can be decoded directly. Likewise, after subtracting the interference from the first layer, the symbols in layer two are decoded. The detection and decoding are the same for other layers.

MMSE-BLAST Receiver

MMSE-BLAST differs from ZF-BLAST in that IS method of MMSE instead of ZF is used. However, they both employ SIC. The flowing table shows the MMSE-BLAST algorithm with ordering.

Set $\mathbf{H}_{t(1)} = \mathbf{H}_t$, $\mathbf{y}_1 = \mathbf{y}$

For $i = 1, 2, \ldots, n_T$

$\mathbf{G}_t^i = [\mathbf{H}_{t(i)}^H \mathbf{H}_{t(i)} + \sigma^2 \mathbf{I}_{n_T}]^{-1} \mathbf{H}_{t(i)}^H$

$k_i = \arg\min_j \|\mathbf{G}_t^i(j)\|^2$

$(\mathbf{w}_t^{k_i})^H = \mathbf{G}_t^i(k_i)$

$r_{k_i} = (\mathbf{w}_t^{k_i})^H \mathbf{y}_i$

$\hat{s}_{k_i} = \text{quantized} \quad r_{k_i}$

$\mathbf{y}_{i+1} = \mathbf{y}_i - \mathbf{H}_t(k_i)\hat{s}_{k_i}$

$\mathbf{H}_{t(i+1)} = \mathbf{H}_{t(i)}^{k_i -}$

End

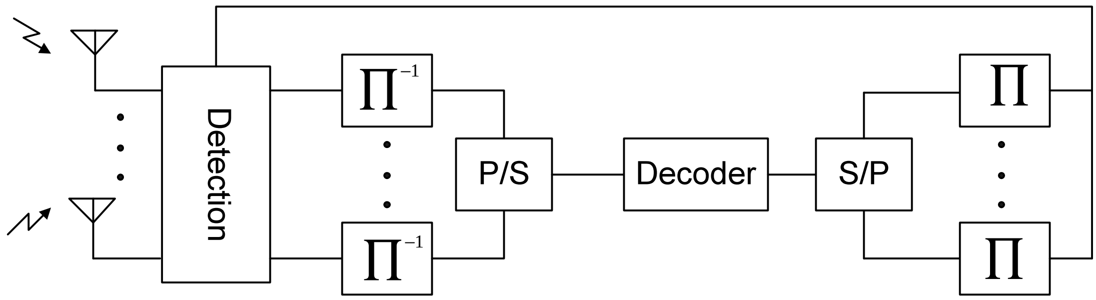

Figure 2.7: One example of the iterative BLAST receiver.

Other Receivers

Some other receivers are also proposed. Many of them are motivated from the fact that the ZF-BLAST and MMSE-BLAST scheme have high computational complexity since calculation of matrix inverse are involved. They are modified algorithms with lower complexity, but are still based on the ZF or MMSE criteria [92], [93].

With the iterative processing principle being extended to the joint detection and decoding, the iterative BLAST receivers were also introduced [94], [95], [96]. However, this kind of receiver can only be applied to the coded BLAST schemes. At each iteration, the decoder soft outputs are used to update the priori probabilities of the transmitted symbols. These updated probabilities are then used to calculate the symbol estimates in the detector. Since the the iterative detection and decoding is out of the scope of the thesis, we will not show the details here. One example of the iterative receiver is shown in Fig. 2.7.

2.3.3 Tradeoff Between Performance and Transmission Rate

From above discussion, we can see that the BLAST systems provide higher spectral efficiency than the STTC and STBC. For example, for the uncoded VBLAST, the spectral efficiency is $n_T m$, where m is constellation size. Since DLST has several zero elements at the left-lower corner as well as the right-upper corner of the codeword matrix, a part of the spectral efficiency will be lost. The spectral efficiency loss depends on the code block length, the number of the transmit antennas, and the diagonal arrangement. Generally, the loss will be high when the code block length is small. For the HLST with code rate r_{code}, the total spectral efficiency will be $r_{code} n_T m$. In general, STTC and STBC have the spectral efficiency less than or equal to m.

It is obvious that with enhanced spectral efficiency, the performance will degrade. We will use HLST as an example to show the tradeoff between spectral efficiency and performance. In a HLST system with QRD receiver, the codeword matrix is decoded row by row, from bottom to top. Let the coding block length is L. $\mathbf{s}_i = [s_1^i, s_2^i, \ldots, s_L^i]$ is the ith row of the codeword matrix. Assuming that the interference from lower layers is canceled out perfectly, we have the conditional PEP for layer i as

$$P(\mathbf{s}_i, \hat{\mathbf{s}}_i | \mathbf{H}_t, 1 \leq t \leq L) \leq \exp\left[-\frac{E_s}{4N_0}\sum_{t=1}^{L}|F_{i,i}^t|^2|c_t^i - \hat{c}_t^i|^2\right]. \tag{2.74}$$

For $\mathbf{H}_t$ is a matrix with i.i.d Gaussian random variables, it has been proved that $|F_{i,i}^t|^2$ is $\mathcal{X}_{2(n_R-i+1)}$ distributed with mean $n_R - i + 1$. When channel is quasi-static,

$F_{i,i}^t = F_{i,i}$ for all t. Then the PEP is upper bounded as

$$P(\mathbf{c}_i, \hat{\mathbf{c}}_i) \leq \left(1 + \frac{E_s}{4N_0}|\mathbf{c}_i - \hat{\mathbf{c}}_i|^2\right)^{-(n_R-i+1)}. \tag{2.75}$$

Similarly, when the channels are fading fast, $|F_{i,i}^t|^2$ will be independent for different t. We have

$$P(\mathbf{c}_i, \hat{\mathbf{c}}_i) \leq \prod_{t\in\Omega}\left(1 + |c_t^i - \hat{c}_t^i|^2\frac{E_s}{4N_0}\right)^{-(n_R-i+1)}, \tag{2.76}$$

where $\Omega = \{t : c_t^i \neq \hat{c}_t^i\}$.

It can be seen that the PEP of HLST has the similar form as that of STTC and STBC. Still using diversity gain and coding gain to measure, we can see that the diversity gain for the ith layer is $n_R - i + 1$, when channel is fading slowly; and $|\Omega|(n_R - i + 1)$, where $|\Omega|$ indicates the cardinality of Ω, when channel is fading fast. This shows that different layers have different diversity gains. Nevertheless, the performance of the whole BLAST system is dominated by the first detected and decoded layer, since SIC is applied. Thus the diversity gain of the system is the diversity gain of the lowest layer, $n_R - n_T + 1$ [22], [103]. On the other hand, the diversity of a STTC can be at most $n_R n_T$, which is much higher than that of a HLST.

Chapter 3

Space-time Code Design for Multiuser Composite Fading Systems

3.1 Introduction

STC is one of the approaches that take advantage of diversity [3], [54]. It introduces temporal and spatial correlation into the signals transmitted from different antennas trying to fully exploit the space and time diversities. Tarokh derived STC design criteria for quasi-static flat fading channels as well as rapid fading channels [3]. Both of the criteria are based on two parameters: diversity gain and coding gain. Handcrafted codes were obtained first, then the code design with improved performance was further discussed [41], [44].

Although the design of STC for single user systems has been extensively studied, code design for narrowband multiuser systems received less attention. Based on the existing single-user STTCs, [13] proposed an interference-resistant modulation, by rotating the STTCs single-user systems before they are transmitted. However, this study only considers a single type of fading, assuming that all the users have quasi-static fading channels. This is not true in many practical multiuser systems, where different users may operate in different fading environments, i.e., some users may undergo quasi-static fading while others may undergo rapid fading.

In this chapter, we analyze the error performance and derive code design criteria of STC for multiuser *composite fading* systems. Composite fading means that the users in the system experience two types of fading: quasi-static fading and rapid fading. It is assumed that different users may have different numbers of transmit antennas while the frame length of the transmitted signal from each user is the same. We find that the PEP depends on two parameters, the rank and the product of nonzero eigenvalues of a matrix $\mathbf{A}$. Code design criteria are then obtained, according to which optimal STCs for composite fading systems are obtained by exhaustive search.

3.2 System Model

There are K users of which K_1 ($K_1 < K$) users suffer quasi-static fading (the channel does not change within one frame) and $K - K_1$ users suffer rapid fading (the fading coefficients are independent over symbols). All the channel coefficients are assumed to be complex Gaussian with variance 0.5 per real dimension. User i has n_{Ti} transmit antennas and receiver has n_R antennas. The system block diagram

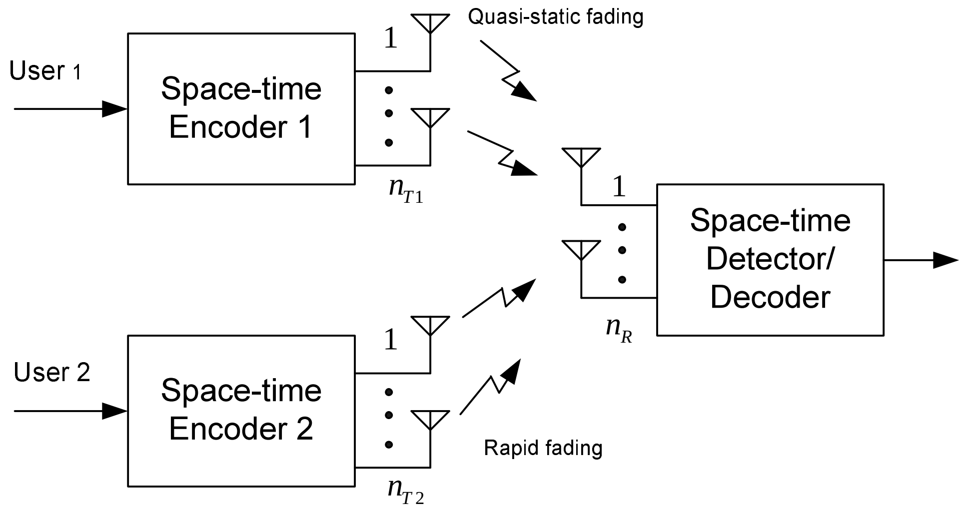

Figure 3.1: The block diagram of a two-user composite fading system.

for $K_1 = 1, K = 2$ is shown in Fig. 3.1. All the users transmit the codes with the same length L . The received signal matrix can be expressed as

$$\mathbf{Y} = \begin{bmatrix} \mathbf{y}_1 & \mathbf{y}_2 & \cdots & \mathbf{y}_L \end{bmatrix}, \tag{3.1}$$

where $\mathbf{y}_t$ is the received signal vector at time t given by

$$\mathbf{y}_t = \sqrt{E_s}\sum_{k=1}^{K_1} \mathbf{H}_k \mathbf{s}_t^k + \sqrt{E_s}\sum_{k=K_1+1}^{K} \mathbf{H}_{kt}\mathbf{s}_t^k + \mathrm{n}_t, \quad t = 1, \cdots, L. \tag{3.2}$$

E_s is the average signal power and is the same for all the users. The normalized transmitted codeword matrix of user k can be expressed as

$$\mathbf{S}_k = \begin{bmatrix} \mathbf{s}_1^k & \mathbf{s}_2^k & \cdots & \mathbf{s}_L^k \end{bmatrix}, \tag{3.3}$$

where $\mathbf{s}_t^k$ is the tth column of it. Since user k, when $K_1 < k \leq K$, has the rapid fading channel, it has statistically independent channel matrices $\mathbf{H}_{kt}$ at different time t. CSI is assumed to be known at the receiver. $\mathbf{n}_t$ is the noise vector at time t, in which each element is zero mean complex Gaussian random variable with variance $N_0/2$ per real dimension.

3.3 Pairwise Error Probability

To derive the code design criteria, we first analyze the pairwise error probability of composite fading systems. The system with two users is considered first. It will be seen that it is easy to extend the two-user case to the case with more users.

3.3.1 Pairwise Error Probability of Two-user Systems

There are two users in systems. User 1 has a quasi-static fading channel and user 2 has a rapid fading channel. The data model in Eq. (3.2) becomes

$$\mathbf{y}_t = \sqrt{E_s}\left(\mathbf{H}_1\mathbf{s}_t^1 + \mathbf{H}_{2t}\mathbf{s}_t^2\right) + \mathbf{n}_t, \quad t = 1, \cdots L \tag{3.4}$$

where $\mathbf{S}_1 \in \mathcal{C}_1$, is the $n_{T1} \times L$ codeword matrix transmitted from user 1 and where $\mathcal{C}_1$ is the set of all possible code matrices of user 1. $\mathbf{S}_2 \in \mathcal{C}_2$, is the $n_{T2} \times L$ codeword matrix transmitted from user 2, where $\mathcal{C}_2$ is the set of all possible code matrices of user 2.

Joint ML decoding and detection is performed at the receiver. The PEP of transmitting $(\mathbf{S}_1, \mathbf{S}_2)$ but deciding $(\hat{\mathbf{S}}_1, \hat{\mathbf{S}}_2)$ is, conditioned on the channel matrices,

$$P\{(\mathbf{S}_1, \mathbf{S}_2) \to (\hat{\mathbf{S}}_1, \hat{\mathbf{S}}_2) \mid \mathbf{H}_1, \mathbf{H}_{2t},\ t = 1, \cdots, L\} \leq \exp\left\{-\frac{E_s}{4N_0} \sum_{t=1}^{L} \|\mathbf{H}_1(\mathbf{s}_t^1 - \hat{\mathbf{s}}_t^1) + \mathbf{H}_{2t}(\mathbf{s}_t^2 - \hat{\mathbf{s}}_t^2)\|^2\right\}, \tag{3.5}$$

where $\mathbf{S}_1, \hat{\mathbf{S}}_1 \in \mathcal{C}_1$ and $\mathbf{S}_2, \hat{\mathbf{S}}_2 \in \mathcal{C}_2$. For the convenience, we denote

$$\Delta^2 = \sum_{t=1}^{L} \|\mathbf{H}_1(\mathbf{s}_t^1 - \hat{\mathbf{s}}_t^1) + \mathbf{H}_{2t}(\mathbf{s}_t^2 - \hat{\mathbf{s}}_t^2)\|^2. \tag{3.6}$$

Then the conditional PEP is upper-bounded by

$$P_2(e) = P\{(\mathbf{S}_1, \mathbf{S}_2) \to (\hat{\mathbf{S}}_1, \hat{\mathbf{S}}_2)\} \leq E\left[\exp\left(-\frac{E_s}{4N_0}\Delta^2\right)\right]. \tag{3.7}$$

It can be seen that Δ^2 is a quadrature form of a sequence of $n_R L$ Gaussian random variables. However, the unchanged channel of user 1 results in the correlation between the random variables. Denoting

$$\mathbf{x}_t = \mathbf{H}_1^*(\mathbf{s}_t^1 - \hat{\mathbf{s}}_t^1)^* + \mathbf{H}_{2t}^*(\mathbf{s}_t^2 - \hat{\mathbf{s}}_t^2)^*, \tag{3.8}$$

where $(\cdot)^*$ indicates the conjugate of $(\cdot)$, we have

$$E[\mathbf{x}_i \mathbf{x}_j^H] = \begin{cases} (\mathbf{s}_j^1 - \hat{\mathbf{s}}_j^1)^H (\mathbf{s}_i^1 - \hat{\mathbf{s}}_i^1) \mathbf{I}_{n_R} & i \neq j \\ (\|\mathbf{s}_i^1 - \hat{\mathbf{s}}_i^1\|^2 + \|\mathbf{s}_i^2 - \hat{\mathbf{s}}_i^2\|^2) \mathbf{I}_{n_R} & i = j \end{cases}. \tag{3.9}$$

With

$$\mathbf{X} = \begin{bmatrix} \mathbf{x}_1^T & \mathbf{x}_2^T & \cdots & \mathbf{x}_L^T \end{bmatrix}^T, \tag{3.10}$$

Δ^2 can be rewritten as

$$\Delta^2 = \mathbf{X}^H \mathbf{X}. \tag{3.11}$$

Define the covariance matrix

$$\mathbf{R}_{XX} = E(\mathbf{X}\mathbf{X}^H) = \begin{bmatrix} \mathbf{R}_{11} & \mathbf{R}_{12} & \cdots & \mathbf{R}_{1L} \\ \mathbf{R}_{21} & \mathbf{R}_{22} & \cdots & \mathbf{R}_{2L} \\ \vdots & \vdots & \ddots & \vdots \\ \mathbf{R}_{L1} & \mathbf{R}_{L2} & \cdots & \mathbf{R}_{LL} \end{bmatrix}, \tag{3.12}$$

where the $[i,j]$th submatrix, $\mathbf{R}_{ij} = E[\mathbf{x}_i \mathbf{x}_j^H]$. $\mathbf{R}_{XX}$ can be further expressed as

$$\mathbf{R}_{XX} = [(\mathbf{B} + \mathbf{D}] \otimes \mathbf{I}_N, \tag{3.13}$$

where $\otimes$ denotes the Kronecker product [104] and

$$\mathbf{B} = (\mathbf{S}_1 - \hat{\mathbf{S}}_1)^H (\mathbf{S}_1 - \hat{\mathbf{S}}_1), \tag{3.14}$$

$$\mathbf{D} = diag(\|\mathbf{s}_1^2 - \hat{\mathbf{s}}_1^2\|^2, \|\mathbf{s}_2^2 - \hat{\mathbf{s}}_2^2\|^2, \cdots, \|\mathbf{s}_L^2 - \hat{\mathbf{s}}_L^2\|^2). \tag{3.15}$$

It has been approved that [25]

$$E\left[\exp\left(-\frac{E_s}{4N_0}\Delta^2\right)\right] = \det{}^{-1}\left(\frac{E_s}{4N_0}\mathbf{R}_{XX} + \mathbf{I}\right). \tag{3.16}$$

Consequently, $P_2(e)$ is upper bounded as

$$\begin{aligned} P_2(e) &\leq \det{}^{-1}\left[\frac{E_s}{4N_0}(\mathbf{B}+\mathbf{D})\otimes \mathbf{I}_N + \mathbf{I}_{NL}\right] \\ &= \det{}^{-1}\left[\frac{E_s}{4N_0}(\mathbf{B}+\mathbf{D}+\mathbf{I}_L)\otimes \mathbf{I}_N\right]. \end{aligned} \tag{3.17}$$

.

Define $\mathbf{A}$ as

$$\mathbf{A} = \mathbf{B} + \mathbf{D}. \tag{3.18}$$

Letting r and $\lambda_1, \lambda_2, \cdots, \lambda_r$ be the rank and the nonzero eigenvalues of $\mathbf{A}$ respectively, we have

$$P_2(e) \leq (\frac{E_s}{4N_0})^{-rn_R}\prod_{i=1}^{r}(\frac{4N_0}{E_s}+\lambda_i)^{-n_R} \tag{3.19}$$

It can be seen that the pairwise error probability depends on the rank and nonzero eigenvalues of $\mathbf{A}$. In the next section, we will extend the above results to K-user systems.

3.3.2 Pairwise Error Probability of K-user Systems

Without loss of generality, we assume that users from 1 to K_1 have quasi-static fading channels and users from $K_1 + 1$ to K have rapid fading channels. The channels of different users are statistically independent. Rewriting the data model in Eq. (3.2) in joint codeword matrix format, we can treat the K-user system, which has two types of fading, as a two-user system. The K_1 users having quasi-static fading can be seen as a virtual user experiencing quasi-static fading, with

$\sum_{k=1}^{K_1} n_{Tk}$ transmit antennas, joint codeword matrix

$$\mathbf{C}_1 = \begin{bmatrix} \mathbf{S}_1^T & \cdots & \mathbf{S}_{K_1}^T \end{bmatrix}^T, \tag{3.20}$$

and joint channel matrix

$$\mathbf{H}_1 = \begin{bmatrix} \mathbf{H}_1 & \cdots & \mathbf{H}_{K_1} \end{bmatrix}. \tag{3.21}$$

Under the assumption that the channels among the different users are independent, $\mathbf{H}_1$ has independent Gaussian random elements. The other $K - K_1$ users having rapid fading can be seen as a virtual user experiencing rapid fading, with $\sum_{k=K_1+1}^{K} n_{Tk}$ transmit antennas, joint codeword matrix

$$\mathbf{C}_2 = \begin{bmatrix} \mathbf{S}_{K_1+1}^T & \cdots & \mathbf{S}_K^T \end{bmatrix}^T, \tag{3.22}$$

and joint channel matrix at time t as

$$\mathbf{H}_{2t} = \begin{bmatrix} \mathbf{H}_{K_1+1,t} & \cdots & \mathbf{H}_{Kt} \end{bmatrix}, \quad t = 1, \ldots, L. \tag{3.23}$$

Similarly, the elements in $\mathbf{H}_{2t}$ are independent, and $\mathbf{H}_{2i}$ is independent of $\mathbf{H}_{2j}$, $\forall i \neq j$. Redefine

$$\mathbf{B} = \left(\mathbf{C}_1 - \hat{\mathbf{C}}_1\right)^H \left(\mathbf{C}_1 - \hat{\mathbf{C}}_1\right) = \sum_{k=1}^{K_1} \mathbf{B}_k = \sum_{k=1}^{K_1} \left(\mathbf{S}_k - \hat{\mathbf{S}}_k\right)^H \left(\mathbf{S}_k - \hat{\mathbf{S}}_k\right), \tag{3.24}$$

,

$$\begin{aligned}\mathbf{D} &= diag\left(\|\mathbf{C}_2^1 - \hat{\mathbf{C}}_2^1\|^2, \|\mathbf{C}_2^2 - \hat{\mathbf{C}}_2^2\|^2, \ldots, \|\mathbf{C}_2^L - \hat{\mathbf{C}}_2^L\|^2\right) \\ &= \sum_{k=K_1+1}^{K} \mathbf{D}_k = \sum_{k=K_1+1}^{K} diag\left(\left\|\mathbf{s}_1^k - \hat{\mathbf{s}}_1^k\right\|^2, \left\|\mathbf{s}_2^k - \hat{\mathbf{s}}_2^k\right\|^2, \ldots, \left\|\mathbf{s}_L^k - \hat{\mathbf{s}}_L^k\right\|^2\right),\end{aligned} \tag{3.25}$$

and $\mathbf{A} = \mathbf{B} + \mathbf{D}$, where $\mathbf{C}_2^t$ represents the tth column of $\mathbf{C}$. Eq. (3.19) results in the following theorem:

Theorem 3.1. *For a K-user system with K_1 users experiencing quasi-static fading and $K - K_1$ users experiencing rapid fading, the pairwise error probability of transmitting $(\mathbf{C}_1, \mathbf{C}_2)$ but deciding $(\hat{\mathbf{C}}_1, \hat{\mathbf{C}}_2)$ is upper bounded as, when SNR is high,*

$$P_2(e) \leq \left(\frac{E_s}{4N_0}\right)^{-rn_R} \prod_{i=1}^{r} \lambda_i^{-n_R}. \tag{3.26}$$

where r and $\lambda_1, \lambda_2, \ldots, \lambda_r$ are rank and nonzero eigenvalues of $\mathbf{A}$ respectively.

3.3.3 The Special Cases

Although the average PEP obtained in Eq. (3.26) is for K-user composite fading systems, it is such a general result that it is applicable for special situations such as multiuser systems with single type of fading and single user systems. When the system has only one type of fading, e.g., quasi-static fading, $K_1 = K$ and $\mathbf{D} = \mathbf{0}$. The PEP is only dependent on the rank and eigenvalues of matrix $\mathbf{B}$. If we assume $K = 1$ in addition, i.e., a single user system with quasi-static fading, $\mathbf{B}$ is reduced to $(\mathbf{S} - \hat{\mathbf{S}})^H(\mathbf{S} - \hat{\mathbf{S}})$. Obviously, we have the same PEP as that in [3]. Similarly, Eq. (3.26) can be used to calculate the PEP for rapid fading multiuser systems and rapid fading ST single user system. It is easy to verify that Eq. (3.26) results in the consistent results as those in [3], when the multiuser composite fading system is reduced to single user system with either kind of fading.

3.4 Code Design Criteria for Multiuser Composite Fading Systems

From Theorem 3.1, it can be seen that the large rank and product of nonzero eigenvalues of $\mathbf{A}$ are desired. Recall that in multiuser composite fading systems, two types of fading exist. However, users are usually not aware of what kind of fading channel they have. Therefore in the code design, $\mathbf{A}$ should be examined for all possible distinct joint code matrices and K_1. This will be too complicated if K is large. Fortunately, the following analysis simplified the code design dramatically.

Some definitions are given first for further discussion. According to Eq. (3.26), the diversity gain η_d and the coding gain η_c are defined respectively as

$$\eta_d = r_{min} n_T \tag{3.27}$$

where r_{min} is the minimum of r's taken over all the distinct pairs of joint code matrices, and

$$\eta_c = \arg\min_{\mathbf{A}\in\Omega} \prod_{i=1}^{\eta_d} \lambda_i^{1/\eta_d}, \tag{3.28}$$

where Ω is the set of all the $\mathbf{A}$'s with rank r_{min}. Based on Eq. (3.24) and Eq. (3.25),

$\mathbf{B}_k$ and $\mathbf{D}_k$ are given for any $1 \le k \le K$ as

$$\mathbf{B}_k = \left(\mathbf{S}_k - \hat{\mathbf{S}}_k\right)^H \left(\mathbf{S}_k - \hat{\mathbf{S}}_k\right) \quad k = 1, 2, \ldots, K, \tag{3.29}$$

and

$$\mathbf{D}_k = diag\left(\left\|\mathbf{s}_1^k - \hat{\mathbf{s}}_1^k\right\|^2, \left\|\mathbf{s}_2^k - \hat{\mathbf{s}}_2^k\right\|^2, \ldots, \left\|\mathbf{s}_L^k - \hat{\mathbf{s}}_L^k\right\|^2\right) \quad k = 1, 2, \ldots, K. \tag{3.30}$$

Note that $\mathbf{B}_k$ is the codeword distance matrix of user k and $\mathbf{D}_k$ has the squares of norms of codeword difference matrix's nonzero column vectors at its diagonal. $\mathbf{D}_k$ is therefore the counterpart of $\mathbf{B}_k$ in the sense that its rank and nonzero eigenvalues decide the diversity gain and coding gain of rapid fading channels. We then refer to $\mathbf{D}_k$ as the *codeword distance matrix for rapid fading* of user k for further reference. Since all the users are independent, there are some pairs of distinct joint code matrices that differ only at one user's codeword matrix. This indicates that $\mathbf{B_k}$ in Eq. (3.24) or $\mathbf{D}_k$ in Eq. (3.25) is equal to $\mathbf{A}$ in certain cases. Assume that $\{\gamma_i^k\}$ and $\{\xi_i^k\}$ are increasingly ordered eigenvalues of $\mathbf{B}_k$ and $\mathbf{D}_k$ respectively. Since $\mathbf{B}_k$ and $\mathbf{D}_k$ are both positive semidefinite, we have $(\eta_c)^{r_{min}} \ge \min_{k\in\Omega}\{\prod_{i=1}^{r_{min}} \gamma_i^k, \prod_{i=1}^{r_{min}} \xi_i^k\}$ and $\eta_d \ge \min\{rank(\mathbf{D}_k), rank(\mathbf{B}_k)\}$. Additionally with the observation that the minimum of $rank(\mathbf{D}_k)$ over all pairs of distinct code matrices is greater or equal to the minimum of $rank(\mathbf{B}_k)$ over these code pairs, we induce that assuring $\mathbf{B}_k$ having maximum available rank over all pairs of distinct $\mathbf{S}_k$ and $\hat{\mathbf{S}}_k$ is sufficient and necessary condition for the STC to achieve the maximum diversity gain. With $n_{Ti} \le L$ in general, r_{min} is less than or equal to $m = \min_i n_{Ti}$. The maximum diversity gain we can get is mn_R.

When all the users do not have the same number of transmit antennas, the code sets for different users may be different. Although the diversity gain and coding gain are decided by the code sets for the users with minimum number of antennas, the pairwise error events with higher diversity gains also affect the error performance. We then have the following code design criteria:

1. Maximize the minimum rank r_{min}^k of codeword distance matrices for quasi-static fading$\mathbf{B}_k$ taken over all pairs of distinct code matrices of each user's code set.

2. The minimum product of nonzero eigenvalues of the codeword distance matrix for quasi-static fading $\mathbf{B}_k$ and the codeword distance matrix for rapid fading $\mathbf{D}_k$ of rank r_{min}^k, taken over all pairs of distinct code matrices of each user's code set has to be maximized.

These code design criteria also imply that the code sets for the users with the same number of transmit antennas should be the same. In specific, if $n_{Ti} = n_T, i = 1, 2, \dots, K$, only one code set is needed for all the users. Otherwise, the decoding and detection at the receiver will be unnecessarily complicated. Since $\mathbf{B}_k$ for all k are the same, we drop the subscript k and use $\mathcal{B}$ and $\mathcal{D}$ instead. Then two code design criteria for multiuser composite fading systems with the same number of transmit antennas for each user are obtained :

1. The minimum rank r_{min} of $\mathcal{B}$ taken over all the pairs of distinct code matrices has to be maximized.

2. The minimum product of nonzero eigenvalues of all possible $\mathcal{B}$ and $\mathcal{D}$ of rank r_{min} has to be maximized.

3.5 The Optimal STTCs for Composite Fading Systems

Based on the STTC encoder model introduced in Chapter 2, we give two examples of STTC codes found by exhaustively searching over all the possible generator matrices with certain parameters. Specifically, we find optimal 4-state and 8-state QPSK STTC codes for two-user composite fading systems, where each user has two transmit antennas.

Optimal QPSK 4-state STTC

$$\mathbf{G}_1^4 = \begin{bmatrix} 3 & 2 \\ 1 & 1 \end{bmatrix}, \quad \mathbf{G}_2^4 = \begin{bmatrix} 2 & 0 \\ 2 & 2 \end{bmatrix}. \tag{3.31}$$

Note that this pair of generator matrix is also for the optimal code presented in [46] for single user rapid fading systems. The corresponding trellis diagram is shown in Fig. 3.2.

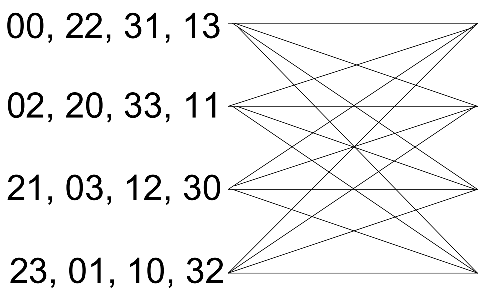

Figure 3.2: Trellis diagram for the new optimal 4-state QPSK STTC.

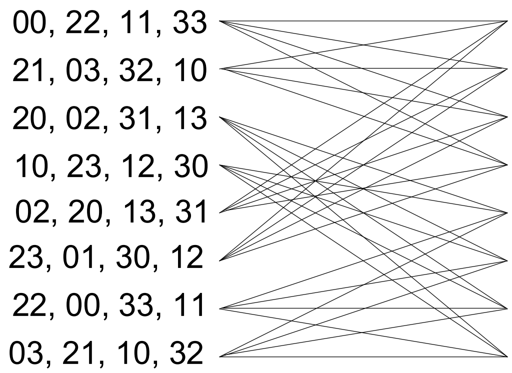

Figure 3.3: Trellis diagram for the new optimal 8-state QPSK STTC.

Optimal QPSK 8-state STTC

$$\mathbf{G}_1^8 = \begin{bmatrix} 1 & 2 & 0 \\ 1 & 0 & 2 \end{bmatrix}, \quad \mathbf{G}_2^8 = \begin{bmatrix} 2 & 2 \\ 2 & 1 \end{bmatrix}, \tag{3.32}$$

whose trellis is shown in Fig. 3.3.

3.6 Simulation results

Simulations are done for the scenario that one user has quasi-static fading channels and the other has rapid fading channels. To evaluate how good the newly designed STTC are, we compare them to several well known space time codes. The codes we use for comparison are the Alamouti code from [53], the 4-state and 8-state QPSK STTC from [3] (referred to as TSC), the optimal 8-state QPSK STTC for quasi-static fading, and the optimal 8-state QPSK STTC for rapid fading [45]. The trellis diagrams for the two TSCs are shown in Fig. 3.4 and Fig. 3.5 respectively.

Fig. 3.6 and Fig. 3.7 compare the performances of several different space-time

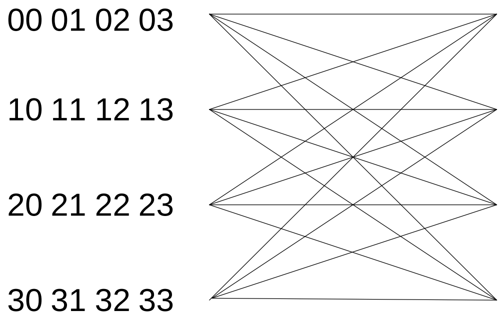

Figure 3.4: Trellis diagram for the 4-state TSC.

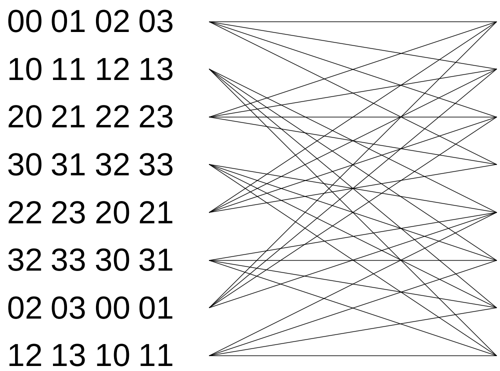

Figure 3.5: Trellis diagram for the 8-state TSC.

codes. All the simulations are done in a two-user system. There is one antenna at the receiver. However, both users have two transmit antennas each. The channels for one user are quasi-static fading and the channels for the other user are rapid fading. The channel gains are complex Gaussian variables with zero mean and variance 0.5 per real dimension. Noises in the channel are white Gaussian with zero mean and variance $\frac{N_0}{2}$ per real dimension. The QPSK modulation is applied. The curves give the average bit error rate of two users versus SNR $= E_a/N_0$, in which E_a is the average power of signals received per receive antenna per user. The STTC codes used have the terminating state zero. It can be seen from Fig. 3.6 that

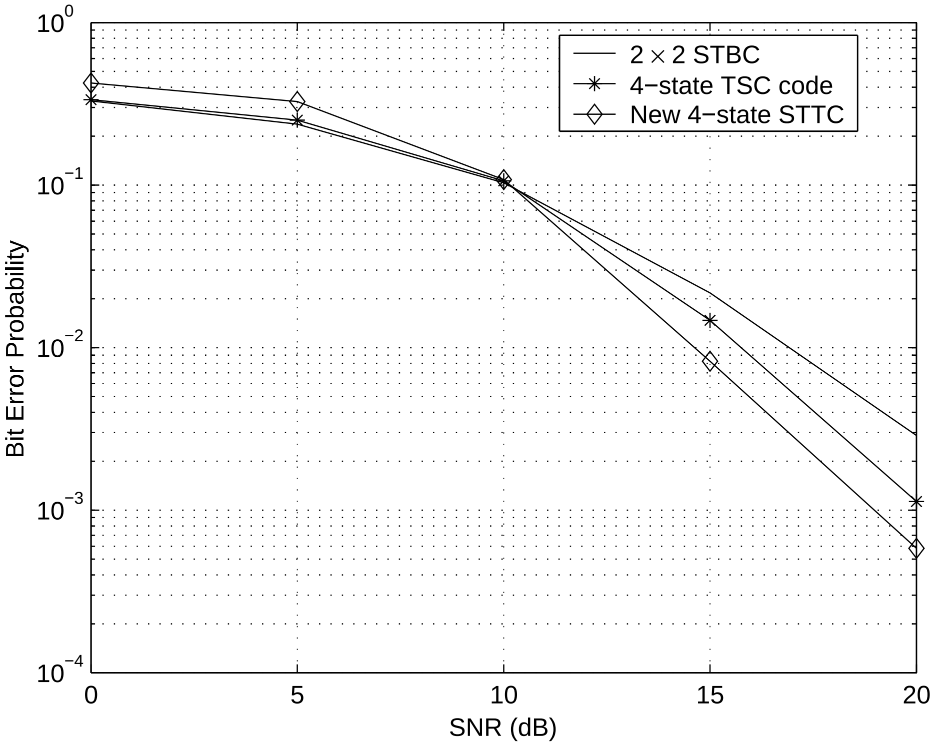

Figure 3.6: Bit error probability for various ST codes, two users with two transmit antennas each, one receive antenna, QPSK modulation, and composite fading.

the new 4-state STTC is about 1 dB better than the 4-state TSC, and 3 dB better than the 2×2 STBC at a BER of 10^{-3}. Note that there is a crossing behavior of BER curves at about 10 dB SNR in Fig. 3.6. This is because that the PEP and code design criteria are derived for high SNRs. Thus the codes obtained based on them might not perform the same supremely in low SNRs. In Fig. 3.7, we compare the performances of 8-state STCs. The performances of the optimal 8-state STTCs for quasi-static and rapid fading channels are almost the same, which are better than, though close to, that of the 8-state TSC code. On the other hand, the new 8-state STTC outperforms them by about 2 dB and outperforms the STBC by over 5 dB at a BER of 10^{-3}.

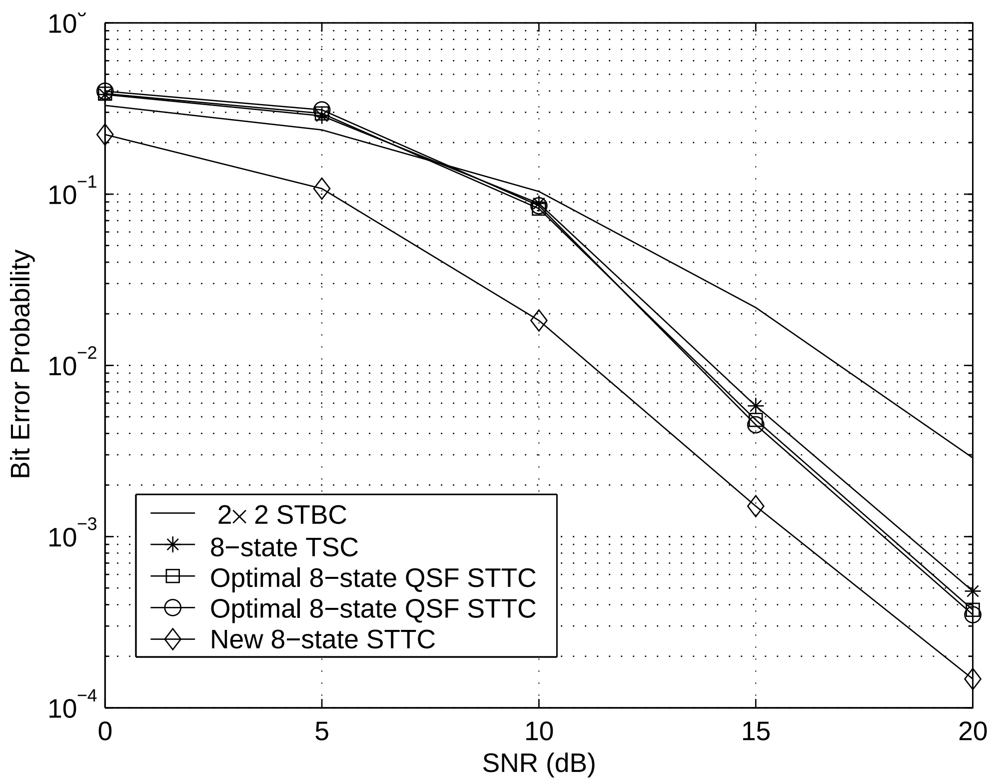

Figure 3.7: Bit error probability for various ST codes, two users with two transmit antennas each, one receive antenna, QPSK modulation, and composite fading.

3.7 Summary

In this chapter, we derive the code design criteria for a composite multiuser system in which different users may suffer different types of fading and have different numbers of transmit antennas. It has been shown that in order to obtain optimal performance, the rank and product of nonzero eigenvalues of codeword distance matrix **A** should be maximized. Based on the fact that pairwise error evens with smaller coding gain and diversity gain dominate the error probability, the code design is targeted at maximizing the minimum rank and product of the nonzero eigenvalues of codeword distance matrices from each user's code set, when different users have different number of transmit antennas. In the case that all the users have the same number of transmit antennas, the code set will be common for different users so that code design is simpler. The new code design criteria can also be applied to multiuser systems with one type of fading and single user systems. The simulation results demonstrate that the STTC obtained from searching based on the new code design criteria perform better than other existing codes in composite fading channels. Noticing that the composite fading is a special case of multiuser correlated fading, we will discuss the code design for a more generally correlated fading system in the next chapter.

Chapter 4

Performance Analysis and STTC Design for MIMO Multiuser Correlated Fading Systems

4.1 Introduction

In last chapter, we discuss the multiuser fading channels with extreme fading correlations: channels with correlation 0 (rapid fading) and channels with correlation 1 (quasi-static fading). In many circumstances, the fading situations cannot be described by these two fading models. More general multiuser correlated fading channels should be considered.

The impacts of the channel correlation have been discussed from view of information theory and performance analysis recently [14], [68] . The results in [14] show that the optimal code design depends on the specific space-time correlation matrix. Nevertheless, to feedback the CSI or its statistics from the receiver may not be useful when channel changes fast; or not be feasible because of the real-time requirement and bandwidth limit. It is desirable to design a class of STCs that achieve robust performance over a wide range of fading situations. [16] presented the general code design criteria for correlated MIMO systems, yet the ST correlation matrix is assumed of full rank. Some examples of designed codes were given, which concatenated the trellis coded modulation and space-time block code to show robust performance over different fading situations.

Recently, Su investigated the robust code design for the case that fading is only time-correlated but not spatially correlated [17], [75]. It is shown that the diversity gain of the square-sized full rank STC is independent of the time correlation matrix. However, consistent with previous work (e.g. [105]), the diversity gain of a rectangular STC is still dependent on the correlation matrix. The lower bound of the coding gain could also be obtained under the assumption that the Hadamard product of the distance matrix and time correlation matrix is positive definite. Although more recent work in [106] analyzed the performance of STCs for different kinds of fading channels, it gave no interesting hints on the STC design for the different correlation situations.

In this chapter, we generalize our investigation to the STTC code performance analysis and design for multiuser correlated MIMO systems. The channels of different users are supposed to be independent and the correlation matrices of distinct users may be different. Three fading circumstances are considered: temporally correlated, spatially correlated and spatio-temporally correlated fading. While the last case includes the former two, it is still desirable to analyze the two special cases individually since more specific and interesting results may be obtained.

Our analysis on the joint pairwise error probability demonstrates that the diversity gain and coding gain are determined by the codeword matrix and channel correlation of individual users. This implies that all the users use the same code set and the code design for multiuser systems is reduced to the code design for single user systems. In discussion on the code design for temporally correlated fading, we relax all the assumptions on dimension of codeword matrix and property of correlation matrix unlike [75]. In this more general case, we still prove that the STC achieving full diversity in quasi-static fading MIMO can achieve full diversity in temporally correlated multiuser MIMO systems. The upper bound of the coding gain depends on the product of the norms of the codeword difference matrix's nonzero column vectors. It is additionally lower bounded by the product of nonzero eigenvalues of the codeword distance matrix when the diversity gain is equal to the minimum rank of the codeword distance matrices as well as the minimum number of the nonzero columns of codeword difference matrices.

With spatial correlation and no temporal correlation presented, the diversity gain relies on the number of nonzero columns of the difference matrices and the ranks of space correlation matrices. More specifically, diversity gain is upper bounded by the product of these two. This makes sense since the diversity gain depends on time diversity and receive diversity though the latter may not be full, when channel is time uncorrelated. The performance analysis for spatio-temporally correlated fading MIMO systems exhibits that the number of, together with the product of the norms of, nonzero columns of codeword difference matrices are desired to be maximized. Based on the code design criteria for all three fading cases, a set of general criteria is obtained appropriate for arbitrary fading.

4.2 Data Model

There are K users in the system with n_T transmit antennas each. The receiver has n_R antennas. All the channels are Rayleigh fading. The received signal at time t can be expressed as

$$\mathbf{x}_t = \sqrt{E_s}\sum_{k=1}^{K}\mathbf{H}_t^k\mathbf{s}_t^k + \mathbf{n}_t, \quad t = 1, 2, \ldots, L, \tag{4.1}$$

where $\mathbf{H}_t^k$ is the channel matrix of user k at time t,

$$\mathbf{H}_t^k = \begin{bmatrix} h_{k1}^1(t) & h_{k2}^1(t) & \cdots & h_{kn_T}^1(t) \\ \vdots & \ddots & \ddots & \vdots \\ h_{k1}^{n_R}(t) & h_{k2}^{n_R}(t) & \cdots & h_{kn_T}^{n_R}(t) \end{bmatrix}.$$

$\mathbf{s}_t^k$ is the signal vector transmitted at time t from user k, which is the tth column of kth user's codeword matrix $\mathbf{S}_k$:

$$\mathbf{S}_k = \begin{bmatrix} \mathbf{s}_1^k & \mathbf{s}_2^k & \cdots & \mathbf{s}_L^k \end{bmatrix}, \quad k = 1, 2, \ldots, K.$$

$\mathbf{n}_t$ is a Gaussian noise vector. By defining

$$\mathbf{y} = \begin{bmatrix} \mathbf{x}_1(1) & \mathbf{x}_2(1) & \cdots & \mathbf{x}_L(1) & \mathbf{x}_1(2) & \cdots & \mathbf{x}_L(2) & \cdots & \mathbf{x}_L(n_R) \end{bmatrix}^T,$$

where $\mathbf{x}_t(i)$ is the ith element of $\mathbf{x}_t$, we have

$$\mathbf{y} = \mathbf{C}\mathbf{g} + \mathbf{w}. \tag{4.2}$$

In Eq. (4.2), $\mathbf{C}$ is a block diagonal matrix:

$$\mathbf{C} = \begin{bmatrix} \mathbf{C}_1 & \mathbf{C}_2 & \cdots & \mathbf{C}_K & \mathbf{0} & \cdots & \mathbf{0} & \cdots & \cdots & \mathbf{0} & \cdots & \cdots & \mathbf{0} \\ \mathbf{0} & \cdots & \mathbf{0} & \cdots & \mathbf{C}_1 & \mathbf{C}_2 & \cdots & \mathbf{C}_K & \mathbf{0} & \cdots & \cdots & \mathbf{0} & \vdots \\ \vdots & \ddots & \ddots & \ddots & \ddots & \ddots & \ddots & \ddots & \ddots & \ddots & \ddots & \ddots & \mathbf{0} \\ \mathbf{0} & \mathbf{0} & \cdots & \cdots & \mathbf{0} & \cdots & \cdots & \mathbf{0} & \mathbf{0} & \mathbf{C}_1 & \mathbf{C}_2 & \cdots & \mathbf{C}_K \end{bmatrix} \tag{4.3}$$

where

$$\mathbf{C}_k = \begin{bmatrix} \mathbf{C}_1^k & \mathbf{C}_2^k & \cdots & \mathbf{C}_{n_T}^k \end{bmatrix}, k = 1, 2, \ldots, K, \tag{4.4}$$

and

$$\mathbf{C}_m^k = diag\left(\mathbf{s}_1^k(m), \mathbf{s}_2^k(m), \cdots, \mathbf{s}_L^k(m)\right), \quad k = 1, 2, \ldots, K, \; m = 1, 2, \ldots, n_T, \tag{4.5}$$

where $\mathbf{s}_t^k(m)$ is the mth element of $\mathbf{s}_t^k$. $\mathbf{g}$ can be expressed as

$$\mathbf{g} = \begin{bmatrix} \mathbf{g}_1^T & \mathbf{g}_2^T & \cdots & \mathbf{g}_{n_R}^T \end{bmatrix}^T, \tag{4.6}$$

where

$$\mathbf{g}_j = \begin{bmatrix} (\mathbf{g}_j^1)^T & (\mathbf{g}_j^2)^T & \cdots & (\mathbf{g}_j^K)^T \end{bmatrix}^T,$$

with

$$\mathbf{g}_j^k = \begin{bmatrix} (\mathbf{h}_{1j}^k)^T & \cdots & (\mathbf{h}_{n_T j}^k)^T \end{bmatrix}^T$$

and

$$\mathbf{h}_{ij}^{k} = \begin{bmatrix} h_{ki}^{j}(1) & h_{ki}^{j}(2) & \cdots & h_{ki}^{j}(L) \end{bmatrix}^{T}.$$

$\mathbf{w}$ is constructed in the same way as $\mathbf{y}$.

4.3 PEP and Code Design Criteria

Assume that $\mathbf{C}$ and $\hat{\mathbf{C}}$ are two matrices associated with the two distinct joint code matrices, $\mathbb{S} = \{\mathbf{S}_1, \mathbf{S}_2, \ldots, \mathbf{S}_K\}$ and $\hat{\mathbb{S}} = \{\hat{\mathbf{S}}_1, \hat{\mathbf{S}}_2, \ldots, \hat{\mathbf{S}}_K\}$. Letting $\mathbf{R} = E[\mathbf{g}\mathbf{g}^H]$ and $\mathbf{Z} = (\mathbf{C} - \hat{\mathbf{C}})\mathbf{R}(\mathbf{C} - \hat{\mathbf{C}})^H$, we have the PEP of transmitting $\mathbb{S}$ but deciding $\hat{\mathbb{S}}$ upper bounded as [14]

$$P_2(e) \leq \begin{pmatrix} 2r_{\mathbf{z}} - 1 \\ r_{\mathbf{z}} - 1 \end{pmatrix} \left(\frac{E_s}{N_0}\right)^{-r_{\mathbf{z}}} \prod_{i=1}^{r_{\mathbf{z}}} \lambda_i^{-1}(\mathbf{Z}), \tag{4.7}$$

where $r_{\mathbf{z}} = rank(\mathbf{Z})$, and $\lambda_i(\cdot)$ denotes the ith nonzero eigenvalue of $(\cdot)$. Without loss of generality, it is assumed that the eigenvalues are ordered such that $\lambda_1(\cdot) \geq \lambda_2(\cdot) \geq \ldots \geq \lambda_r(\cdot)$. Furthermore, from Eq. (4.7), two important factors, diversity gain η_d and coding gain η_c, are defined as

$$\eta_d = \min_{(\mathbb{S}, \hat{\mathbb{S}})} r_{\mathbf{z}}, \tag{4.8}$$

and

$$\eta_c = \min_{(\mathbb{S}, \hat{\mathbb{S}}) \in \nu} \left(\prod_{i=1}^{\eta_d} \lambda_i(\mathbf{Z}) \right)^{1/\eta_d}, \tag{4.9}$$

where

$$\nu = \{(\mathbb{S}, \hat{\mathbb{S}}) : rank(\mathbf{Z}) = \eta_d\}. \tag{4.10}$$

In the following, we will discuss the diversity gain, coding gain and code design under different channel correlation situations.

4.3.1 Channels are Only Temporally Correlated

Suppose that channels are not spatially correlated and the channel between each pair of transmit and receive antennas has the same temporal correlation, i.e.,

$$E[\mathbf{h}_{ij}^{k}\mathbf{h}_{ij}^{kH}] = \mathbf{R}_{TP}^{k}, \forall i, j \tag{4.11}$$

and

$$E[\mathbf{h}_{ij}^{k}\mathbf{h}_{mn}^{kH}] = \mathbf{0}, \forall i \neq m \text{ or } n \neq j. \tag{4.12}$$

Moreover, we assume that the channels of different users are uncorrelated, that means,

$$E[\mathbf{h}_{ij}^{k}\mathbf{h}_{mn}^{lH}] = \mathbf{0}, \forall i, j, m, n; k \neq l. \tag{4.13}$$

Then we have

$$\mathbf{R} = \mathbf{I}_{n_R} \otimes diag(\mathbf{I}_{n_T} \otimes \mathbf{R}_{TP}^{1}, \mathbf{I}_{n_T} \otimes \mathbf{R}_{TP}^{2}, \ldots, \mathbf{I}_{n_T} \otimes \mathbf{R}_{TP}^{K}), \tag{4.14}$$

where $\otimes$ indicates the Kronecker product. Together with Eq. (4.3), $(\mathbf{C}-\hat{\mathbf{C}})\mathbf{R}(\mathbf{C}-\hat{\mathbf{C}})^{H}$ can be rewritten as

$$\begin{aligned} \mathbf{Z} &= \mathbf{I}_{n_R} \otimes \left(\sum_{k=1}^{K} \sum_{m=1}^{n_T} \mathbf{C}_{m}^{k} \mathbf{R}_{TP}^{k} \mathbf{C}_{m}^{kH} \right) \\ &= \mathbf{I}_{n_R} \otimes \left[\sum_{k=1}^{K} (\mathbf{S}_k - \hat{\mathbf{S}}_k)^T (\mathbf{S}_k - \hat{\mathbf{S}}_k)^* \circ \mathbf{R}_{TP}^{k} \right], \end{aligned} \tag{4.15}$$

where $\circ$ denotes the Hadamard product [104]. We define

$$\mathbf{D}_k = [(\mathbf{S}_k - \hat{\mathbf{S}}_k)^H (\mathbf{S}_k - \hat{\mathbf{S}}_k)]^*, \tag{4.16}$$

and

$$\mathbf{A}_k = \mathbf{D}_k \circ \mathbf{R}_{TP}^k, \ \mathbf{A} = \sum_{i=1}^{K} \mathbf{A}_k \tag{4.17}$$

for denotation simplicity. Note that $\mathbf{D}_k$ is the codeword distance matrix of user k. Let d be the rank of $\mathbf{A}$. Eq. (4.7) becomes

$$P_2(e) \leq \begin{pmatrix} 2n_R d - 1 \\ n_R d - 1 \end{pmatrix} \left(\frac{E_s}{N_0}\right)^{-n_R d} \prod_{i=1}^{d} \lambda_i^{-n_R}(\mathbf{A}). \tag{4.18}$$

And the diversity gain is,

$$\eta_d = \min_{(\mathbb{S},\hat{\mathbb{S}})} d n_R. \tag{4.19}$$

Theorem 4.1. *With $d = rank(\mathbf{A})$ and $d_k = rank(\mathbf{A}_k)$, the diversity gain of the system is*

$$\eta_d = \min_{(\mathbb{S},\hat{\mathbb{S}})} d n_R = d_{min} n_R, \tag{4.20}$$

where $d_{min} = \min_{1 \leq k \leq K} \min_{(\mathbf{S}_k, \hat{\mathbf{S}}_k)} d_k$, in which the inner minimum is taken among all the pairs of distinct code matrices of each user, and the outer minimum is taken on the K minimums obtained from the inner minimum operator. The coding gain is

$$\eta_c = \min_{1 \leq k \leq K} \min_{(\mathbf{S}_k, \hat{\mathbf{S}}_k), k \in \mu} \left(\prod_{i=1}^{d_{min}} \lambda_i(\mathbf{A}_k) \right)^{1/d_{min}}, \tag{4.21}$$

where $\mu = \{k : \min_{(\mathbf{S}_k, \hat{\mathbf{S}}_k)} d_k = d_{min}\}$.

Proof. Since $\mathbf{D}_k$ and $\mathbf{R}_{TP}^k$ are both Hermitian and positive semidefinite, so is $\mathbf{A}_k$ [107]. According to Weyl's theorem [108], we have

$$\max\{\lambda_i(\mathbf{A}_p), \lambda_i(\mathbf{A}_q)\} \leq \lambda_i(\mathbf{A}_p + \mathbf{A}_q), \;\; 1 \leq p, q \leq K; \; 1 \leq i \leq L. \tag{4.22}$$

Thus

$$\max_{1 \leq k \leq K} \lambda_i(\mathbf{A}_k) \leq \lambda_i(\mathbf{A}), \; i = 1, 2, \ldots, L. \tag{4.23}$$

This implies that the number of nonzero eigenvalues of $\mathbf{A}$ will be greater than or equal to the maximum number of nonzero eigenvalues of all users. In other words, for a specific pair $(\mathbb{S}, \hat{\mathbb{S}})$,

$$d \geq \max_{1 \leq k \leq K} d_k. \tag{4.24}$$

Since each user transmits signals independently, the two distinct joint code matrices $\mathbb{S}$ and $\hat{\mathbb{S}}$ may have all the same elements except one. That means, there is a case that $\mathbf{A} = \mathbf{A}_{k_0}$, with $\mathbf{A}_k = 0, \forall k \neq k_0$. Eq. (4.24) implies that $\mathbf{A}$ associated with the pair of distinct code matrices that are different in more elements besides the k_0th element, will have rank not less than d_{k_0}. Therefore, $\min_{(\mathbb{S},\hat{\mathbb{S}})} d = \min_{1 \leq k \leq K} \min_{(\mathbf{S}_k, \hat{\mathbf{S}}_k)} d_k$. Based on Eq. (4.22), for $\mathbf{A}$ with rank d_{min}, we also have

$$\prod_{i=1}^{d_{min}} \lambda_i(\mathbf{A}_k) \leq \prod_{i=1}^{d_{min}} \lambda_i(\mathbf{A}). \tag{4.25}$$

According to the definition of the coding gain, Eq. (4.21) can be proved in a similar way to the above discussion. $\square$

Theorem 4.1 suggests that the minimum of d_k's taken over all the distinct signal matrices of each user should be maximized in the code design. However, d_k

still depends on the temporal correlation matrix. In the rest of this section, we will discuss the code design criteria, which are independent of specific correlation matrix.

Denote $rank(\mathbf{D}_k) = r_k$. Since $\mathbf{D}_k$ is positive semi-definite, all the r_k-by-r_k principal minors are non-negative. Furthermore, there exists one r_k-by-r_k positive definite principal submatrix, which is denoted as $\mathbf{P}$. The corresponding submatrix of $\mathbf{R}_{TP}^k$, which is composed of the rows and columns with the same indices as those used for constructing $\mathbf{P}$, is denoted as $\mathbf{Q}$. Then $\mathbf{P} \circ \mathbf{Q}$ is the corresponding submatrix of $\mathbf{A}_k$.

According to Oppenheim's inequality [108], we have $det(\mathbf{P} \circ \mathbf{Q}) \geq det(\mathbf{P})$, for the diagonal elements of $\mathbf{Q}$ are all 1. It is known that

$$\zeta_{r_k} = \sum_{\{u_1,u_2,\ldots,u_{r_k}\}\in\Gamma} \prod_{i=1}^{r_k} \lambda_{u_i}(\mathbf{A}_k),$$

where

$$\Gamma = \{\{u_1, u_2, \ldots, u_{r_k}\} | 1 \leq u_i \leq L, u_i \neq u_j, \forall i \neq j\},$$

is equal to the sum of all the r_k-by-r_k principal minors of $\mathbf{A}_k$. With the fact that $\mathbf{A}_k$ is positive semidefinite, $\zeta_{r_k} \geq det(\mathbf{P} \circ \mathbf{Q}) \geq det(\mathbf{P}) > 0$. So the number of nonzero eigenvalues of $\mathbf{A}_k$ must not be less than r_k, otherwise, ζ_{r_k} will be zero. This means that the rank of $\mathbf{A}_k$ is equal or greater than the rank of $\mathbf{D}_k$.

Moreover, since $\mathbf{D}_k$ and $\mathbf{R}_{TP}^k$ are normal and positive semidefinite, we have [107]

$$\prod_{i=1}^{m} \lambda_i(\mathbf{A}_k) \leq \left(\lambda_1(\mathbf{R}_{TP}^k)\right)^m \prod_{i=1}^{m} a_i^H(\mathbf{X}) a_i(\mathbf{X}), m = 1, 2, \ldots, L. \tag{4.26}$$

where $\mathbf{D}_k = \mathbf{X}^H\mathbf{X}$ and $a_1(\cdot), \ldots, a_m(\cdot)$ are the first m largest norms of column vectors of $(\cdot)$. It can been seen that $a_i(\mathbf{X})$ is the ith largest among $\{\|\mathbf{s}_t^k - \mathbf{s}_t^k\|^2, t = 1, 2, \ldots, L\}$. Thus the number of nonzero eigenvalues, i.e., the rank of $\mathbf{A}_k$, is less than or equal to the number of nonzero columns of $\mathbf{S}_k - \hat{\mathbf{S}}_k$. Together with the inequality that $rank(\mathbf{A}_k) \leq rank(\mathbf{D}_k) \cdot rank(\mathbf{R}_{TP}^k)$, we have the following theorem

Theorem 4.2. *The diversity gain is bounded by*

$$n_R \cdot \min_{1\leq k\leq K} \min_{(\mathbf{S}_k, \hat{\mathbf{S}}_k)} rank(\mathbf{D_k}) \leq \eta_d \leq n_R \cdot \min\{\min_{1\leq k\leq K} \min_{(\mathbf{S}_k, \hat{\mathbf{S}}_k)} rank(\mathbf{D_k}) \cdot rank(\mathbf{R}_{TP}^k), \min_{1\leq k\leq K} \min_{(\mathbf{S}_k, \hat{\mathbf{S}}_k)} \delta_k\} \tag{4.27}$$

where δ_k is the number of nonzero columns of $\mathbf{D}_k$ and $\min_{(\mathbf{S}_k, \hat{\mathbf{S}}_k)} \delta_k$ is denoted as δ_k^{min}, which is the length of shortest error event.

Theorem 4.2 demonstrates that the rank of $\mathbf{D}_k$ and the number of different columns between $\mathbf{S}_k$ and $\hat{\mathbf{S}}_k$ should be maximized. It is also implied that when the minimum of $r_k = rank(\mathbf{D}_k)$ is equal to the minimum of δ_k over all the distinct signal matrix pairs, the available maximum diversity gain is fixed. Generally, we have $L \geq n_T$, and thus r_k can be n_T at most. That means, in the STTC design, the number of states of encoder should be chosen such that $\delta_k \geq n_T$ to fully use transmit antenna diversity. Specially, when $L = n_T$ (e.g., Alamouti's code) and all of $\mathbf{D}_k$'s are of full rank, according to Theorem 4.2, the diversity gain will be $n_T n_R$. From Eq. (4.27), it is also observed that for a STC that can achieve full space diversity in quasi-static fading channels can achieve full space diversity in arbitrarily temporally correlated fading situations as well.

Based on Eq. (4.26), it is found that

$$\prod_{i=1}^{d_k} \lambda_i(\mathbf{A}_k) \leq \left(\lambda_1(\mathbf{R}_{TP}^k)\right)^{d_k} \prod_{t=1}^{d_k} \|\mathbf{s}_t^k - \hat{\mathbf{s}}_t^k\|^2, \tag{4.28}$$

where $\{\|\mathbf{s}_{t_i}^k - \hat{\mathbf{s}}_{t_i}^k\|^2\}$ are assumed to be ordered decreasingly. Exchanging $\mathbf{D}_k$ and $\mathbf{R}_{TP}^k$ in Eq. (4.26), the following inequality can be obtained,

$$\prod_{i=1}^{d_k} \lambda_i(\mathbf{A}_k) \leq (\lambda_1(\mathbf{D}_k))^{d_k} \tag{4.29}$$

for the diagonal elements of $\mathbf{R}_{TP}^k$ are all 1. Consequently, we have

$$\eta_c \leq \min_{1\leq k\leq K} \min_{\substack{(\mathbf{s}_k, \hat{\mathbf{s}}_k) \\ k\in\mu}} \lambda_1(\mathbf{R}_{TP}^k) \prod_{t=1}^{d_{min}} \|\mathbf{s}_t^k - \hat{\mathbf{s}}_t^k\|^{2/d_{min}} \tag{4.30}$$

and

$$\eta_c \leq \min_{1\leq k\leq K} \min_{\substack{(\mathbf{s}_k, \hat{\mathbf{s}}_k) \\ k\in\mu}} \lambda_1(\mathbf{D}_k) \tag{4.31}$$

Since $\prod_{t=1}^{n_k} \|\mathbf{s}_t^k - \hat{\mathbf{s}}_t^k\|^2 \leq (\lambda_1(\mathbf{D}_k))^{r_k}$, we will use Eq. (4.30) in code design. Using the same way as the proof of Theorem 4.1, we have

$$\prod_{i=1}^{r_k} \lambda_i(\mathbf{D}_k) \leq \prod_{i=1}^{r_k} \lambda_i(\mathbf{A}_k). \tag{4.32}$$

The derivation uses the fact that for any matrix $\mathbf{Y} \in \mathcal{C}^{n\times n}$, $\lambda_i(\mathbf{Y}_p) \leq \lambda_i(\mathbf{Y})$, where $\mathbf{Y}_p$ is the p-by-p principal submatrix of $\mathbf{Y}$. When $\min\limits_{(\mathbf{S}_k, \hat{\mathbf{S}}_k)} r_k = \delta_k^{min}$, the coding gain is bounded as

$$\min_{1\le k\le K}\prod_{i=1}^{\delta_k^{min}}\lambda_i(\mathbf{D}_k)\le\eta_c\le\min_{1\le k\le K}\min_{\substack{(\mathbf{s}_k,\hat{\mathbf{s}}_k)\\ k\in\mu}}\lambda_1(\mathbf{R}_{TP}^k)\prod_{t=1}^{\delta_k^{min}}\|\mathbf{s}_t^k-\hat{\mathbf{s}}_t^k\|^{2/\delta_k^{min}} \tag{4.33}$$

Similarly, we have [17], when $L = n_T = r_k$,

$$\max\{det(\mathbf{D_k}), det(\mathbf{R_{TP}^k})\prod_{t=1}^{L}\|\mathbf{s}_t^k-\hat{\mathbf{s}}_t^k\|^2\}\le det(\mathbf{A}_k)\le\lambda_1^L(\mathbf{R}_{TP}^k)\prod_{t=1}^{L}\|\mathbf{s}_t^k-\hat{\mathbf{s}}_t^k\|^2. \tag{4.34}$$

From above discussions, it is found that although we do not specify that all the users use the same code set, it should be the case since the diversity gain and coding gain of the system depend on the diversity gain and coding gain of individual user. Otherwise, the decoding at the receiver will be unnecessarily complicated.

Then the evaluation of the codeword difference and distance matrices is within one code set as the code design of single user system does. With respect to the diversity gain and coding gain, the following two code design criteria for the temporally correlated fading channels are obtained, which are independent of specific fading correlation.

1. Maximize the minimum rank d_{min} of codeword distance matrices and the minimum number of different columns taken over all pairs of distinct code matrices.

2. The minimum products of norms of nonzero column vectors of $\mathbf{S}-\hat{\mathbf{S}}$, taken over all pairs of distinct code matrices should be maximized. When the number of the states of ST trellis encoder or the dimension of STBC is chosen such that $\min_{(\mathbf{S},\hat{\mathbf{S}})}\delta$ is equal to the maximum available $\min_{(\mathbf{S},\hat{\mathbf{S}})} n$, i.e. n_T,

the minimum of the products of nonzero eigenvalues of codeword distance matrices taken over all pairs of distinct code matrices should be maximized additionally.

Note that $\mathbf{S}$, $\hat{\mathbf{S}}$, δ and n are the corresponding symbols used in above discussion with k dropped.

4.3.2 Channels are Only Spatially Correlated

When channels are only spatially correlated, it is assumed that, i) there is no temporal correlation between channels of each user, ii) channels of different transmit antennas of one user are correlated, and the correlation at each time is the same and iii) channels of different users are uncorrelated. That means

$$E[\mathbf{h}_{ij}^{k}\mathbf{h}_{ij}^{kH}] = \mathbf{I}_L, \forall i, j \tag{4.35}$$

$$E[\mathbf{h}_{ij}^{k}\mathbf{h}_{i'j'}^{kH}] = \alpha_k(i, i', j, j')\mathbf{I}_L, 1 \leq i, i' \leq M.$$

$$E[\mathbf{h}_{i'j'}^{k}\mathbf{h}_{i'j'}^{k'H}] = \mathbf{0},\ 1 \leq i, i' \leq n_T,\ 1 \leq j, j' \leq n_R; 1 \leq k \neq k' \leq K$$

where $\alpha_k(i, i', j, j')$ is the spatial correlation between the two channels from transmit antenna i to receive antenna j and transmit antenna i' to receive antenna j'

of user k. We define the following matrices for further discussion:

$$\Phi_{ij}^{k} = \begin{bmatrix} \alpha_k(1,1,i,j) & \alpha_k(1,2,i,j) & \cdots & \alpha_k(1,n_T,i,j) \\ \alpha_k(2,1,i,j) & \alpha_k(2,2,i,j) & \cdots & \alpha_k(2,n_T,i,j) \\ \vdots & \ddots & \ddots & \vdots \\ \alpha_k(n_T,1,i,j) & \alpha_k(n_T,2,i,j) & \cdots & \alpha_k(n_T,n_T,i,j) \end{bmatrix}, \tag{4.36}$$

$$\Lambda_{ij}^{t} = \sum_{k=1}^{K} \mathbf{s}_t^{kH} \Phi_{ij}^{k} \mathbf{s}_t^{k}, \tag{4.37}$$

and

$$\Lambda_{ij} = diag(\Lambda_{ij}^{1}, \Lambda_{ij}^{2}, \ldots, \Lambda_{ij}^{L}). \tag{4.38}$$

Then we have

$$\mathbf{Z} = \begin{bmatrix} \Lambda_{11} & \Lambda_{12} & \cdots & \Lambda_{1n_R} \\ \Lambda_{21} & \Lambda_{22} & \cdots & \Lambda_{2n_R} \\ \vdots & \ddots & \ddots & \vdots \\ \Lambda_{n_R1} & \Lambda_{n_R2} & \cdots & \Lambda_{n_Rn_R} \end{bmatrix}. \tag{4.39}$$

Exchanging the rows and columns of $\mathbf{Z}$ in a way such that the ith row (column) exchanges with the $nL+i$th row (column), where $1 \le i \le L,\ 1 \le n \le n_R$,

$$\tilde{\mathbf{Z}} = diag(\mathbf{B}_1, \mathbf{B}_2, \ldots, \mathbf{B}_L), \tag{4.40}$$

where

$$\mathbf{B}_t = \begin{bmatrix} \Lambda_{11}^t & \Lambda_{12}^t & \cdots & \Lambda_{1n_R}^t \\ \Lambda_{21}^t & \Lambda_{22}^t & \cdots & \Lambda_{2n_R}^t \\ \vdots & \ddots & \ddots & \vdots \\ \Lambda_{n_R1}^t & \Lambda_{n_R2}^t & \cdots & \Lambda_{n_Rn_R}^t \end{bmatrix}. \tag{4.41}$$

Note that $\mathbf{Z}$ and $\tilde{\mathbf{Z}}$ has the same rank and eigenvalues. It can be seen that the rank and nonzero eigenvalues of $\mathbf{B}_t$ decide the performance of spatially correlated system. $\mathbf{B}_t$ can be rewritten as

$$\mathbf{B}_t = \sum_{k=1}^{K} \mathbf{B}_t^k = \sum_{k=1}^{K} \tilde{\mathbf{D}}_t^k \mathbf{R}_{SP}^k \tilde{\mathbf{D}}_t^{kH}, \tag{4.42}$$

where $\mathbf{R}_{SP}^k = [\Phi_{ij}^k] \in \mathcal{C}^{n_T n_R \times n_T n_R}$ and

$$\tilde{\mathbf{D}}_t^k = \mathbf{I}_{n_R} \otimes (\mathbf{s}_t^k - \hat{\mathbf{s}}_t^k)^T. \tag{4.43}$$

Following the discussion in above sections, to get high diversity, the rank and product of nonzero eigenvalues of $\mathbf{B}_t^k$ have to be maximized. We have the following theorem.

Theorem 4.3. *Defining $R_k = rank(\mathbf{B}_t^k)$ with $\mathbf{B}_t^k \neq 0$, $N_k = \min\{rank(\mathbf{R}_{SP}^k), n_R\}$ and $\delta_k^{min} = \min_{(\mathbf{s}_k, \hat{\mathbf{s}}_k)} \delta_k$, we have*

$$\eta_d = \min_{1 \le k \le K} R_k \delta_k^{min} \le \min_{1 \le k \le K} N_k \delta_k^{min}, \tag{4.44}$$

and

$$\eta_c \le \min_{k \in \Omega} \lambda_1(\mathbf{R}_{SP}^k) \prod_{t=1}^{\delta_k^{min}} \|\mathbf{s}_t^k - \hat{\mathbf{s}}_t^k\|^{2/R_k}, \tag{4.45}$$

where $\Omega = \{k : R_k \delta_k^{min} = \eta_d\}$.

Proof. Based on Eq. (4.24) and the argument that $\mathbb{S}$ and $\hat{\mathbb{S}}$ may differs on one user's codeword matrix since all users independently transmit signals, we have

$$\eta_d = \min_k \min_{(\mathbf{s}_k, \hat{\mathbf{s}}_k)} rank(\tilde{\mathbf{B}}^k),$$

where

$$\tilde{\mathbf{B}}^k = diag\left(\mathbf{B}_1^k, \mathbf{B}_2^k, \ldots, \mathbf{B}_L^k\right).$$

It is easy to see that $rank(\tilde{\mathbf{B}}^k) = \sum_{t=1}^{L} rank(\mathbf{B}_t^k)$. For t where $\mathbf{s}_t^k - \hat{\mathbf{s}}_t^k \neq 0$, $rank(\mathbf{B}_t^k) \leq N_k$; for t where $\mathbf{s}_t^k - \hat{\mathbf{s}}_t^k = 0$, $rank(\mathbf{B}_t^k) = 0$. Therefore, $\eta_d \leq \min_{(\mathbf{s}_t^k, \hat{\mathbf{s}}_t^k)} \delta_k N_k = \min_k \delta_k^{min} N_k$. Eq. (4.44) is proved. It is known that $\lambda_i(\mathbf{B}_t^k) \leq \lambda_i(\tilde{\mathbf{D}}_t^k \tilde{\mathbf{D}}_t^{kH}) \lambda_1(\mathbf{R}_{SP}^k)$. Thus the inequality in Eq. (4.45) holds. □

Similarly, we have the conclusion that all the users use the same code set. The following code design criteria are for spatially correlated fading channels:

1. Maximize the number of nonzero columns of codeword difference matrices taken over all possible distinct code matrices.

2. The minimum products of norms of nonzero column vectors of difference matrices, taken over all pairs of distinct code matrices, should be maximized.

It can be seen that the code design for spatially correlated fading channels is reduced to the code design for rapid fading channels [3].

4.3.3 Channels are spatio-temporally Correlated

In this case, we only assume that

$$E[\mathbf{h}_{i'j'}^{k}\mathbf{h}_{i'j'}^{k'H}] = \mathbf{0},\ 1 \le i, i' \le n_T,\ 1 \le j, j' \le n_R; 1 \le k \ne k' \le K, \tag{4.46}$$

by denoting

$$E[\mathbf{g}_i^k \mathbf{g}_j^k] = \mathbf{R}_{ij}^k \tag{4.47}$$

and

$$\mathbf{R}_k = \begin{bmatrix} \mathbf{R}_{11}^k & \mathbf{R}_{12}^k & \cdots & \mathbf{R}_{1n_R}^k \\ \mathbf{R}_{21}^k & \mathbf{R}_{22}^k & \cdots & \mathbf{R}_{2n_R}^k \\ \vdots & \vdots & \ddots & \vdots \\ \mathbf{R}_{n_R1}^k & \mathbf{R}_{n_R2}^k & \cdots & \mathbf{R}_{n_Rn_R}^k \end{bmatrix}, \tag{4.48}$$

we have

$$\mathbf{Z} = \sum_{k=1}^{K} \mathbf{\Delta}_k \mathbf{R}_k \mathbf{\Delta}_k^H, \tag{4.49}$$

where

$$\mathbf{\Delta}_k = \mathbf{I}_{n_R} \otimes \mathbf{C}_k.$$

So that the diversity gain and coding gain depend on the minimum rank and product of nonzero eigenvalues of each $\mathbf{\Delta}_k \mathbf{R}_k \mathbf{\Delta}_k^H$.

It is easy to verify that

$$\lambda_i(\mathbf{\Delta}_k \mathbf{R}_k \mathbf{\Delta}_k^H) \le \lambda_i(\mathbf{\Delta}_k^H \mathbf{\Delta}_k)\lambda_1(\mathbf{R}_k) = \|\mathbf{s}_t^k - \hat{\mathbf{s}}_t^k\|^{2n_R}\lambda_1(\mathbf{R}_k), 1 \le i \le n_R L; t = \lfloor \frac{i}{n_R} \rfloor \tag{4.50}$$

and

$$\lambda_i(\mathbf{\Delta}_k\mathbf{R}_k\mathbf{\Delta}_k^H) \leq \lambda_1(\mathbf{\Delta}_k^H\mathbf{\Delta}_k)\lambda_i(\mathbf{R}_k) = \|\mathbf{s}_1^k - \hat{\mathbf{s}}_1^k\|^{2n_R}\lambda_i(\mathbf{R}_k),\ 1 \leq i \leq n_R L, \quad (4.51)$$

where $\{\|\mathbf{s}_t^k - \hat{\mathbf{s}}_t^k\|, t = 1, \ldots, L\}$ are assumed to be ordered decreasingly. Eq. (4.50) and Eq. (4.51) imply that

$$rank(\mathbf{\Delta}_k\mathbf{R}_k\mathbf{\Delta}_k^H) \leq \min\{rank(\mathbf{R}_k), \delta_k n_R\}. \quad (4.52)$$

We have the following theorem:

Theorem 4.4. *For spatio-temporally correlated fading systems, the coding gain and diversity gain will be bounded as*

$$\eta_d \leq \min_{1\leq k\leq K} \min\{rank(\mathbf{R}_k), \delta_k n_R\}, \quad (4.53)$$

and

$$\eta_c \leq \min_{1\leq k\leq K} \lambda_1(\mathbf{R}^k)\left(\prod_{t=1}^{m} \|\mathbf{s}_t^k - \hat{\mathbf{s}}_t^k\|^{2n_R}\|\mathbf{s}_{m+1}^k - \hat{\mathbf{s}}_{m+1}^k\|^{2(\eta_d - mn_R)}\right)^{1/\eta_d}. \quad (4.54)$$

where $m = \lfloor \frac{\eta_d}{n_R} \rfloor$.

Theorem 4.4 also verifies the results in [105]. The above discussion suggests that without any information on the correlation matrix, we will maximize the minimum number of nonzero columns of codeword difference matrices, and the minimum product of the norms of these columns in the code design. That means, the code design criteria for spatio-temporally correlated and spatially correlated fading channels are the same as those for single user rapid fading channels.

4.3.4 Further Discussions

It has been shown that for all three fading cases, only one code set is employed for all the users. The code design is affected by the following factors: the minimum number of the nonzero columns of codeword difference matrices, the minimum product of nonzero column vectors of codeword difference matrices, the minimum rank of nonzero eigenvalues of codeword distance matrices, and the minimum product of nonzero eigenvalues of the codeword distance matrices. For illustration simplicity, we use c_d, p_d, R_D and P_D to indicate these four factors respectively. In general, there are many STTCs such that c_d, p_d and R_D can be maximized at the same time. Since it is not sure if p_d and P_D can be maximized at the same time, it is reasonable to choose the code with the largest P_D from the ones that have the maximized c_d, p_d and R_D. Then more general code design criteria are obtained:

1. Maximize the c_d and R_D taken over all possible distinct code matrices.
2. p_d taken over all pairs of distinct code matrices should be maximized.
3. Choose the code with the largest P_D from the ones that have the maximized c_d, p_d and R_D.

4.4 Optimal STTCs and Simulation Results

Based on the criteria obtained above, we use the STTC encoder model introduced in Chapter 2 to get the optimal code generator matrices for the system with users equipped with two antennas each.

Simulations are done for two-user systems. The number of transmit antennas for each user is two while the number of antennas at the receiver is one. Channels for each user are correlated Rayleigh fading, which are simulated with model introduced in Chapter 2 with variance 1. Recall that channel correlation depends on the parameters that are shown below:

b	scatter ring radius
d_0	mobile distance to the center of the antenna pair
β	mobile position angle with respect to the end-fire of the antennas
ξ	mobile moving direction with respect to the end-fire of the base station antennas
d_{sp}	space separation between transmit antennas
f_D	Doppler spread

and different users have independent channels. Noise is Gaussian with variance $N_0/2$ per real dimension. QPSK is used for all the simulations. We compare our newly designed codes with the optimal STTC codes for quasi-static Rayleigh fading channels obtained in [109], which are referred to as YBCs. The simulation results give the average bit error probability of two users versus SNR $= E_a/N_0$, where E_a is the average power of the signals received per receive antenna per user.

After exhaustive search, we obtain the following optimal code generator matrices for 4-state and 8-state STTCs. It should be emphasized that the optimal generator matrix set with respect to the criteria is not unique.

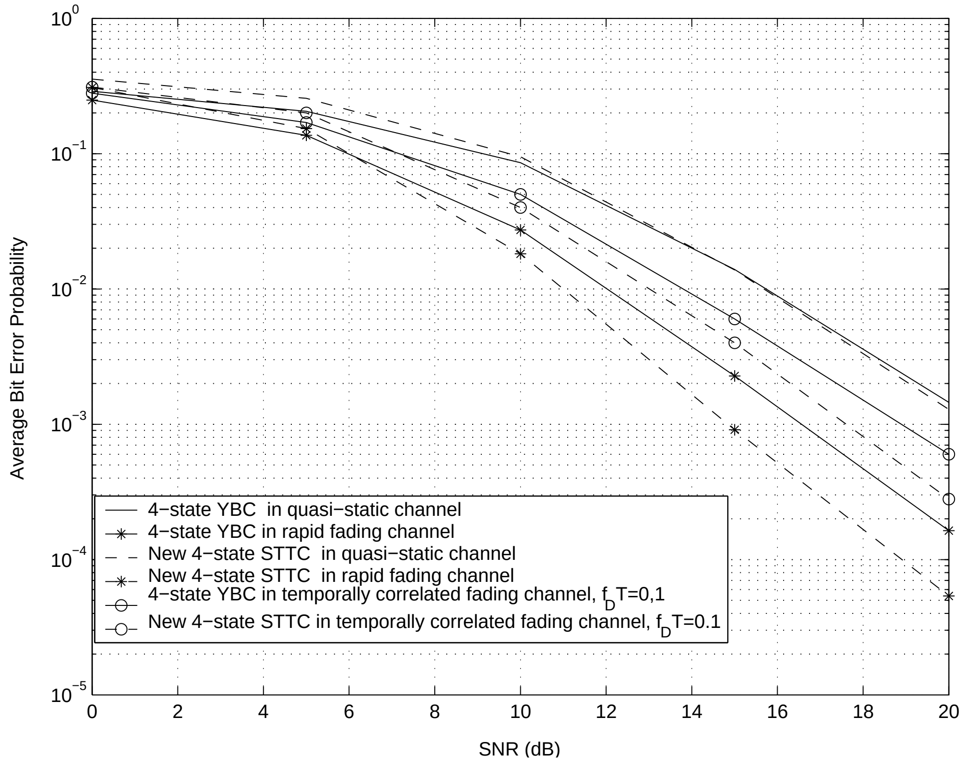

Figure 4.1: Performance comparison of 4-state STTCs under temporally correlated fading channels.

Optimal 4-state STTC for temporally correlated fading

$$\mathbf{G}_1^4 = \begin{bmatrix} 1 & 2 \\ 2 & 2 \end{bmatrix} \quad \text{and} \quad \mathbf{G}_2^4 = \begin{bmatrix} 2 & 2 \\ 3 & 0 \end{bmatrix}$$

Optimal 8-state STTC for temporally correlated fading

$$\mathbf{G}_1^8 = \begin{bmatrix} 2 & 2 & 0 \\ 0 & 0 & 1 \end{bmatrix} \quad \text{and} \quad \mathbf{G}_2^8 = \begin{bmatrix} 2 & 3 \\ 2 & 2 \end{bmatrix}$$

In Fig. 4.1 and Fig. 4.2 , we compare the BER performance of the 4-state and 8-state newly designed codes with the YBCs under different temporally correlated

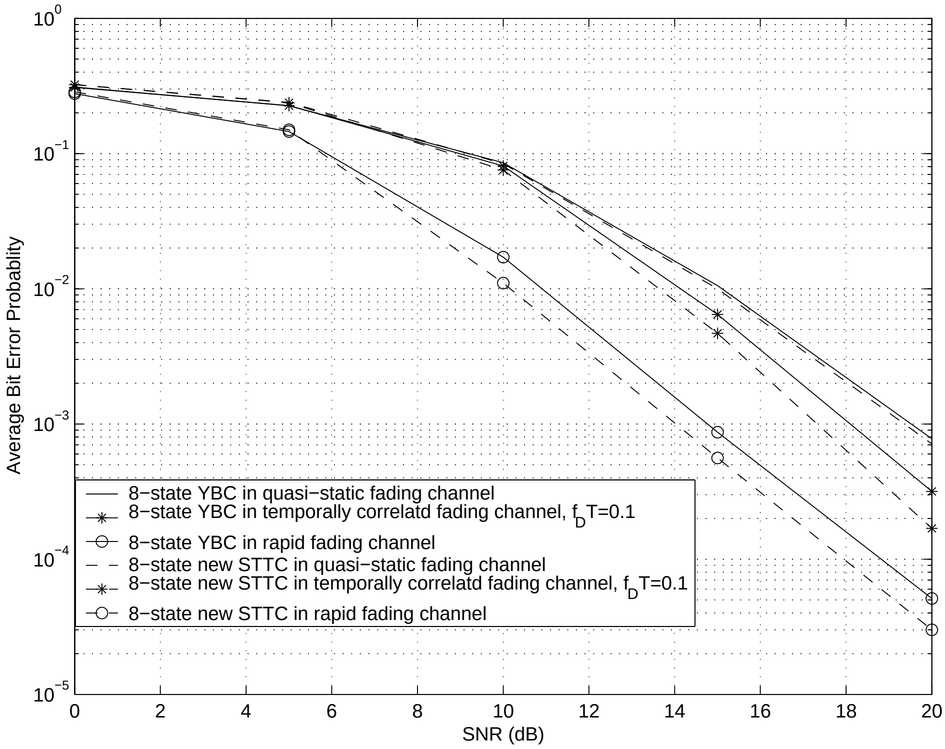

Figure 4.2: Performance comparison of 8-state STTCs under temporally correlated fading channels.

situations. It can be seen that the newly designed STTC outperforms the YBCs in channels with low to high correlations. It is expected that the performance for the case where channel has the highest time correlation, i.e., quasi-static fading, is the worst. Fig. 4.3 and Fig. 4.4. compare the performances of 4-state STTCs in differently spatially correlated fading and spatio-temporally correlated fading channels respectively. The performances of 8-state STTCs under variant spatially and spatio-temporally correlated fading systems are presented in Fig. 4.5 and Fig. 4.6. It can be seen that the newly design codes have better performances than the YBCs. Moreover, the channel correlations have large impact on the performance of STCs. Since the diversity gains are different when different spatial

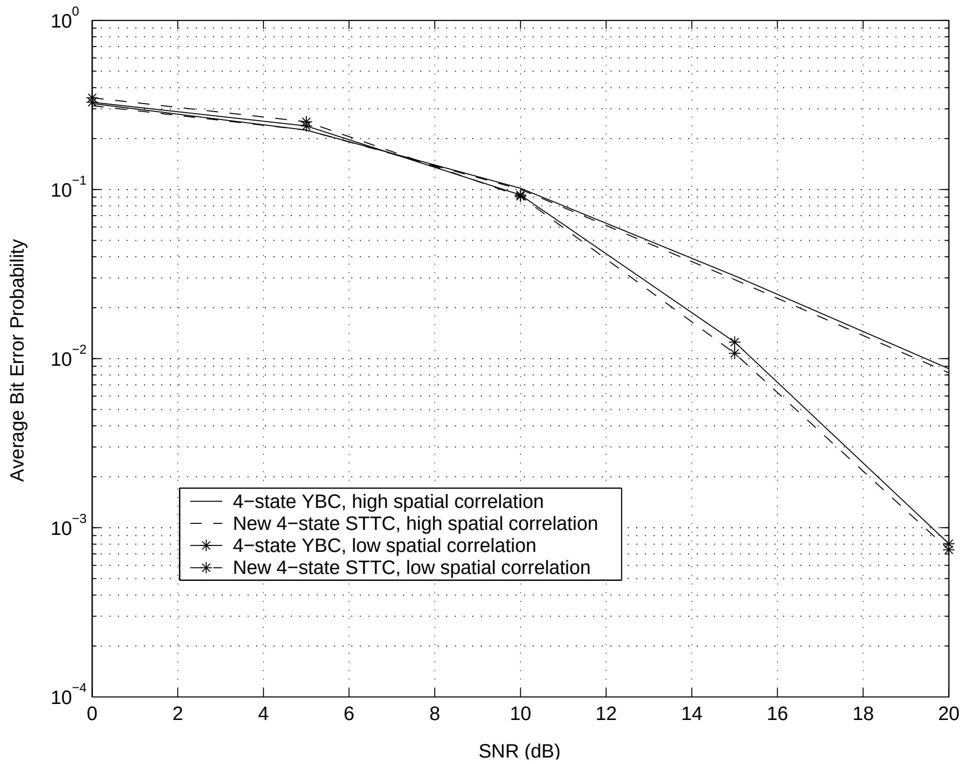

Figure 4.3: Performance comparison of 4-state STTCs in spatially correlated fading channels. Low correlation: $\xi = \beta = 1/6\pi$, $a = 50\lambda$, $d_{sp} = 5\lambda$, $d = 1500\lambda$. High correlation: $\xi = 1/6\pi$, $\beta = 2/3\pi$, $a = 10\lambda$, $d_{sp} = 1/2\lambda$, $d = 1500\lambda$.

correlations present, we can observe that the performance curves drop faster in spatial or spatio-temporally correlated fading channels with lower correlations.

4.5 Summary

In this chapter, we generalize our discussion to the STTC code design for multiuser correlated MIMO systems. Three fading circumstances are considered: temporally correlated, spatially correlated, and spatio-temporally correlated fading.

It has been reasoned that all users use the same code set. Without any assumption on the dimension of codeword matrix and property of correlation matrix, we prove

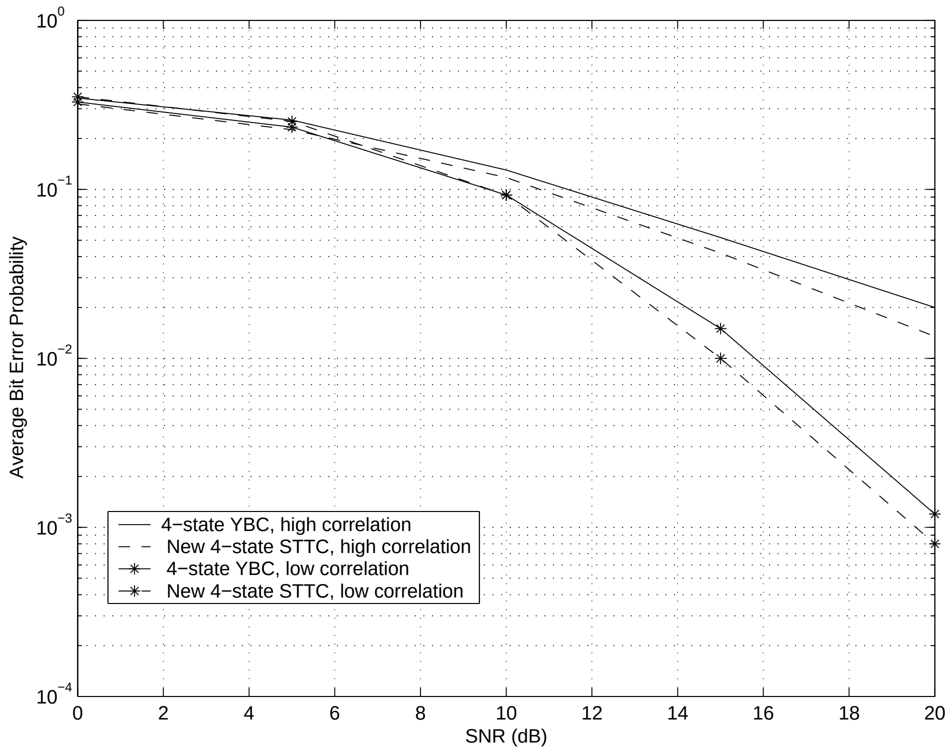

Figure 4.4: Performance comparison of 4-state STTCs in spatio-temporally correlated fading channels. Low correlation: $f_D T = 0.8$, $\xi = \beta = 1/6\pi$, $a = 50\lambda$, $d_{sp} = 5\lambda$, $d = 1500\lambda$. High correlation: $f_D T = 0.003$, $\xi = 1/6\pi$, $\beta = 2/3\pi$, $a = 10\lambda$, $d_{sp} = 1/2\lambda$, $d = 1500\lambda$.

that the STC achieving full diversity in quasi-static fading systems can achieve full diversity in temporally correlated fading systems. It is shown that the product of the norms of codeword difference matrices' columns vectors and the product of the nonzero eigenvalues of codeword distance matrices should be maximized to have the high coding gain. On the other hand, the performance analysis for spatially correlated and arbitrarily correlated fading systems exhibits that the code design for these two cases is equivalent to the code design for single user rapid fading channels. Based on these facts, we further obtained a set of general code design criteria applicable for all three fading situations. Note that the composite fading

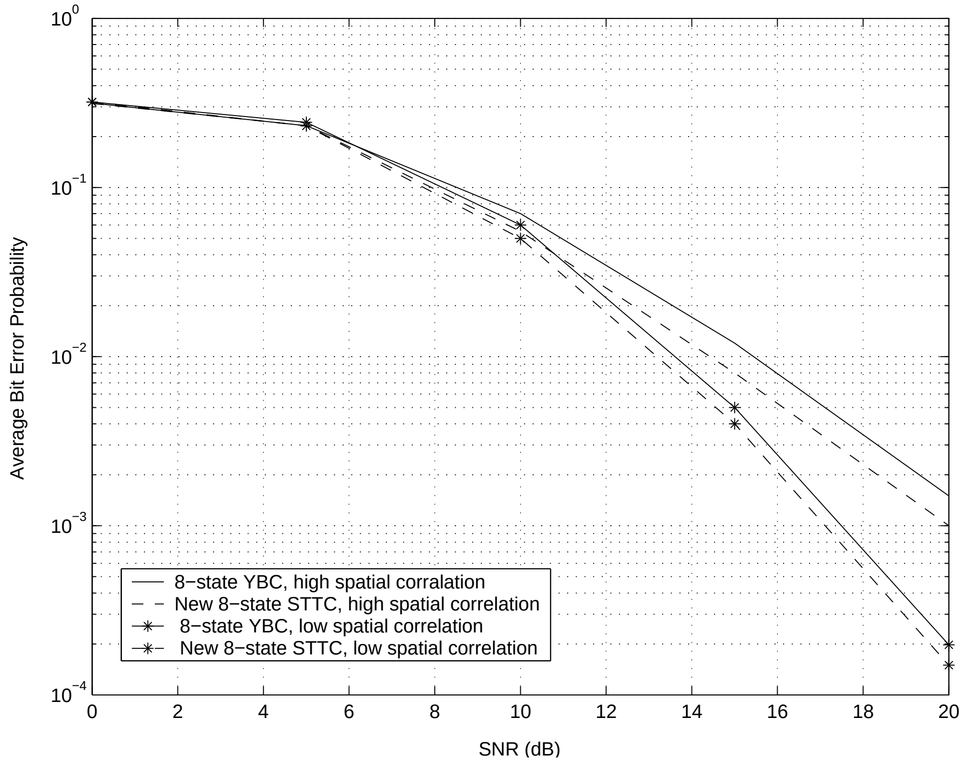

Figure 4.5: Performance comparison of 8-state STTCs in spatially correlated fading channels. Low correlation: $\xi = \beta = 1/6\pi$, $a = 50\lambda$, $d_s p = 5\lambda$, $d = 1500\lambda$. High correlation: $\xi = 1/6\pi$, $\beta = 2/3\pi$, $a = 10\lambda$, $d_s p = 1/2\lambda$, $d = 1500\lambda$.

discussed in Chapter 3 is a special case of multiuser correlated fading situations. It is easy to be verified that the results of Chapter 3 are in consistence with those of this chapter.

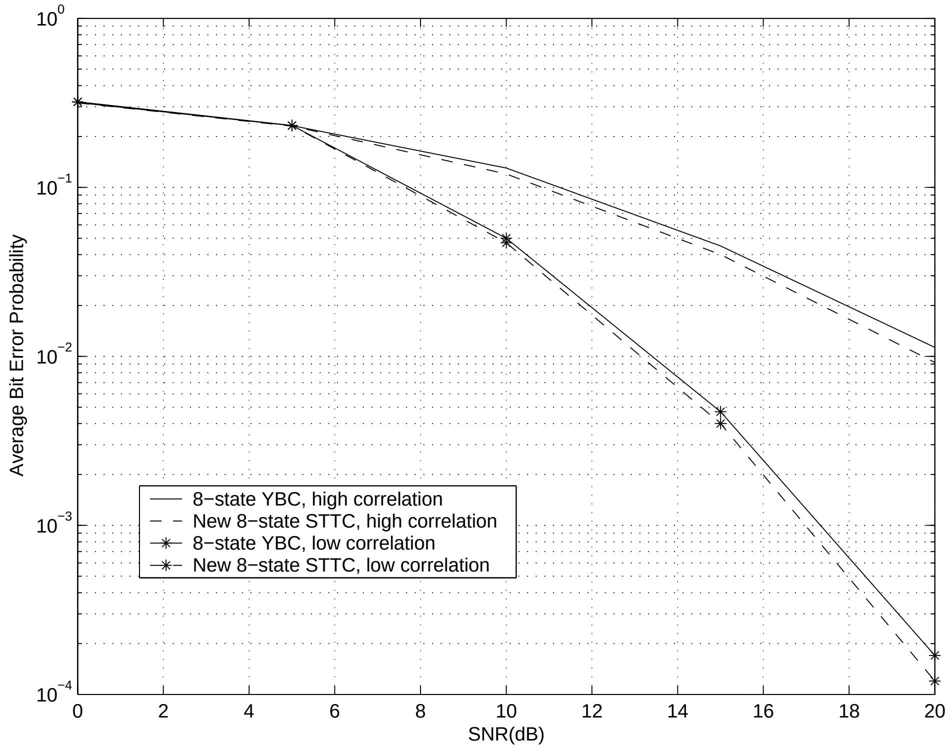

Figure 4.6: Performance comparison of 8-state STTCs in spatio-temporally correlated fading channels. Low correlation: $f_D T = 0.8$, $\xi = \beta = 1/6\pi$, $a = 50\lambda$, $d_s p = 5\lambda$, $d = 1500\lambda$. High correlation: $f_D T = 0.003$, $\xi = 1/6\pi$, $\beta = 2/3\pi$, $a = 10\lambda$, $d_s p = 1/2\lambda$, $d = 1500\lambda$.

Chapter 5

STBC-VBLAST for MIMO Wireless Communication Systems

5.1 Introduction

It has been shown that multiple antenna systems have the potential to achieve a much higher bandwidth efficiency than single antenna systems in fading environment [1]. In addition to STC, many BLAST schemes were proposed to exploit this potential. The first BLAST structure is DLST proposed by Foschini [6], which distributes the code blocks along the diagonals, called layers, of the transmit codeword matrix. Consequently, VBLAST architecture was introduced [7], [20], [90]. In VBLAST, each layer is either uncoded or coded independently and associated with a certain transmit antenna. Unlike DLST, the vertical arrangement of the layers enables detection and coding with lower complexity, but having different performance for different layers. Coded VBLAST is also called HLST [68], [91], which is later generalized to refer to as horizontally coded BLAST schemes with dependently coded layers [103].

Treating a BLAST system as a multiuser system enables IS and ordered SIC [6], [19] to be used in detection. Examples include [7], which proposed ZF-VBLAST, and [20], [90], which proposed MMSE-VBLAST. However, both algorithms involve the computation of pseudo-inverses of matrices, which has high order complexity. The work in [68] traded the performance for the less complexity by using a QRD approach. Although the performance is degraded (when the decomposition order is not optimal), the computational effort at the receiver is reduced enormously.

Since all the algorithms discussed above use SIC in the detection, we refer to them as SIC BLAST. As in multiuser detection (MUD), the error propagation inherent in SIC considerably degrades the performance of SIC BLAST systems [41]. To improve the performance, the turbo processing principle can be applied, so that the detection block and decoding block share information in an iterative fashion to do joint detection and decoding [94], [95], [96]. Iterative detection and decoding has its own challenges, such as complexity, convergence and decoding delay.

The challenge of BLAST systems is to design a low-complexity detector, which can suppress and cancel inter-layer interference efficiently. SIC BLAST, such as VBLAST using QRD, has lower computational complexity than BLAST using iterative detection but worse performance resulting from error propagation. Power allocation has been considered to combat the error propagation problem in VBLAST systems [97]. The limitation is that CSI is required at both transmitter and receiver. Note that because of error propagation, the performance of the SIC BLAST system is mainly dependent on the worst performance of the layers. The lowest layer, which is detected first, has the minimum diversity gain amongst all the layers. It is more susceptible to noise, and this will affect the performance of the whole system.

We therefore propose a new STBC-VBLAST scheme, which increases the minimum diversity gain by integrating STBC [4] into the VBLAST architecture. CSI is only required to be known or estimated at the receiver and low-complexity computation is performed. In a STBC-VBLAST system having n_T transmit and n_R receive antennas, nG antennas transmit G STBCs. The data transmitted on the rest of antennas are independent and uncoded. Although we assume uncoded transmission, the STBC-VBLAST can easily incorporate channel coded transmission, yielding better performance due to the coding gain of the code.

At the receiver, low-complexity QRD and SIC detection are applied. In addition, the decoding of STBC is linear and separate for every information symbol [5], [54]. All these make it the fact that the detection process of the STBC-VBLAST has low complexity. With n_T transmit antennas and n_R receive antennas, the minimum diversity gain of the STBC-VBLAST is increased to be the minimum of $n_R - n_T + nG + 1$ and $n(n_R - n_T) + n^2$, larger than $n_R - n_T + 1$ for other VBLAST schemes. Our simulations show that the new STBC-VBLAST scheme significantly outperforms other VBLAST schemes. The performance improvement is accompanied by the loss of spectral efficiency because STBC is used. Trying to be fair, we use the higher-order modulation for the STBC-VBLAST and do the performance comparison. It is demonstrated that even with higher spectral efficiency, the STBC-VBLAST outperforms other VBLAST systems at the medium to high SNRs due to its high diversity gain. Although the better performance of the new scheme is achieved by integrating the STBC, it is not always true that the performance is improved with the increasing number of STBC used. We found a threshold of G, in terms of n_R, n_T and n, above which there are only diminishing performance improvement at the price of spectral efficiency loss. The tradeoffs between the performances and spectral efficiencies of STBC-VBLAST systems with different combinations of (n, G) are also discussed.

The case when the channel is not perfectly estimated is considered. The effect of the estimation errors is to cause an error floor in performance curve. We show that the STBC-VBLAST has lower error floors than other BLAST systems because of the higher diversity gain.

We also compare STBC-VLBAST to VBLAST employing STTC. The simulations show VBLAST using the best STTC for quasi-static Rayleigh fading performs worse than the STBC-VBLAST. The reason is that the STTC design criteria for Rayleigh fading channel are not suitable for VBLAST systems, since the effective channel after interference suppression and cancellation is not Rayleigh. Moreover, the decoding complexity of STTC is higher than that of STBC. Noting that DLST is famous for its high diversity, we compare it with the STBC-VBLAST from views of performance, complexity and applicability. Performance comparison is done through simulations that involve DLST using RS code and trellis code.

Noticing that SQRD [93] uses ordering without increasing complexity very much, we study the ordered STBC-VBLAST as well. It is no doubt that the performance is improved at the price of computational complexity. In effect, the diversity gain of the STBC-VBLAST is the lower bound for that of the ordered STBC-VBLAST as presented in simulations. In spite that G_{th} is derived for the STBC-VBLAST in the first place, the simulations demonstrate that it is also valid for the ordered STBC-VBLAST as well.

5.2 STBC-VBLAST Transmitter

We consider a system with n_T transmit antennas and n_R receive antennas. Fig. 5.1 depicts the block diagram for the STBC-VBLAST transmitter. The information symbol sequence is divided into $n_T - (n-1)G$ streams. Streams 1 to $n_T - nG$ are transmitted on the first $n_T - nG$ antennas. The remaining G streams go through corresponding G STBC encoders before being transmitted on nG antennas. To be specific, each group of n antennas is used to transmit an $n \times m$ STBC, denoted by $\mathcal{G}_n$, where n and m indicate the number of transmit antennas and symbol intervals occupied by the STBC respectively. We call each of the G STBC encoded streams a *STBC layer* and the system an (n, m, G) STBC-VBLAST system. Note that the codeword matrix $\mathcal{G}_n$ here is the transpose of that in [4]. Although it is possible to allow for different STBC at the layers, we assume that all the STBC layers use codes of the same size, i.e., $n \times m$.

The transmitted signal can be expressed in matrix form as

$$\mathbf{S} = \begin{bmatrix} \mathbf{C}_1 & \mathbf{C}_2 & \cdots & \mathbf{C}_L \\ \mathcal{G}_{n1}^1 & \mathcal{G}_{n2}^1 & \cdots & \mathcal{G}_{nL}^1 \\ \vdots & \vdots & \ddots & \vdots \\ \mathcal{G}_{n1}^G & \mathcal{G}_{n2}^G & \cdots & \mathcal{G}_{nL}^G \end{bmatrix}, \tag{5.1}$$

where the signal frame is of length mL. $\mathbf{C}_l$, the uncoded signal in block l, can be

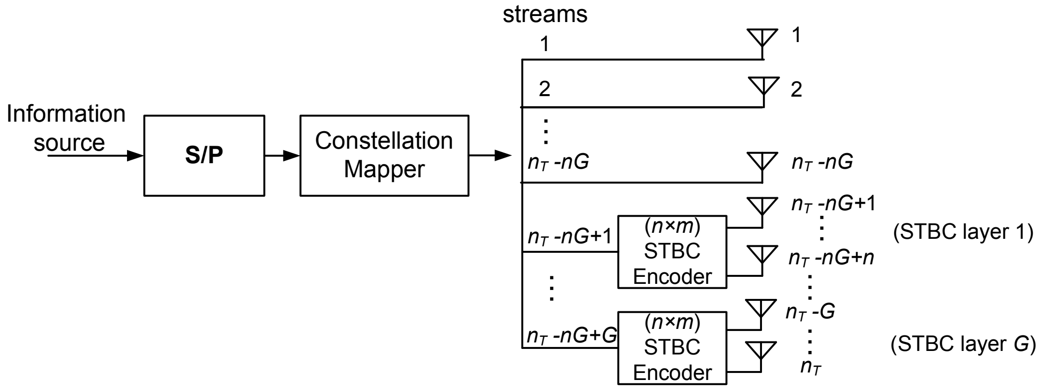

Figure 5.1: Block diagram for the STBC-VBLAST transmitter.

written as

$$\mathbf{C}_l = \begin{bmatrix} s^1_{ml-m+1} & s^1_{ml-m+2} & \cdots & s^1_{ml} \\ s^2_{ml-m+1} & s^2_{ml-m+2} & \cdots & s^2_{ml} \\ \vdots & \vdots & \ddots & \vdots \\ s^{n_T-nG}_{ml-m+1} & s^{n_T-nG}_{ml-m+2} & \cdots & s^{n_T-nG}_{ml} \end{bmatrix},$$

where element s^i_j indicates the jth symbol in the ith information symbol stream. $\mathcal{G}^i_{nl}$ denotes the $n \times m$ STBC in the ith STBC layer at block l, which is associated with $(n_T - nG + i)$th information symbol stream and constructed by N information symbols, their negatives and conjugates, as stated in Chapter 2. The average energy of each information symbol, hence each transmitted symbol, is $E_s = E[|s^j_i|^2]$, where $i = 1, 2, \ldots, n_T - (n-1)G; j = 1, 2, \ldots, mL$. For convenience, we call each block with m symbol intervals as a *STBC interval*.

5.3 STBC-VBLAST Receiver

The signals transmitted from the n_T antennas undergo Rayleigh fading channels and interfere with each other at the receiver. It is assumed that channels do not change within one STBC interval. At the receiver, decoding and detection are performed in one STBC interval. The signal received in STBC interval l is

$$\mathbf{X}_l = \mathbf{H}_l \mathbf{S}_l + \mathbf{W}_l, \tag{5.2}$$

where $\mathbf{W}_l \in \mathbb{C}^{n_R \times m}$ is the complex AWGN noise matrix, in which all the elements are i.i.d $\mathcal{CN}(0, N_0)$. Every element in channel matrix, $\mathbf{H}_l \in \mathbb{C}^{n_R \times n_T}$, is i.i.d. $\mathcal{CN}(0, 1)$. $\mathbf{S}_l$ is the signal transmitted at STBC interval l, written as

$$\mathbf{S}_l = \left[\ \mathbf{C}_l^T, (\mathcal{G}_{nl}^1)^T, \cdots, (\mathcal{G}_{nl}^G)^T \ \right]^T. \tag{5.3}$$

The STBC layers are processed first, with decoding and detection done within each layer. Interference cancellation is performed at every STBC and uncoded layer except for the Gth STBC layer (since it is decoded first). The block diagram for the receiver is shown in Fig. 5.2. With assumption that $n_R \geq n_T$, we have QR decomposition of $\mathbf{H}_l$ as $\mathbf{H}_l = \mathbf{QR}$, where $\mathbf{Q}$ is an $n_R \times n_T$ matrix with orthonormal

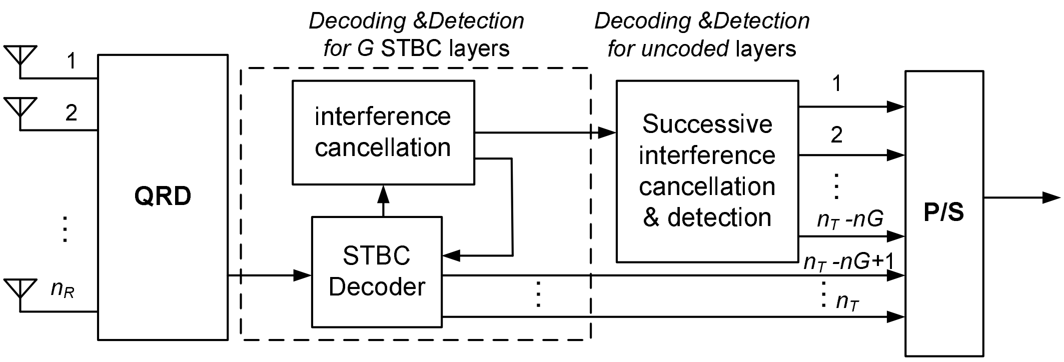

Figure 5.2: Block diagram for the STBC-VBLAST receiver.

columns and $\mathbf{R} = [R_{i,j}]$ is an $n_T \times n_T$ upper triangular matrix expressed as

$$\mathbf{R} = \begin{bmatrix} R_{1,1} & R_{1,2} & R_{1,3} & \cdots & R_{1,n_T} \\ 0 & R_{2,2} & R_{2,3} & \cdots & R_{2,n_T} \\ \vdots & \vdots & \ddots & \ddots & \vdots \\ 0 & 0 & \cdots & R_{n_T-1,n_T-1} & R_{n_T-1,n_T} \\ 0 & 0 & \cdots & 0 & R_{n_T,n_T} \end{bmatrix}. \tag{5.4}$$

The process of obtaining $\mathbf{R}$ and $\mathbf{Q}$ is as follows [104]:

$\mathbf{R} = 0,\ \ \mathbf{Q} = H,\ \ \textbf{index} = [1, 2, \ldots, n_T]$

For $\quad i = 1 \ldots n_T - 2$

$k_i = \arg \min_{j=i,\ldots,n_T} \|\mathbf{q}_j\|$

Exchange column i and k_i of $\mathbf{Q}$, $\mathbf{R}$ and **index** respectively

$R_{i,i} = \|\mathbf{q}_j\|, \quad \mathbf{q}_i = \mathbf{q}_i/\mathbf{R}_{i,i}$

$R_{i,j} = \mathbf{q}_i^H \mathbf{q}_i, \quad \mathbf{q}_j = \mathbf{q}_j - R_{i,j}\mathbf{q}_i, \quad \text{for } j = i+1, \ldots, n_T$

End

Multiplying $\mathbf{X}_l$ in Eq. (5.2) by $\mathbf{Q}^H$, we have

$$\mathbf{Y}_l = \mathbf{Q}^H \mathbf{X}_l = \mathbf{R}\mathbf{S}_l + \mathbf{N}_l, \tag{5.5}$$

where $\mathbf{N}_l = \mathbf{Q}^H \mathbf{W}_l$. It can be verified that every entry of $\mathbf{N}_l$ is i.i.d. $\mathcal{CN}(0, N_0)$ distributed. After substracting the interference from the lower $G-k$ STBC layers, the decision statistic for the kth STBC layer is

$$\mathbf{Y}_l^k = \mathbf{Y}_l - \sum_{i=k+1}^{G} \mathcal{H}_l^i \hat{\mathcal{G}}_{nl}^i, \tag{5.6}$$

where $\hat{\mathcal{G}}_{nl}^i$ is the estimation of $\mathcal{G}_{nl}^i$. $\mathbf{Y}_l^k$ and $\mathcal{H}_l^i$ are defined as:

$$\mathbf{Y}_l^k = \begin{bmatrix} \mathbf{Y}_l(\beta_1, 1) & \mathbf{Y}_l(\beta_1, 2) & \cdots & \mathbf{Y}_l(\beta_1, m) \\ \vdots & \vdots & \ddots & \vdots \\ \mathbf{Y}_l(\beta_n, 1) & \cdots & \cdots & \mathbf{Y}_l(\beta_n, m) \end{bmatrix} \tag{5.7}$$

and

$$\mathcal{H}_l^i = \begin{bmatrix} R_{k'+1,i'+1} & R_{k'+1,i'+2} & \cdots & R_{k'+1,i'+n} \\ \vdots & \vdots & \ddots & \vdots \\ R_{k'+n,i'+1} & \cdots & \cdots & R_{k'+n,i'+n} \end{bmatrix}, \tag{5.8}$$

where $\beta_i = k' + i$, $k' = n_T - (G-k+1)n$ and $i' = n_T - (G-i+1)n$. $(\cdot)(j,k)$ denotes the (j,k)th elements of $(\cdot)$, which will be used for the rest of this chapter. $\tilde{\mathbf{Y}}_l^k$ can be further expressed as

$$\tilde{\mathbf{Y}}_l^k = \tilde{\mathbf{H}}_l^k \mathcal{G}_{nl}^k + \tilde{\mathbf{N}}_l^k + \mathbf{E}, \tag{5.9}$$

where $\mathbf{E}$ comes from the detection errors at the lower layers. $\tilde{\mathbf{H}}_l^k$ is a square matrix composed of $k'+1$ to $k'+n$ rows and $k'+1$ to $k'+n$ columns of $\mathbf{R}$, written as

$$\tilde{\mathbf{H}}_l^k = \begin{bmatrix} R_{k'+1,k'+1} & R_{k'+1,k'+2} & \cdots & R_{k'+1,k'+n} \\ \vdots & \vdots & \ddots & \vdots \\ R_{k'+n,k'+1} & \cdots & \cdots & R_{k'+n,k'+n} \end{bmatrix}. \tag{5.10}$$

$\tilde{\mathbf{N}}_l^k$ is composed of $k'+1$ to $k'+n$ rows of $\mathbf{N}_l$, written as

$$\tilde{\mathbf{N}}_l^k = \begin{bmatrix} \mathbf{N}_l^k(k'+1,1) & \mathbf{N}_l^k(k'+1,2) & \cdots & \mathbf{N}_l^k(k'+1,m) \\ \vdots & \vdots & \ddots & \vdots \\ \mathbf{N}_l^k(k'+n,1) & \cdots & \cdots & \mathbf{N}_l^k(k'+n,m) \end{bmatrix}. \tag{5.11}$$

Base on Eq. (5.9), each STBC layer can be considered as a virtual (n,n) STBC system, in which $\tilde{\mathbf{H}}_l^k$ is the channel matrix. It is well known that the decoding of STBC can be done linearly. Assuming that the residual interference from the previously detected layers is independent Gaussian, we have the separate decision rules for the symbols in the kth STBC layer as

$$\hat{s}_{N(l-1)+i}^{n_T-nG+k} = \underset{s_{N(l-1)+i}^{n_T-nG+k}}{\arg} \min \left| (\mathbf{h}_{li}^k)^H \mathbf{y}_l^k - a\rho_k s_{N(l-1)+i}^{n_T-nG+k} \right|^2, \tag{5.12}$$

or

$$\hat{s}_{N(l-1)+i}^{n_T-nG+k} = \underset{s_{N(l-1)+i}^{n_T-nG+k}}{\arg} \min \left| (\mathbf{y}_l^k)^H \mathbf{h}_{li}^k - a\rho_k s_{N(l-1)+i}^{n_T-nG+k} \right|^2, \tag{5.13}$$

where $1 \leq i \leq N$ and $1 \leq k \leq G$. $\hat{s}_q^p$ is the estimation of qth information symbol in stream p. a is a constant dependent on the type of STBC used for the

STBC-VBLAST [4], [5]. For example, for $\mathcal{G}_2$, $a = 1$, and for $\mathcal{G}_4$ with complex symbols, $a = 2$. $\mathbf{y}_l$ and $\mathbf{h}_{li}$ are constructed by the elements and their negatives and conjugates of $\tilde{\mathbf{Y}}_l^k$ and $\tilde{\mathbf{H}}_l^k$ respectively. ρ_k is defined as the Frobenius norm of $\tilde{\mathbf{H}}_l^k$:

$$\rho_k = \|\tilde{\mathbf{H}}_l^k\|_F^2. \tag{5.14}$$

The symbols of uncoded layer can be detected in a successive way by

$$\begin{aligned}
\hat{s}^k_{m(l-1)+j} = & \arg \min_{s^k_{m(l-1)+j}} \left| \frac{1}{R_{k,k}} \left\{ \mathbf{Y}_l^k(k,j) \right. \right. \\
& \left. \left. - \sum_{i=1}^{G} \mathcal{H}_l^i \hat{\mathcal{G}}_{nl}^i(j) - \sum_{i=k+1}^{n_T-nG} R_{k,i}\hat{s}^i_{m(l-1)+j} \right\} - s^k_{m(l-1)+j} \right|^2, \\
& k = 1, 2, \ldots, n_T - nG, j = 1, 2, \ldots, m,
\end{aligned} \tag{5.15}$$

where $\hat{\mathcal{G}}_{nl}^i(j)$ denotes the jth column of $\hat{\mathcal{G}}_{nl}^i$.

5.4 Performance Analysis

In this section, we analyze the performance of the new proposed STBC-VBLAST systems under Rayleigh fading. CSI is known or perfectly estimated at the receiver. Based on the fact that the performance of whole system is dependent on the performance of the lowest layer that has the smallest diversity gain, we define the diversity gain d of the system as the minimum diversity gain among all the layers. The following theorem gives an exact result for the diversity gain of the STBC-VBLAST system, which shows that the new system has much higher diversity gain than other VBLAST systems.

Theorem 5.1. *For an* (n, m, G) *STBC-VBLAST system having* n_T *transmit and* n_R *receive antennas, the diversity gain of the system is the minimum of* $n(n_R - n_T) + n^2$ *and* $n_R - n_T + Gn + 1$.

Proof. For each STBC layer k, $\tilde{\mathbf{Y}}_l^k$ defined in Eq. (5.9) is the decision statistics. Based on the fact that the STBC has unitary structure and the way $\mathbf{h}_{li}^k$ constructed, $\tilde{S}_i^k = (\mathbf{h}_{li}^k)^H \mathbf{y}_l^k$, has the same information as $\tilde{\mathbf{Y}}_l^k$ for decoding of $s_{N(l-1)+i}^{n_T-nG+k}$ in kth STBC layer. Moreover, with assumption that the residual interference from the lower STBC layers is independent Gaussian with variance N_e^k, the decision statistics $\tilde{S}_i^k$, can be expressed as

$$\tilde{S}_i^k = a\rho_k s_{N(l-1)+i}^{n_T-nG+k} + \tilde{n}_i^k, \quad i = 1, 2, \ldots, N, \tag{5.16}$$

where $\tilde{n}_i^k$ is complex Gaussian noise with variance $a\rho_k(N_0 + N_e^k) = a\rho_k N_0^k$. ρ_k are defined in Eq. (5.14) and a is the constant dependent on the STBC used.

Provided that the channel is known or perfectly estimated at the receiver, the conditional pairwise symbol error probability (PSEP) of transmitting $s_{N(l-1)+i}^{n_T-nG+k}$ but deciding $\hat{s}_{N(l-1)+i}^{n_T-nG+k}$ is

$$P_2^k(e|\mathbf{H}_l) = Q\left(\sqrt{\frac{a\rho_k E_s \Delta}{2N_0^k}}\right), \tag{5.17}$$

where $\sqrt{\Delta}$ is the normalized Euclidean distance between the two constellation points and E_s is the average energy of symbols of the STBC.

For elements of channel matrix are independent complex Gaussian, $\mathbf{Q}$ and $\mathbf{R}$ obtained from QRD of $\mathbf{H}_l$, are statistically independent [110]. It has been shown that all the nonzero elements R_{ij}'s of $\mathbf{R}$, where $i = 1, 2, \ldots, n_T, i < j$, are independent and $R_{i,j} \sim \mathcal{CN}(0, 1)$. In addition, the square of diagonal element, $R_{i,i}^2$, is $\chi^2_{2(n_R-i+1)}$ distributed with variance $n_R - i + 1$. Its probability density function (p.d.f.) is [111]

$$f_{R_{ii}^2}(r) = \frac{r^{n_R-i}e^{-r}}{\Gamma(n_R - i + 1)}, \quad r \geq 0, \quad i = 1, 2, \ldots, n_T. \tag{5.18}$$

Therefore ρ_k is a chi-squared variate with freedom

$$\begin{aligned}&\sum_{i=1}^{n} 2[n_R - n_T + n(G-k) + i] + \sum_{i=1}^{n-1} 2i \\ &= 2n[n_R - n_T + n(G - k + 1)], \quad k = 1, 2, \ldots, G,\end{aligned} \tag{5.19}$$

for STBC layer k. Typically, interference coming from lower layers is assumed to be perfectly canceled out, i.e., $N_0^k = N_0$. Then, averaging Eq. (5.17) with respect to $\mathbf{H}_l$, we get the approximate PSEP of kth STBC layer, when SNR $= E_s/N_0$ is high [27], as

$$P_2^k(e) \approx \left(\frac{aE_s\Delta}{N_0}\right)^{-d_k} \begin{pmatrix} 2d_k - 1 \\ d_k \end{pmatrix}, \quad k = 1, 2, \ldots, G, \tag{5.20}$$

where $d_k = n[(n_R - n_T + n(G - k + 1)]$, is the diversity gain of the kth STBC layer. The layers transmitting uncoded stream $\{s_j^i\}$ can be seen as a special case of STBC layers with $a = 1$ and $\rho_i = R_{i,i}^2 \sim \chi^2_{2(n_R-i+1)}$. Thus the ith uncoded layer has the diversity gain $n_R - i + 1$, where $i = 1, 2, \ldots, n_T - nG$ [68]. As a sequence, the minimum diversity gain d, among all the layers, is the minimum of $n_R - n_T + nG + 1$ and $n(n_R - n_T + n)$. $\square$

Since the diversity gain of the STBC-VBLAST system, i.e., the minimum diversity gain of all the layers is enhanced, the error propagation is suppressed very efficiently. For example, the STBC-VBLAST system with one layer of 2×2 STBC and $n_R = n_T$, the diversity gain is increased to 3 other than one for other VBLAST systems. Simulations show that even with one STBC layer, the STBC-VBLAST outperforms other VBLAST greatly.

5.5 Some Discussions

An analog of the STBC-VBLAST is the VBLAST integrating STTC, which is, for notation simplicity, indicated as STTC-VBLAST. It has been shown that well designed STTC outperforms the STBC in Rayleigh fading system because of higher coding gain [3]. However, the previous analysis demonstrates the virtual channel matrix for each coded layer is upper triangular, and not all the elements are Gaussian. That implies, the STTC, which is designed based on the criteria in [3], may not have a good performance when used for STTC-VBLAST. It can be seen that Theorem 5.1 still holds for STTC-VBLAST, if the STTC used is unitary [76]. We also show in simulation that STTC-VBLAST with the optimal STTC designed for the quasi-static Rayleigh fading does not perform better than the STBC-VBLAST, but with higher detection complexity.

In the sense of having high diversity gain, DLST is one of the competitors of the STBC-VBLAST. As the first proposed layered space-time code, DLST may have a very large diversity gain [68]. However, a necessary condition to own this virtue is that the first layer must be free of the interference. This is why the the layers of a

DLST are along the "diagonals". Nevertheless, this is accompanied by a spectral loss since no symbols will be employed in the left-lower and right-upper parts of transmit signal matrix. The second necessary condition is that the codeword length should be equal to the layer length, or at least that the symbols in each layer can be decoded at a time. This implies that the layer length and the codeword length should be matched. Otherwise, the diversity gain will degrade to be the same as that of HLST.

With all these conditions satisfied, the number of distinct symbols between each pair of layers determines the diversity gain of the DLST. That means, to achieve a large diversity gain, the channel coding with the large free distance should be used for the DLST. With a specific number of transmit antennas, a range of layer lengths can be implemented. Although the longer layer can more likely accommodate the codes with larger free distance, it also results in the larger loss of the spectral efficiency. In fact, the larger number of transmit antennas also means the larger loss of the spectral efficiency [112].

A reasonable choice of the channel coding is the Reed-Solomon code (RS code), which has a great error correction capability. Nevertheless, it can only use modulation with order higher than that of 8PSK and the codeword length is usually greater than or equal to 4. Although using the binary block codes can relax the constraint on the modulation, the free distance of the modulated code may decrease as the exponential function of the order of modulation. An alternative choice is the trellis code whose decision depth is as the same as the layer length. However, the unpleasant fact is that the decision depth is usually the 5 times of the trellis code constraint length.

All these facts reveal that the DLST has a nominal spectral efficiency loss when it is used for systems with the short signal block or large number of transmit antennas. This is also the main reason why the DLST is not applied into realistic communication systems. However, in the sense of performance, DLST is an attractive scheme. It is, in general, a more flexible scheme than the STBC-VBLAST since the STBC has the particular requirement on the dimension and format of the codeword matrix. On the other hand, the computational complexity of the DLST with either trellis codes or RS codes is higher than that of the STBC-VBLAST. We show in the simulations that the DLST with a shortened (4,2) RS code has the similar performance with the (2,2,1) STBC-VBLAST in the (4,4) system. The simulation result of the DLST with the trellis code, which has a decision depth greater than the layer length, verify our statement of the second necessary condition.

5.6 Detection and Performance of the STBC-VBLAST in the Presence of Channel Estimation Error

In this section we will analyze the performance of STBC-VBLAST systems in the absence of ideal CSI. The estimated channel matrix can be expressed as [65], [113]

$$\hat{\mathbf{H}}_l = \mathbf{H}_l + \mathbf{Z}, \tag{5.21}$$

where $\mathbf{Z}$ is the estimation error matrix. Every element of $\mathbf{Z}$ is i.i.d $\mathcal{N}(0, 2\sigma_z^2)$ distributed and $\mathbf{Z}$ is statistically independent of $\mathbf{H}_l$. Thus the elements of $\hat{\mathbf{H}}_l$ are i.i.d $\mathcal{N}(0, 2\sigma_{\hat{h}}^2)$ distributed, where $\sigma_{\hat{h}}^2 = \sigma_z^2 + 0.5$. Similarly, QRD is performed to get $\hat{\mathbf{H}}_l = \hat{\mathbf{Q}}\hat{\mathbf{R}}$. Multiplying the received signal $\mathbf{X}$ in Eq. (5.2) with $\hat{\mathbf{Q}}^H$, we have

$$\hat{\mathbf{Y}}_l = \hat{\mathbf{Q}}^H(\mathbf{H}_l\mathbf{S}_l + \mathbf{W}_l). \tag{5.22}$$

Since the elements of $\hat{\mathbf{H}}_l$ and $\mathbf{H}_l$ are jointly Gaussian, $\mathbf{H}_l$ can be expressed as, conditioned on $\hat{\mathbf{H}}_l$,

$$\mathbf{H}_l = \beta\hat{\mathbf{H}}_l + \Xi, \tag{5.23}$$

where $\beta = 1/(2\sigma_z^2 + 1)$. $\hat{\mathbf{H}}_l$ and Ξ are independent and the elements of Ξ are i.i.d $\mathcal{N}(0, 2\sigma_\Xi^2)$ distributed, where $\sigma_\Xi^2 = \sigma_z^2/(2\sigma_z^2 + 1)$. Substituting Eq. (5.23) into Eq. (5.22), we have

$$\hat{\mathbf{Y}}_l = \beta\hat{\mathbf{R}}\mathbf{S}_l + \hat{\mathbf{Q}}^H\Xi\mathbf{S}_l + \hat{\mathbf{Q}}^H\mathbf{W}_l. \tag{5.24}$$

Based on Eq. (5.24), following the same detection process in Section 5.4, we can obtain the decision statistic, $\hat{\mathbf{Y}}_l^k$, for the kth STBC layer, which is composed of $k' + 1$ to $k' + n$ rows of $\hat{\mathbf{Y}}_l$, where $k' = n_T - (G - k + 1)n$. Then we have

$$\hat{\mathbf{Y}}_l^k = \beta\hat{\mathbf{R}}^k\mathcal{G}_{nl}^k + \mathbf{\Phi}_k, \tag{5.25}$$

where $\mathbf{\Phi}_k$ and $\beta\hat{\mathbf{R}}^k$ are the corresponding virtual channel matrix and noise matrix. Thus $\mathbf{\Phi}_k$ consists of $k' + 1$ to $k' + n$ rows of $\hat{\mathbf{Q}}^H\Xi\mathbf{S}_l + \hat{\mathbf{Q}}^H\mathbf{W}_l$. Note that the columns of $\hat{\mathbf{Q}}$ are orthonormal, $\hat{\mathbf{Q}}^H\Xi$ and $\hat{\mathbf{Q}}^H\mathbf{W}_l$ are still complex Gaussian with the same distribution as Ξ and $\mathbf{W}_l$ respectively. However, the fact that $\hat{\mathbf{Q}}^H\Xi$ is right multiplied by $\mathbf{S}_l$ may result in time correlation between elements of $\mathbf{\Phi}_k$, unless the STBC is square.

To separately detect the symbols in STBC, we apply the decision rules similar to

Eq. (5.12) and Eq. (5.13) though they are suboptimal when STBC is not square. Note that the distribution of (i,j)th element of $\hat{\mathbf{R}}$ is $\mathcal{CN}(0, 2\sigma_{\hat{h}}^2)$, when $i < j$. The square of diagonal element $\hat{R}_{ii}$ has the distribution

$$f_{\hat{R}_{ii}^2}(r) = \frac{(2\sigma_{\hat{h}}^2)^{-(n_R-i+1)}}{\Gamma(n_R - i + 1)} r^{n_R-i} e^{-\frac{1}{2\sigma_{\hat{h}}^2} r}, \quad r \geq 0, \quad i = 1, 2, \ldots, n_T. \tag{5.26}$$

With $E[\mathbf{\Phi}_k(i,j)\mathbf{\Phi}_k^*(i,j)] = 2\sigma_{\Xi}^2 n_T E_s + N_0$, we have the exact PSEP of the kth STBC layer in the M-ary PSK STBC-VBLAST with channel estimation error as

$$P_s^k(e) = \left(\frac{1-\mu}{2}\right)^{d_k} \sum_{i=0}^{d_k-1} \left(\begin{array}{c} d_k - 1 + i \\ i \end{array} \right) \left(\frac{1+\mu}{2}\right)^i, \quad k = 1, 2, \ldots, G, \tag{5.27}$$

where $d_k = n[n_R - n_T + n(G - k + 1)]$. $\mu = \sqrt{\alpha/(1+\alpha)}$, in which

$$\alpha = \frac{\frac{1}{4} a E_s \Delta}{2(n_T E_s + N_0)\sigma_z^2 + N_0}. \tag{5.28}$$

Similarly, PSEP of the kth uncoded layer has the same form as Eq. (5.27) with a different $d_k = n_R - k + 1$, where $k = 1, 2, \ldots, n_T - nG$.

Note that when $E_s/N_0 \to \infty$, $\alpha \to a\Delta/8n_T\sigma_z^2$. This means the performance curve of the STBC-VBLAST has an error floor dependent on σ_z, n_T and d_k, when imperfect channel estimation presents. Eq. (5.27) also shows that the error floor is a decreasing function of d_k. Recalling that $d = \arg\min_k d_k$, it is deduced that error floor is a decreasing function of system diversity gain d. It is expected that Eq. (5.27) is identical to Eq. (5.20), when there is no channel estimation error and SNR is high.

5.7 Tradeoff Between Performance and Spectral efficiency

For a BLAST system, the spectral efficiency can be expressed as $\eta = r_{\text{code}} K n_T$ bits/s/Hz, where K is the number of bits in a modulated symbol and r_{code} is the code rate, e.g., $r_{\text{code}} = 1$ for for uncoded VBLAST systems. For an (n, m, G) STBC-VBLAST system, $\eta = K(n_T - nG + Gr_{\text{STBC}})$ bits/s/Hz, where r_{STBC} is the code rate for STBC. For an $n \times m$ STBC, $r_{\text{STBC}} = N/m \leq 1$. Thus the price to pay for the increment of the minimum diversity gain of the STBC-VBLAST is a reduction in the spectral efficiency by a factor of $G(n - r_{\text{STBC}})/n_T$ with respect to uncoded VBLAST. This value is small when n_T is large. To show the tradeoff between diversity gain and spectral efficiency, we give in Table 5.1 the diversity gain and spectral efficiency of a STBC-VBLAST system, which has n_T transmit and n_R receive antennas and uses G $n \times m$ STBCs.

However, increasing the number of the STBC layers used cannot always trade the spectral efficiency for diversity gain. Note that the diversity gain of the STBC-VBLAST is upper bounded by $n(n_R - n_T) + n^2$, when n_R and n_T are fixed and a particular STBC has been chosen. This implies that a larger G does not necessarily lead to higher diversity gain. On the other hand, a larger G does result in a lower spectral efficiency. The following theorem demonstrates how to choose G to use bandwidth efficiently.

Theorem 5.2. *For an (n, m, G) STBC-VBLAST system having n_T transmit and n_R receive antennas, in order to use the bandwidth efficiently, G should be chosen*

Table 5.1: Summary of the minimum diversity gain and spectral efficiency for the STBC-VBLAST and VBLAST.

Schemes	(n, m, G) STBC-VBLAST	uncoded BLAST
Diversity gain (d)	$\min \left\{ \begin{array}{c} n(n_R - n_T) + n^2, \\ n_R - n_T + Gn + 1 \end{array} \right\}$	$n_R - n_T + 1$
Spectral Efficiency (η)	$K(n_T - nG + Gr_{\text{STBC}})$	Kn_T

such that

$$G \leq G_{th} = n + (n_R - n_T) - \left\lfloor \frac{n_R - n_T + 1}{n} \right\rfloor, \tag{5.29}$$

where $\lfloor (\cdot) \rfloor$ *indicates the largest integer equal to or smaller than* $(\cdot)$.

Proof. Since the diversity gain d of the system is the smaller of $n(n_R - n_T) + n^2$ and $n_R - n_T + nG + 1$, the maximum diversity gain possible by varying G, when n_R, n_T and a particular STBC (i.e., n) have been chosen, is $n(n_R - n_T) + n^2$. Thus the number of STBC layers that maximizes the diversity gain is given by

$$G' = n + (n_R - n_T) - \frac{n_R - n_T + 1}{n}, \tag{5.30}$$

This is because that the diversity gain is $n(n_R - n_T) + n^2$ for any $G > G'$. Imposing the integer constraint on G gives Eq. ((5.29)). $\square$

Remark: Recall from Theorem 5.1 that for an (n, m, G) STBC-VBLAST system having n_T transmit and n_R receive antennas, the diversity gain of the system is $\min\{n(n_R - n_T) + n^2, n_R - n_T + Gn + 1)\}$. For $G < G_{th}$ the diversity gain is $n_R - n_T + Gn + 1$, while for $G \geq G_{th}$, the diversity gain is $n(n_R - n_T) + n^2$. We note that although the (n, m, G) STBC-VBLAST, with $G \geq G_{th}$ has the same diversity gain as the (n, m, G_{th}) STBC-VBLAST, the former has better performance than the latter. However, the difference is very small and can be ignored especially when nG_{th} is large. This conclusion is based on the fact that $(G - G_{th})$ STBCs are used to improved the performance of layers higher than nG_{th}. Even without STBC, these layers already have large diversity gain $d > nG_{th}$, which enables their error probabilities to be much smaller than those of lower layers. Therefore the performance improvement of these layers due to STBC contributes little to the performance of the whole system. It is not worth sacrificing the spectral efficiency for the ignorable performance improvement.

Table 5.1 and Eq. (5.29) indicate that when $G < G_{th}$, the (n_1, m_1, G_1) STBC-VBLAST has the same diversity gain as the (n_2, m_2, G_2) STBC-VBLAST provided $n_1 G_1 = n_2 G_2$. However, their spectral efficiencies are different.

We plot the tradeoff lines of schemes with different (n, G) for systems with $n_T = 9, n_R = 13$ in Fig 5.3. n is chosen to be 2, 3 and 4. For each specific n, G is set to the integers such that $1 \leq G < G_{th}$. QPSK is assumed; $r_{\mathrm{STBC}} = 1$ for $n = 2$ and $r_{\mathrm{STBC}} = 1/2$ for $n = 3, 4$. Each line is connecting points of (d, η) pairs for a specific n with different G (It is straight line since every line between two adjacent points has the same slope). It can be seen that to get the same diversity gain, the schemes with steep slope, i.e., smaller n are preferred. For example, the $(2, 2, 2)$ QPSK STBC-VBLAST is a better choice than the $(4, 4, 1)$ QPSK STBC-VBLAST, since the former has 3 bits/s/Hz more spectral efficiency. It can be seen that the choice of the scheme depends on what diversity gain (data rate) you desire.

We discuss above how to choose G and n to improve performance while using the channel more efficiently. Although the STBC-VBLAST outperforms the VBLAST

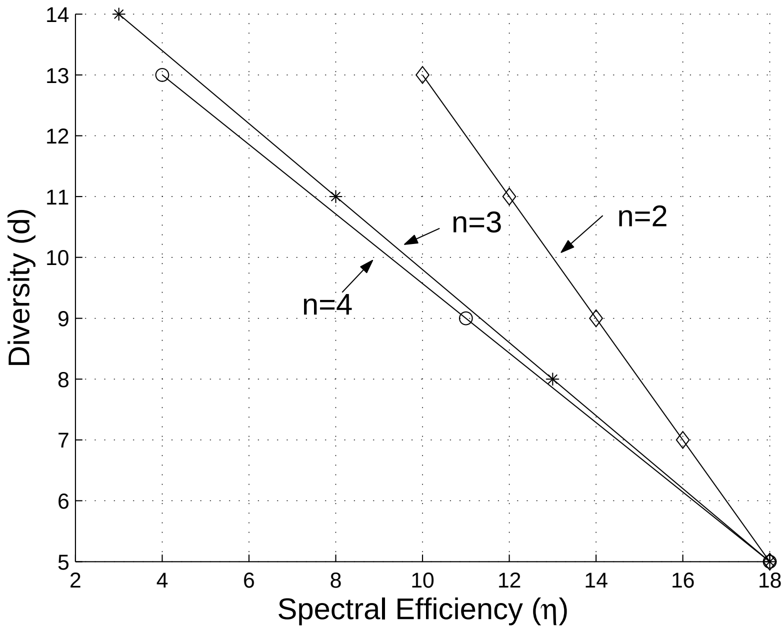

Figure 5.3: Tradeoff lines of different schemes.

considerably, it does suffer a partial spectral efficiency loss compared with uncoded VBLAST. To do a fair performance comparison, we can use a higher modulation for the STBC-VBLAST to ensure that it has a spectral efficiency not less than that of uncoded BLAST systems. It will be shown in Section 5.10 that the STBC-VBLAST still outperforms the existing VBLAST schemes, even with a higher spectral efficiency.

5.8 Complexity Comparison

Profiting from the orthogonal structure of STBC and simplicity of QRD, the STBC-VBLAST has lower computational complexity than ZF-VBLAST and MMSE-VBLAST algorithms which involves complicated calculation of matrix inverse.

We next compare the computational complexities of ZF-VBLAST and the (2,2,1) STBC-VBLAST in the number of multiplications and additions in one STBC interval. One addition and multiplication is counted for one real valued addition and multiplication respectively. The transmitted symbols are assumed to be complex.

For ZF-VBLAST, the computations occur in the detection of each symbol and QR decomposition, which is following the procedure in [104]. The number of multiplications and additions for ZF-VBLAST in one STBC interval are

$$n_T^4 + \left(\frac{2}{3}n_R + \frac{4}{3}\right) n_T^3 + \left(2n_R^2 + n_R - \frac{1}{2}\right) n_T^2 + \left[2n_R^2 + (8m - \frac{1}{3})n_R - \frac{1}{6}\right] n_T \quad (5.31)$$

and

$$\frac{1}{4}n_T^4 + \frac{1}{6}(8n_R + 1)n_T^3 + \left(2n_R^2 - \frac{1}{2}\right) n_T^2 + \left[\left(8m - \frac{1}{3}\right) n_R - \left(2m - \frac{1}{3}\right)\right] n_T \quad (5.32)$$

respectively. Note that the computational complexity of MMSE-VBLAST is even higher.

In addition to the computations in QR decomposition, the computational complexity of the STBC-VBLAST counts the computations in STBC decoding and the detection of symbols in uncoded layers. The number of multiplications for the (2,2,1) STBC-VBLAST is

$$4n_R n_T^2 + n_T + 4n^2 m G^2 + (nm - 4n^2 m)G - m + (4nm + 1)N + n^2 - n, \quad (5.33)$$

and the number of additions for the STBC-VBLAST is

$$(4n_R-1)n_T^2-2n_Rn_T+2(n^2m+n^2)G^2-2n^2mG+(4mn-2)N+n^2-1. \quad (5.34)$$

From Eq. (5.31)∼ Eq. (5.34), we can see that the number of calculations in ZF-VBLAST is of order $O(n_T^4+n_Rn_T^3)$ However, the computational complexity of the STBC-VBLAST is only of order $O(n_Rn_T^2)$. It is obvious that the complexity of the STBC-VBLAST is lower than that of ZF-VBLAST and MMSE-VBLAST. Compared with STTC-VBLAST, the linear decoding of STBC in a STBC-VBLAST system is much simpler than ST Viterbi decoding algorithm whose complexity, in the sense of the trellis states, is the exponential function in the product of the transmission rate and the number of antennas used for the STTC. Similarly, the decoding of HLST, which uses trellis code generally, have higher computational complexity than the STBC-VBLAST, even though without iterative decoding.

5.9 Ordered STBC-VBLAST

Our new STBC-VBLAST system uses the standard QRD to keep the detection complexity low. To take advantage of ordering, we have the ordered STBC-VBLAST, which applies modified SQRD at the receiver. For the ordered STBC-VBLAST, the SQRD [93] is first employed to get the ordering for the upper n_T-nG layers, denoted by **index1**, which is a permutation of $\{1,2,\ldots,n_T-n_G\}$. The ordering of the lowest G STBC layers, denoted by **index2**, is done differently. Based on Eq. (5.12) and Eq. (5.13), the SNR for decoding in each STBC layer is proportional to ρ. Thus the STBC layers are ordered such that the STBC layer with smaller ρ is decoded later. Note that changing the order of n sublayers within each STBC layer does not change the value of ρ. The ordering algorithm is as follows.

Set $\mathbf{R} = 0, \mathbf{Q} = \mathbf{H}_l, \mathbf{index1} = [1, 2, \ldots, n_T - nG]$

Run SQRD [93] to get $\mathbf{index1}, \mathbf{Q}, \mathbf{R}$

Set $\mathbf{index2} = [n_T - nG + 1, n_T - nG + 2, \ldots, n_T]$

For $p = 1, 2, \ldots, G$

$k_p = \arg \min\limits_{g=p,\ldots,G} \sum_{u=1}^{n} \|\mathbf{q}_v\|^2,$

where $v = n_T - n(G - g + 1) + u.$

Exchange columns from $n_T - n(G - p + 1) + 1$

to $n_T - n(G - p)$ with corresponding columns

from $n_T - n(G - k_p + 1) + 1$ to $n_T - n(G - k_p)$

of $\mathbf{Q}$, $\mathbf{R}$ and $\mathbf{index2}$ respectively.

For $i = n_T - n(G - p + 1) + 1, \ldots, n_T - n(G - p)$

$R_{i,i} = \|\mathbf{q}_i\|, \quad \mathbf{q}_i = \mathbf{q}_i / R_{i,i}, \quad R_{i,j} = \mathbf{q}_i^H \mathbf{q}_j,$

$\mathbf{q}_j = \mathbf{q}_j - R_{i,j}\mathbf{q}_i, j = i + 1, \ldots, n_T.$

End

End

With the updated $\mathbf{Q}$ and $\mathbf{R}$, detection is done using Eq. (5.12), Eq. (5.13) and Eq. (5.15). The estimated information symbols are then obtained by reordering the detected symbol sequence according to **index1** and **index2**.

It is no doubt that the computational complexity of the ordered STBC-VBLAST becomes higher, but it is still much lower than that of ZF-VBLAST. To be specific, the number of multiplications and additions for the ordered STBC-VBLAST are

$$\begin{aligned}&4n_Rn_T^2-(2n_R-1)n_T+(n_Rn+4n^2m)G^2+(n_Rn-2n^2m+3nm)G\\&+(4mn+1)N+n(n-1)\end{aligned} \tag{5.35}$$

and

$$\begin{aligned}&(4n_R-1)n_T^2-(4n_R-1)n_T+[4n^2-(m+n_R-\frac{1}{2})]G^2\\&-[2n^2m+(n_R-3m-\frac{1}{2})n]G+(4mn-2)N+n^2-2\end{aligned} \tag{5.36}$$

respectively, which are of the same order as those of the STBC-VBLAST. We summarize the computational complexity of different schemes in Table 5.2.

With the increased complexity, the ordered STBC-VBLAST performs better than the STBC-VBLAST. In fact, the exact diversity gain of the STBC-VBLAST stated in Theorem 5.1 only serves as the lower bound of the diversity gain of the ordered STBC-VBLAST as shown in simulation. This assures that the ordered STBC-VBLAST has more robust performance in the presence of channel estimation errors. The simulations also demonstrate that the threshold in Theorem 5.2 is still applicable for the ordered STBC-VBLAST to get a good tradeoff between performance and spectral efficiency.

Table 5.2: Summary of the computational complexities of the STBC-VBLAST and VBLAST.

Schemes	Order of number of addition/multiplications
ZF-VBLAST	$O(n_T^4 + n_R n_T^3)$
$(2, 2, 1)$ STBC-VBLAST	$O(n_R n_T^2)$
$(2, 2, 1)$ ordered STBC-VBLAST	$O(n_R n_T^2)$

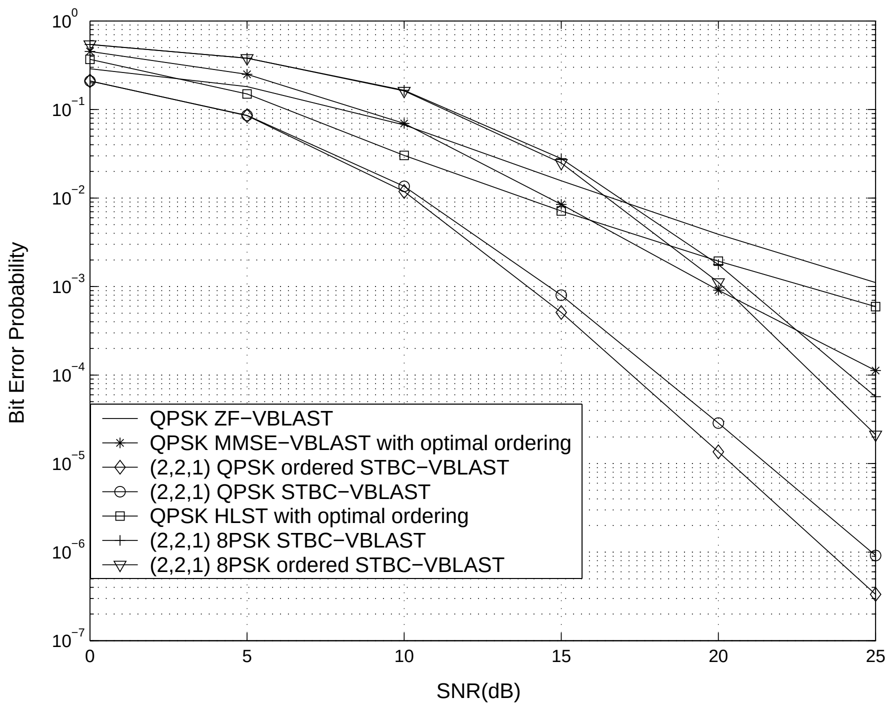

Figure 5.4: Performance comparison of different STBC-VBLAST and VBLAST systems, $n_R = n_T = 4$.

5.10 Simulation Results

In this section, we compare the performance of the new STBC-VBLAST systems with other BLAST systems. The channel is Rayleigh quasi-static fading channel, known or estimated at the receiver. The elements of the channel matrix are modeled as samples of independent complex Gaussian random variables with variance 0.5 per real dimension. The noise is complex white Gaussian with variance $N_0 = E_s n_T/\mathrm{SNR}$, where SNR is signal to noise ratio, E_s is the average symbol energy at each transmit antenna. PSK modulations are used to compare the performance of the different systems with different spectral efficiencies. A rate 1/2 convolutional code, with generator polynomial of (5,7) in octal form, is employed for HLST.

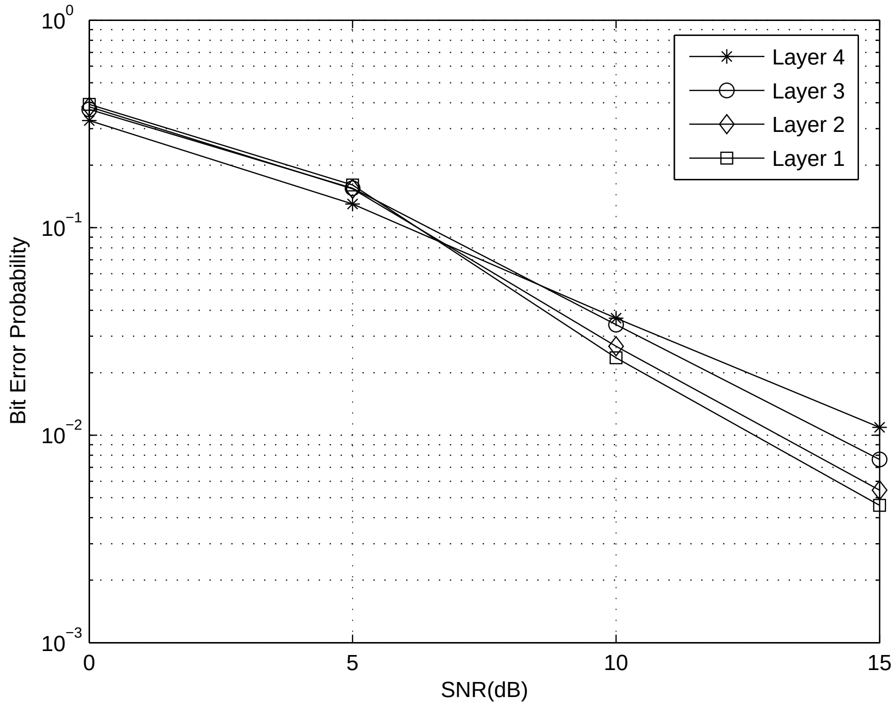

Figure 5.5: Bit error probability of each layer of QPSK HLST, $n_R = n_T = 4$.

Fig. 5.4 shows the bit error probabilities of different BLAST schemes in systems with $n_R = n_T = 4$. The $(2, 2, 1)$ QPSK, 8-PSK STBC-VBLAST and ordered STBC-VBLAST are used for comparison. The Viterbi algorithm and SIC are performed in the decoding and detection of HLST. It can be seen that, as SNR

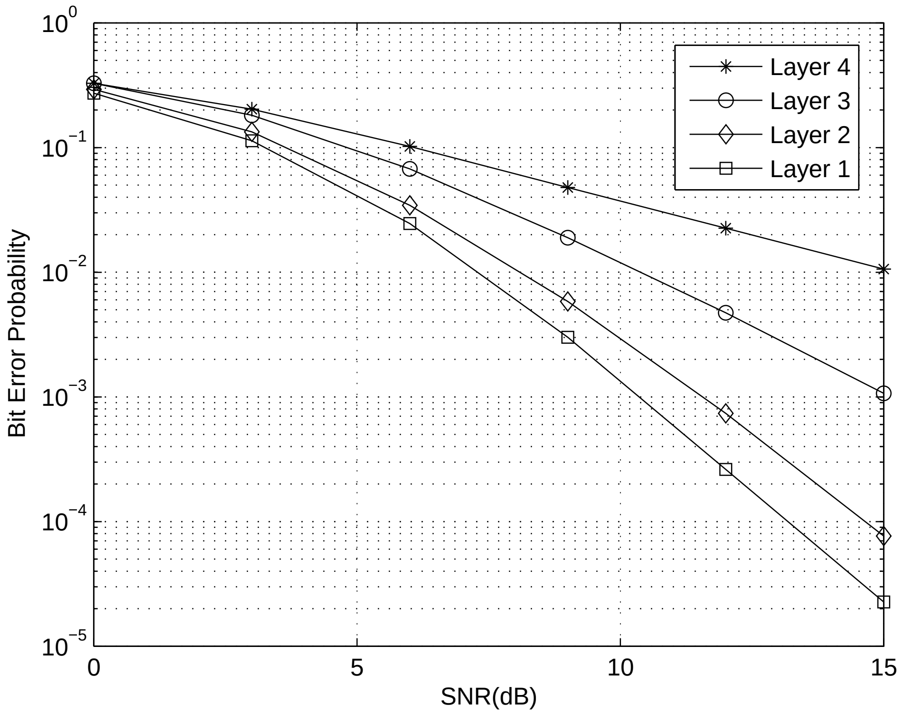

Figure 5.6: Bit error probability of each layer of QPSK HLST with perfect interference cancelation, $n_R = n_T = 4$.

increases, the performance curves for the (ordered) STBC-VBLAST drop much faster than those of others because of the larger diversity gain. There is a very wide gap between performance of the other QPSK VBLAST schemes and the new QPSK STBC-VBLAST, which has little loss of special efficiency. The 8-PSK STBC-VBLAST system with higher bit rate, 9 bits/s/Hz, still outperforms the 8 bits/s/Hz ZF-VBLAST system. The former also has better performance than 8 bits/s/Hz MMSE-VBLAST systems with optimal ordering, at high SNR. The 4 bits/s/Hz QPSK HLST is outperformed by 6 bits/s/Hz QPSK STBC-VBLAST considerably, since it only uses time-dimensional coding without enhancing the diversity gain. It is expected that the ordering results in a better performance for the ordered STBC-VBLAST.

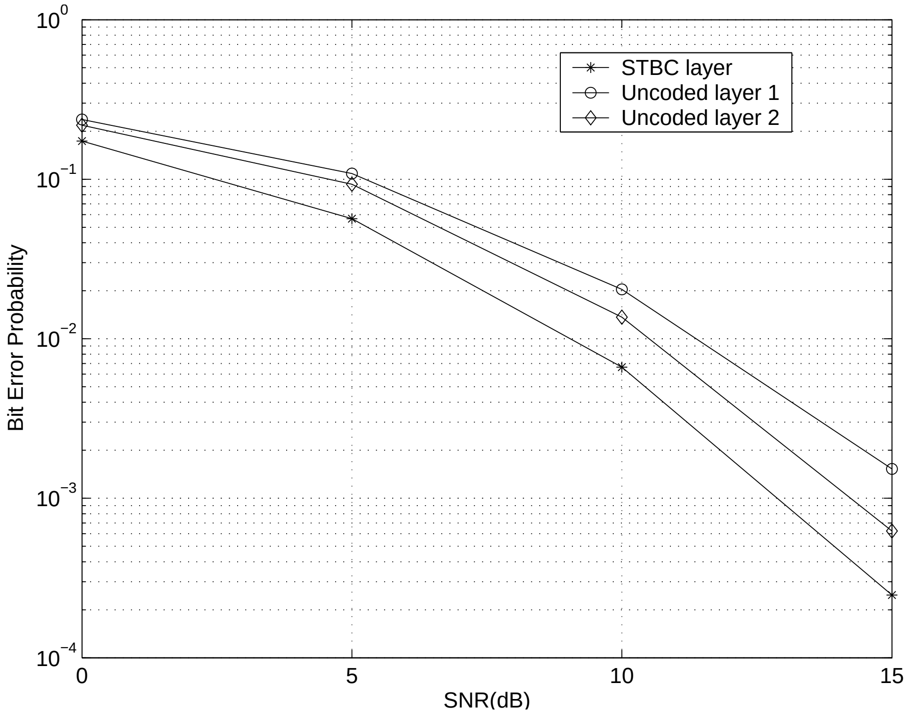

Figure 5.7: Bit error probability of each layer of the (2,2,1) QPSK STBC-VBLAST, $n_R = n_T = 4$.

In Fig. 5.5 $\sim$ Fig. 5.8 we show the new STBC-VBLAST combats the error propagation efficiently by comparing layer performances of the (2,2,1) STBC-VBLAST and HLST. The bit error probability of each layer of the HLST and STBC-VBLAST is presented respectively in Fig. 5.5 and Fig. 5.7. By comparing layer performances of the (2,2,1) STBC-VBLAST and HLST, we show the new STBC-VBLAST combats the error propagation efficiently. Note that there is a crossing behavior of BER curves at about 7dB SNR in Fig. 5.5. The reason for this is that the first layer is free of the interference and the diversity gain does not help much on improving the performance when SNR is not high.

Fig. 5.6 and Fig. 5.8 present the performance for the "genie" case, which means that we perform real interference suppression for each layer, but perfect cancelation

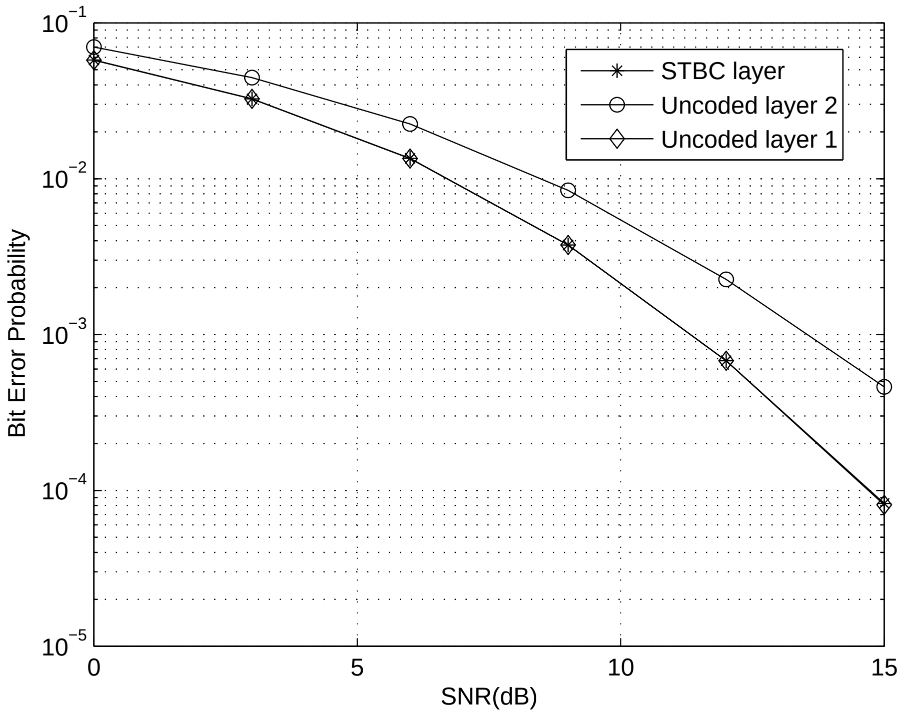

Figure 5.8: Bit error probability of each layer of the (2,2,1) QPSK STBC-VBLAST with perfect interference cancelation, $n_R = n_T = 4$.

is assumed for subsequent layers. It can be seen that layers from 4 to 1 of HLST have diversity gain 1 to 4 respectively in genie case. Similarly, uncoded layer 2 of the STBC-VBLAST has the minimum diversity 3 among all the layers. The curves of STBC layer and uncoded layer 1 coincide exactly if perfect cancelation is assumed, because the two layers have the same SNR when detected.

Comparing Fig. 5.7 and Fig. 5.4, we find that the performance of a STBC-VBLAST system depends on the layer with the minimum diversity gain amongest all layers. This justifies our definition of the system diversity gain as the minimum diversity gain of all the layers. On the other hand, Fig. 5.5 and Fig. 5.4 show that the diversity gain of HLST systems is one, which is the same as that of the lowest layer.

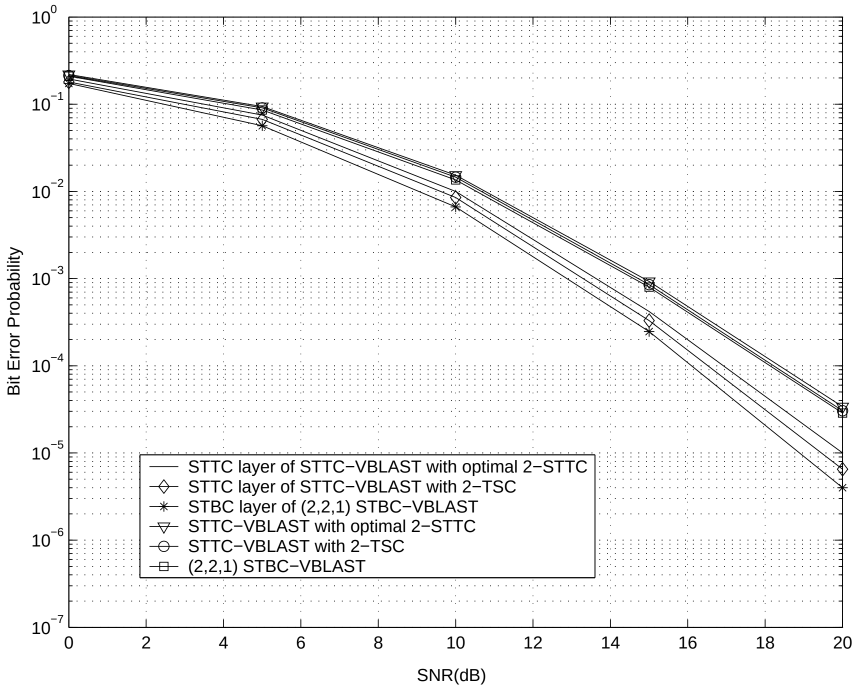

Figure 5.9: Performance comparison of the (2,2,1) QPSK STBC-VBLAST and QPSK STTC-VBLAST using 2-STTCs, $n_R = n_T = 4$.

In Fig. 5.9, we compares $(2, 2, 1)$ STBC-VBLAST with the STTC-VBLAST using one STTC layer. QPSK is used and $n_R = n_T = 4$. Two of STTC are used: one is the optimal 2-STTC (STTC using two transmit antennas, following the notation in [3]) for quasi-static Rayleigh fading, the other is 2-STTC designed by Tarokh *et.al.*, indicated as 2-TSC. The performance curves of the STBC and STTC layers are plotted. It is observed that although STTCs have higher coding gain for Rayleigh fading channel, they show lower coding gain in STTC-VBLAST systems. This also makes the STBC-VBLAST outperform the STTC-VBLAST.

In Fig. 5.10, we compare the performance of the DLST to those of the HLST and STBC-VBLAST. Two DLST schemes are taken into consideration, including the

DLST with a (5,7) trellis code and the DLST with a shortened (4,2) RS code. The HLST also uses the (5,7) trellis code. Since the DLST layer length and the decision depth of the (5,7) trellis code is not matched, it can be seen that the DLST has the same diversity gain as that of the HLST. Nevertheless, the latter has a better performance. This is because that the HLST performs decoding before interference cancellation yet the former does interference cancellation first since the layers are along the diagonals. On the other hand, the DLST with (4,2) RS has the similar performance with the (2,2,1) STBC-VBLAST but slightly higher diversity. However, the spectral efficiency of the DLST is much less than that of the STBC-VBLAST especially when the signal block length is small.

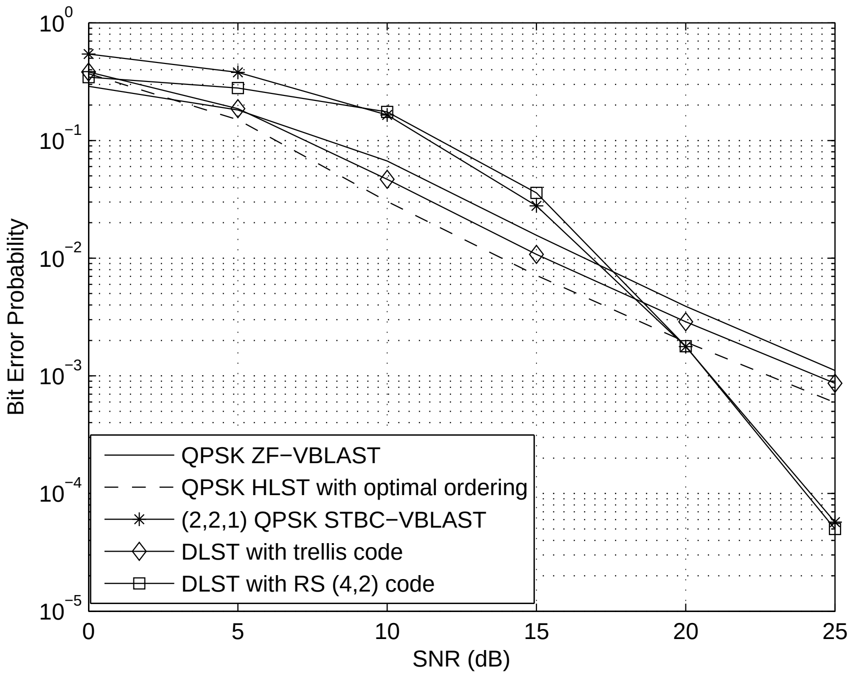

Figure 5.10: Performance comparison of the (2,2,1) STBC-VBLAST , HLST and DLST, $n_R = n_T = 4$.

To verify the result in Section 5.7, we show in Fig. 5.11 the performances of $(2, 2, 1)$, $(2, 2, 2)$ and $(2, 2, 3)$ QPSK (ordered) STBC-VBLAST systems with $n_R = n_T = 6$. Note that $G_{th} = 2$ in this case. It is observed that a $(2, 2, 2)$ STBC-VBLAST system has better performance than that of a $(2, 2, 1)$ STBC-VBLAST system since the former has higher diversity gain. However, performance difference between the $(2, 2, 2)$ and $(2, 2, 3)$ STBC-VBLAST systems is very small, while the $(2, 2, 3)$ STBC-VBLAST has less 2bits/s/Hz spectral efficiency than the $(2, 2, 2)$ STBC-VBLAST. The same happens to the ordered STBC-VBLAST systems. It can be seen that the performance curves of the $(2, 2, 2)$ and $(2, 2, 3)$ STBC-VBLAST converge with the increasing SNR because they share the same diversity gain of 4. Furthermore, the convergence of performance curves of the $(2, 2, 2)$ and $(2, 2, 3)$ ordered STBC-VBLAST demonstrates that G_{th} is also suitable for the ordered STBC-VBLAST.

Finally, the performances of the $(2, 2, 1)$ ordered STBC-VBLAST and ZF-VBLAST, in the presence of channel estimation error, are shown in Fig. 5.12. The number of transmit and receive antennas are both four. Channel to channel estimation error ratio (CER) is defined as $1/2\sigma_z^2$, which is the ratio of variances of channel coefficients and channel estimation error. Performances under four different CERs are presented. It is shown that the channel estimation error results in the error floor in the performance curves. The performance curves of ordered STBC-VBLAST systems have lower error floors than ZF-VBLAST for the higher diversity gain.

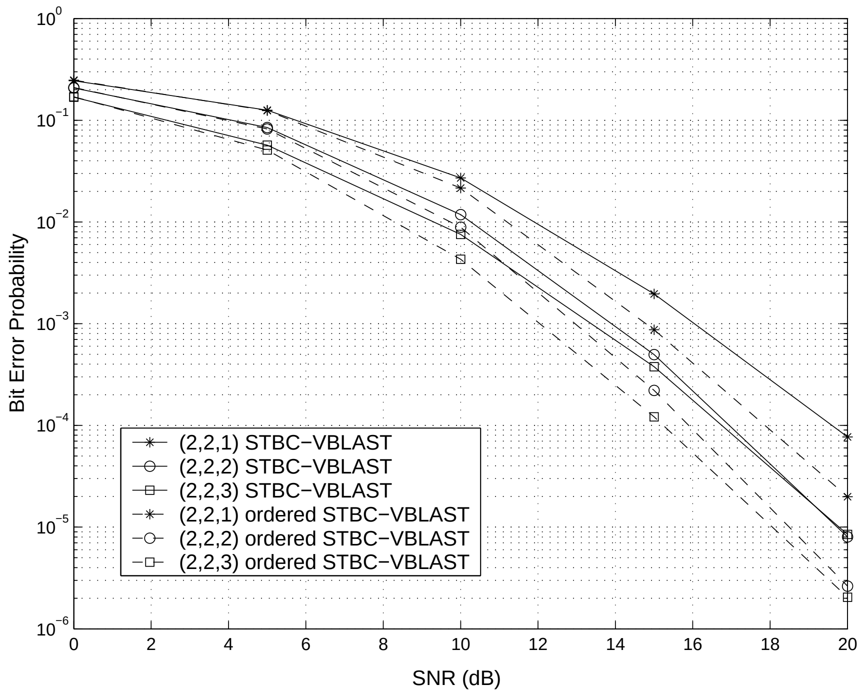

Figure 5.11: Performance comparison of QPSK (ordered) STBC-VBLAST systems using different numbers of STBC layers, $n_R = n_T = 6$.

5.11 Summary

In this chapter, we introduce a new STBC-VBLAST scheme. Due to the the integration of STBC into VBLAST, the (n, m, G) STBC-VBLAST system increase the diversity gain d, to be the minimum of $n(n_R - n_T) + n^2$ and $n_R - n_T + Gn + 1$, which is much higher than $n_R - n_T + 1$ for VBLAST system.

Although a part of the spectral efficiency is lost because of the use of STBC, the loss can be minimized by properly choosing the number of group G. A threshold G_{th} is obtained such that a good tradeoff between diversity gain and spectral efficiency will be achieved if $G \leq G_{th}$. With appropriately selected G and higher-order modulation, the STBC-VBLAST systems still perform better, even with higher

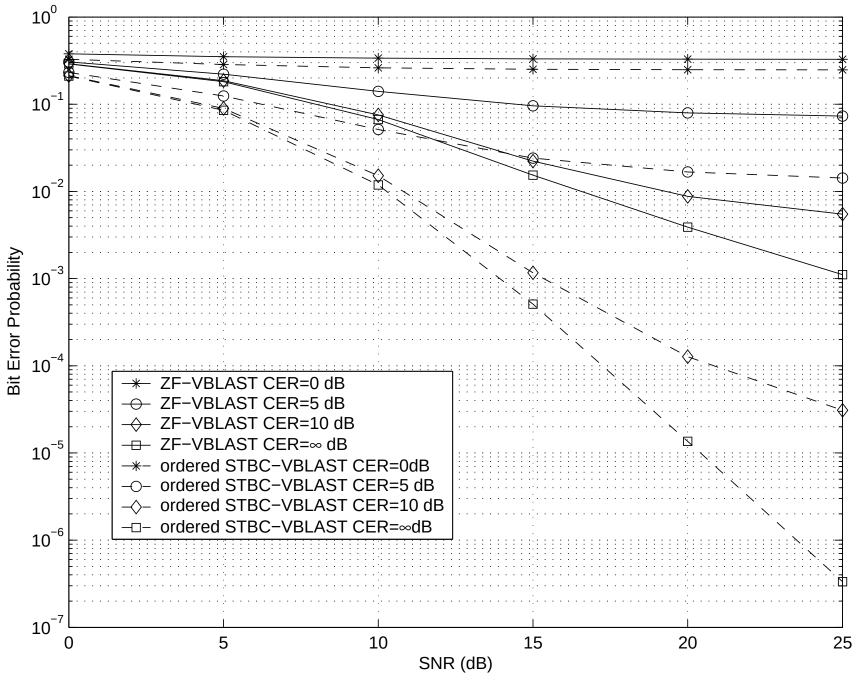

Figure 5.12: Bit error probabilities of the (2,2,1) QPSK ordered STBC-VBLAST and ZF-VBLAST in the presence of channel estimation error, $n_R = n_T = 4$.

spectral efficiency, at moderate to high SNRs due to the high diversity gain.

Also benefiting from the large d, the STBC-VBLAST shows more robust performance when unperfect channel estimation presents, since the error floor is a decreasingly function of diversity gain d. In addition, because of the linear decoding of the STBC and simplicity of QRD, the computational complexity of the new system is of order $O(n_R n_T^2)$, compared to $O(n_T^4)$ for ZF-VBLAST.

In order to obtain more gain from ordering, we also consider the ordered STBC-VBLAST with modified SQRD. The simulations demonstrate that it outperforms the STBC-VBLAST due to higher diversity gain. However, the method to get threshold of G for the STBC-VBLAST is still appropriate for the ordered STBC-VBLAST.

Chapter 6

Conclusions

In this thesis, the STTC design for multiuser systems under different fading situations is studied. Optimal codes are obtained based on the specific code design criteria, which show better performance than the existing STCs. Combining VBLAST and STBC, a new STBC-VBLAST scheme is proposed with a good performance as well as a high data rate. It is demonstrated that the STBC-VBLAST not only achieves a very good tradeoff between the spectral efficiency and performance but has low computational complexity.

The STC design for multiuser composite fading systems is discussed, in which some users undergo quasi-static fading, while the others experience rapid fading. The analysis of the pairwise error probability demonstrates that the rank and non-zero eigenvalues of a codeword distance matrix $\mathbf{A}$ determine the performance of the system, which is the sum of two matrices: one characterizing quasi-static fading and the other characterizing rapid fading. Based on further matrix analysis, two code design criteria are obtained first, for the case that all the users do not have the same number of transmit antennas. It is shown that the minimum rank and non-zero eigenvalues of codeword distance matrices for both quasi-static and rapid fading from each user's code set should be maximized. When all the users are equipped with the same number of transmit antennas, the code design criteria will be simplified since there exits only one code set. According to the criteria, we obtain the optimal QPSK STTCs for a two-user composite fading system through exhaustive searching. It is shown that the new codes have better performance than the existing STBCs and STTCs in composite fading channels.

In order to get more general STC design criteria that are suitable for a wide range of fading situations, we analyze the error performances of different correlated fading channels. It is demonstrated that the diversity gain and coding gain are determined by the channel correlation matrix, the coding gain, and the diversity gain of individual user. The fact that users are independent of each other implies that all users should use the same code set and code design for multiuser systems is equivalent to the code design for single user systems. Without any assumption on the dimension of the codeword matrix and the rank of correlation matrix, we proved that the STC achieving full diversity in quasi-static fading systems can also achieve full diversity in temporally correlated fading systems. The upper bound of the coding gain depends on the product of the norms of codeword difference matrix's nonzero column vectors. It is additionally lower bounded by the product of the nonzero eigenvalues of the codeword distance matrix when the diversity gain is equal to the minimum rank of codeword distance matrices as well as the minimum number of the nonzero columns of codeword difference matrices.

For the fading channel with spatial correlation but no temporal correlation, it is shown that the diversity gain is upper bounded by the product of the minimum number of the nonzero columns of the code difference matrices and the minimum rank of space correlation matrices. The performance analysis for MIMO tempo-spatially correlated fading systems exhibits that the number of, together with the product of the norms of, nonzero column vectors of code difference matrices are desired to be maximized. These results indicate that the code design for the last two cases is reduced to the code design for rapid fading channels. Based on these code design criteria, we obtain a set of general code design criteria suitable for all three fading situations. Accordingly, the optimal STTCs are obtained through computer searching showing more robust performance than other STTCs.

The VBLAST scheme can be used to exploit the capacity potential provided by the multiple transmit antenna systems. However, SIC used in VBLAST detection degrades performance because of the small minimum diversity gain and error propagation. Although the ordered ZF or MMSE is applied to improve the performance, such as in ZF-VBLAST or MMSE-VBLAST, the computational complexity is high, since the calculation of matrix inverse is involved. In this thesis, we introduce a new STBC-VBLAST scheme. Due to the the linear decoding of STBC and simplicity of QRD, the computational complexity of the new system is of order $O(n_R n_T^2)$, compared to $O(n_T^4)$ for ZF-VBLAST.

Both theoretical analysis and simulations show that the (n, m, G) STBC-VBLAST system has much better performance than other VBLAST systems since it increases the exact system diversity gain d to be the minimum of $n(n_R - n_T) + n^2$ and $n_R - n_T + Gn + 1$. From the fact that d is upper bounded by $n(n_R - n_T) + n^2$ when n_R and n_T are fixed and a particular STBC has been chosen, it is proved that the number of the STBC layers should not be greater than a threshold G_{th} to use the bandwidth efficiently.

Although a part of the spectral efficiency is lost compared to the uncoded VBLAST because STBC is used, it can be compensated by using the higher-order modulation. With appropriately selected G and high diversity gain, the STBC-VBLAST system still performs better than existing VBLAST systems at moderate to high SNRs, even with higher spectral efficiency.

The analysis of the performance under imperfect channel CSI indicates that the error floor exits since there is a fixed noise increment coming from the channel estimation errors. The error floor of the STBC-VBLAST is much lower than those of other VBLAST systems due to the higher d.

To further improve the performance, we also consider the ordered STBC-VBLAST with modified SQRD instead of standard QRD. The ordered STBC-VBLAST has higher diversity gain with a little increment of the computational complexity, which is however, in the same order as that of the STBC-VBLAST. It is also demonstrated by simulations that the theorem for calculating Gth for the STBC-VBLAST still holds for the ordered STBC-VBLAST.

Based on the work of this thesis, the following topics are worthwhile for further research.

As we mentioned in Chapter 5, the STTC-VBLAST is the counterpart of the STBC-VBLAST, which integrated STTC to the lower layers of VBLAST. It is attractive because a STTC can supply the same diversity gain as but higher coding gain than a STBC generally. However, since the virtual channel after the QRD is not Rayleigh, the STTC code design for STTC-VBLAST cannot be based on the criteria obtained in previous research. It is worthy to investigate the STTC design for STTC-VBLAST system to obtain the optimal performance.

When the STBC-VBLAST is used for a multiuser uplink channel, QRD can hardly be applied directly since the total number of transmit antennas is usually greater than the number of antennas at receiver. It is reasonable to partially suppress the interference before QRD is used for the desired users or layers. The problem that how to apply the group interference suppression together with QRD to have the best performance is an interesting topic for consideration. This may also give hints on how to choose the number of STBCs for each user to use the bandwidth efficiently in this circumstance.

Note that the ML joint decoding and detection are used when code design for multiuser systems is studied in this thesis. When suboptimal multiuser detection is employed at the receiver. The design criteria may be different since the interference suppression or cancellation is used, similar to the case of STTC-VBLAST. It is desirable to investigate the code performance and code design under this circumstance.

Bibliography

[1] G. J. Foschini and M. J. Gans, "On limits of wireless communications in a fading environment when using multiple antennas," *Wireless Personal Communication*, vol. 6, pp. 311–335, Mar. 1998.

[2] E. Telatar, "Capacity of multi-antenna gaussian channels," *Technical Report, AT&T Bell Labs*, vol. 10, June 1995.

[3] V.Tatokh, N. Seshadri, and A. Calderbank, "Space-time codes for high data rate wireless communication: performance criterion and code construction," *IEEE Trans. Inform. Theory*, vol. 44, pp. 744–765, Mar. 1998.

[4] V. Tarokh, H. Jfarkhani, and A. Calderbank, "Space-time block codes from orthogonal designs," *IEEE Trans. Inform. Theory*, vol. 45, pp. 1456–1467, 1999.

[5] A. F. Naguib, N. Sechadri, and R. Calderbank, "Space-time coding and signal processing for high date rate wireless communications," *IEEE Signal Processing Mag.*, vol. 17, pp. 76–92, Mar. 2000.

[6] G. J. Foschini, "Layered space-time architecture for wireless communication in a fading environment when using multielement antennas," *Bell Labs Tech. J.*, pp. 41–59, 1996.

[7] G. Golden, R. Valenzuela, P. Wolniansky, and G. J. Foschini, "V-BLAST: an architecture for realizing very high data rates over the rich-scattering wireless channel," in *International Symposium on Signals, Systems, and Electronics*, Sept. 1998, pp. 295–300.

[8] G. Foschini, D. Chizhik, M. J. Gans, C. Papadias, and R. R. A. Valenzuela, "Analysis and performance of some basic space-time architectures," *IEEE J. Select. Areas Commun.*, vol. 21, pp. 303–320, Apr. 2003.

[9] D. Gesbert, M. Shafi, D. S. Shiu, P. J. Smith, and A. Naguib, "From theory to practice: an overview of MIMO space-time coded wireless systems," *IEEE J. Select. Areas Commun.*, vol. 21, pp. 281–302, Apr. 2003.

[10] J. W. C. Jakes, *Microwave Mobile Communications.* John Wiley & Sons, 1994.

[11] Z. Chen, J. Yuan, and B. Vucetic, "Imroved space-time trellis coded modulation scheme on slow Rayleigh fading channels," *IEE Electronics Letters*, vol. 37, pp. 440–442, Apr. 2001.

[12] M. Tao and R. S. Cheng, "Improved design criteria and new trellis codes for space-time coded modulation in slow flat fading channels," *IEEE Commun. Lett.*, vol. 5, pp. 314–315, July 2001.

[13] B. K. Ng and E. S. Sousa, "On bandwidth-efficient multiuser-space-time signal design and detection," *IEEE J. Select. Areas Commun.*, vol. 20, pp. 320–329, Feb. 2002.

[14] S. Siwanogsatham, M. Fitz, and J. H. Grimm, "A new view of performance analysis of transmit diversity schemes in correlated Rayleigh fading," *IEEE Trans. Inform. Theory*, vol. 48, pp. 950–956, Apr. 2002.

[15] H. E. Gammal, "On the robustness of space-time coding," *IEEE Trans. Signal Processing*, vol. 50, pp. 2417–2428, Oct. 2002.

[16] S. Siwanogsatham and M. Fitz, "Robust space-time codes for correlated Rayleigh fading channels," *IEEE Trans. Signal Processing*, vol. 50, pp. 2408–2416, Oct. 2002.

[17] W. Su, Z. Safar, and K. J. R. Liu, "Diversity analysis of space-time modulation over time-correlated Rayleigh fading channels," *IEEE Trans. Inform. Theory*, vol. 50, pp. 1832–1840, Aug. 2004.

[18] K. L. Lo, S. Marinkovic, Z. Chen, and B. Vucetic, "Performance comparison of layered space time codes," in *Proc. IEEE International Conf. Commun.*, May 2002, pp. 1382–1387.

[19] S. Verdu, *Multiuser Detection.* Cambridge University Press, 1998.

[20] G. D. Golden, G. J. Foschini, R. A. Valenzuela, and P. W. Wolniansky, "Detection algorithm and initial laboratory results using v-blast space-time communication architecture," *Electron. Lett.*, vol. 35, pp. 14–16, Nov. 1998.

[21] S. Baro, G. Bauch, A. Pavlic, and A. Semmler, "Improving blast performance using space-time block codes and turbo decoding," in *Proc. IEEE Globecom*, Dec. 2000, pp. 1067–1071.

[22] D. Shiu and J. Kahn, "Layered space-time codes for wireless communications using multiple transmit antennas," in *Proc. IEEE International Conf. Commun.*, June 1999, pp. 436–440.

[23] M. Tao and R. S. Cheng, "Generalized layered space-time codes for high data rate wireless communications," *IEEE Trans. Commun.*, vol. 3, pp. 1067–1075, July 2004.

[24] R. G. Gallager, *Information Theory and Reliable Communication.* Wiley, 1968.

[25] M. Schwarts, W. Bennett, and S. Stein, *Communication Systems and Techniques.* McGraw-Hill, 1966.

[26] M. Simon and M. Alouini, *Digital Communication over Fading Channels: A Unified Approach to Performance Analysis.* John Wiley & Sons, 2000.

[27] J. G. Proakis, *Digital Communications*, 4th ed. McGraw-Hill, 2001.

[28] T. Rappaport, *Wireless Communications: Principles and Practice*, 2nd ed. Prentice Hall, 2001.

[29] S. K. et al, "Base station polarization diversity reception for mobile radio," *IEEE Trans. Veh. Technol.*, vol. 33, pp. 301–306, Nov. 1985.

[30] P. Baiaban and E. A. Sweedyk, "Angle diversity with two antennas and experimental results," in *Proc. IEEE International Conf. Commun.*, 1986, pp. 400–406.

[31] T. Eng, N. Kong, and L. B. Milstein, "Comparison of diversity combining technieqies for Rayleigh fading channels," *IEEE Trans. Commun.*, vol. 44, pp. 1117–1129, Sept. 1996.

[32] A. Wittneben, "Base station modulation diversity for digital simulcast," in *Proc. IEEE Vehicular Technology Conf.*, St Louis, May 1991, pp. 848–853.

[33] H. Olofsson, M. Almgren, and M. Hook, "Transmitter diversity with antenna hopping for wireless communication," in *Proc. IEEE Vehicular Technology Conf.*, May 1997, pp. 1743–1747.

[34] A. Hiroike, F. Adachi, and N. Nakajima, "Combined effects of phase sweeping transmitter diversity and channel coding," *IEEE Trans. Veh. Technol.*, vol. 41, pp. 170–176, 1992.

[35] J. Winters, "Switched diveristy with feedback for DPSK mobile radio systems," *IEEE Trans. Veh. Technol.*, vol. 32, pp. 134–150, 1983.

[36] A. Hottinen and R. Wichman, "Transmit divesity by antenna selection in CDMA downlink," in *Proc. IEEE 5th Inter. Symp. Spread Spectrum Tech. App*, Sept. 1998, pp. 767–770.

[37] R. Heath and A. Paulraj, "A simple scheme for transmit diversity using partial channel feedback," in *Proc. Asilomar Conf. Signals, Systems, and computers*, Pacific Grore, CA, Nov. 1998, pp. 1073–1078.

[38] N. Seshadri and J. H. Winters, "Two signaling schemes for improving the error performance of frequency division duplex (FDD) transmission systems using transmitter antenna diversity," in *Proc. IEEE Vehicular Technology Conf.*, May 1993, pp. 508–511.

[39] A. Wittneben, "A new bandwidth efficient transmit antenna modulation diversity scheme for linear digital modulation," in *Proc. IEEE International Conf. Commun.*, 1993, pp. 1630–1634.

[40] J. Guey, M. P. Fitz, M. R. Bell, and W. Y. Kuo, "Signal design for transmitter diversity wireless communication systems over Rayleigh fading channels," Atalanta, GA, Apr. 1996, pp. 136–140.

[41] S. Baro, G. Bauch, and A. Hansmann, "Improved codes for space-time trellis-coded modulation," *IEEE Commun. Lett.*, vol. 4, pp. 20–22, Jan. 2000.

[42] J. Grimm, M. P. Fitz, and J. V. Krogmeier, "Further results in space-time coding for Rayleigh fading," in *Proc. 36th Annual Allerton Conf. on Communication, Control, and Computing*, Monticello, Illinois, USA, Sept. 1998, pp. 391–400.

[43] R. S. Blum, "Some analytical tools for design of space-time convolutional codes," *IEEE Trans. Commun.*, vol. 50, pp. 1593–1599, Oct. 2002.

[44] D. M. Ionescu, K. K. Mukkavilli, Z. Yan, and J. Lilleberg, "Improved 8- and 16-state space-time codes for 4PSK with two transmit antennas," *IEEE Commun. Lett.*, vol. 5, pp. 301–303, July 2001.

[45] W. Firmanto, B. Vucetic, and J. Yuan, "Space-time TCM with improved performance on fast fading channels," *IEEE Commun. Lett.*, vol. 5, pp. 154–156, Apr. 2001.

[46] B. Vucetic and J. Yuan, *Space-time Coding.* John Wiley & Sons, 2003.

[47] Q. Yan and R. S. Blum, "Optimum space-time convolutional codes," in *Proc. IEEE WCNC*, Sept. 2000.

[48] J. A. R. Hammons and H. E. Gammal, "On the theory of space-time codes for PSK modulation," *IEEE Trans. Inform. Theory*, vol. 46, pp. 524–542, Mar. 2000.

[49] Z. Safar and K. J. F. Liu, "Systematic space-time trellis code design for an arbitrary number of transmit antennas," in *Proc. IEEE Vehicular Technology Conf.*, 2001, pp. 8–12.

[50] Z. Chen, J. Yuan, and B. Vucetic, "An imroved space-time trellis coded modulation scheme on slow Rayleigh fading channels," in *Proc. IEEE International Conf. Commun.*, June 2001, pp. 1110–1116.

[51] J. Yuan, Z. Chen, B. Vucetic, and W. Firmanto, "Performance and design of space-time coding in fading channels," *IEEE Trans. Commun.*, vol. 51, pp. 1991–1996, Dec. 2003.

[52] Z. Chen, B. Vucetic, J. Yuan, and K. L. Lo, "Space-time trellis codes for 4-PSK with three and four transmit antennas in quasi-static flat fading channels," *IEEE Commun. Lett.*, vol. 6, pp. 67–69, Feb. 2002.

[53] S. Alamouti, "A simple transmitter diversity scheme for wireless communications," *IEEE J. Select. Areas Commun.*, vol. 12, pp. 1451–1458, Oct. 1998.

[54] H. Jafarkhani and A. R. Calderbank, "Space-time block coding for wireless communications: performance results," *IEEE J. Select. Areas Commun.*, vol. 17, pp. 451–460, Mar. 1999.

[55] G. Ganesan and P. Stoica, "Space-time diversity using orthogonal and amicable orthogonal designs," *Wireless Personal Commun.*, vol. 18, pp. 165–178, Aug. 2001.

[56] H. Jafarkhani, "A quasi-orthogonal space-time block code," *IEEE Trans. Commun.*, vol. 49, pp. 1–4, Jan. 2001.

[57] O. Trikkonen, A. Boariu, and A. Hottinen, "Minimal nonorthogonality rate one space-time block code for 3+ antennas," in *Proc. IEEE Int. Symp. Spread Spectrum Technology*, 2000, pp. 429–432.

[58] O. Tirkkonen and A. Hottinen, "Improved MIMO performance with nonorthogonal space-time block codes," in *IEEE Globecom*, Nov. 2001, pp. 1122–1126.

[59] M. O. Damen, K. Abed-Meraim, and J. C. Belfiore, "Diagonal algebraic space-time block codes," *IEEE Trans. Inform. Theory*, vol. 48, Mar. 2002.

[60] J. H. E. Gamaland A. R. Hammons, "On the design of algebraic space-time codes for MIMO block-fading channels," *IEEE Trans. Inform. Theory*, vol. 49, Jan. 2003.

[61] Y. Liu, M. P. Fitz, and O. Y. Takeshita, "Space-time codes performance criteria and design for frequency selective fading channels," in *Proc. IEEE International Conf. Commun.*, June 2001, pp. 2277–2292.

[62] H. E. Gamal, J. A.R. Hammons, Y. Liu, M. P. Fitz, and O. Y. Takeshita, "On the design of space-time and space-frequency codes for MIMO frequency-selective fading channels," *IEEE Trans. Inform. Theory*, vol. 49, pp. 2800–2804, Sept. 2003.

[63] Z. Liu, X. Ma, and G. Giannakis, "Space-time coding and kalman filtering for diversity transmissions through doubly-selective fading channels," in *Proc. of MILCOM Conf*, Oct. 2000, pp. 1529–1539.

[64] Z. Liu, G. B. Giannakis, and B. L. Hughes, "Double differential space-time block coding for time-selective fading channels," *IEEE Trans. Commun.*, vol. 49, pp. 1529–1539, Sept. 2001.

[65] V. Tarokh, A. Naguib, N. Seshadri, and A. R. Calderbank, "Space-time codes for high data rate wireless communication: performance criteria in the presence of channel estimation errors, mobility and multiple paths," *IEEE Trans. Commun.*, vol. 47, pp. 199–206, Feb. 1999.

[66] R. H. Clarke, "A statistical theory for mobile-radio reception," *Bell System Technical Journal*, pp. 957–1000, July 1968.

[67] T. A. Chen, M. P. Fitz, W. Y. Kuo, and M. D. Zoltowski, "A space-time model for frequency nonselective Rayleigh fading channels with applications

to space-time modems," *IEEE J. Select. Areas Commun.*, vol. 18, pp. 1175–1190, July 2000.

[68] D. S. Shiu, D. Foschini, M. Gans, and J. Kahn, "Fading correlation and its effect on the capacity of multi-element antenna systems," *IEEE Trans. Commun.*, vol. 48, pp. 502–513, Mar. 2000.

[69] H. Bolcskei and A. J. Paulraj, "Performance of space-time codes in the presence of spatial fading correlation," in *Proc. Asilomar Conf. Signals, Systems, Computers*, Pacific Grove, CA, Oct. 2000, pp. 687–693.

[70] C. Fragouli, N. Al-Dharir, and W. Turin, "Effect of spatio-temporal channel correlation on the performance of space-time codes," in *Proc. IEEE International Conf. Commun.*, Apr. 2002, pp. 826–830.

[71] A. Safar and K. J. R. Liu, "Performance analysis of space-time codes over correlated Rayleigh fading channels," in *Proc. IEEE International Conf. Commun.*, May 2003, pp. 3185–3189.

[72] L. T. Younkins, W. Su, and R. Liu, "On the robustness of space-time coding for spatially and temporally correlated wireless channels," in *Proc. IEEE WCNC*, 2004, pp. 587–592.

[73] M. Godbout and H. Leib, "Space-time modulation and coding over transmit correlated fading channels," *IEEE Trans. Wireless Commun.*, vol. 3, pp. 1405–1410, Sept. 2004.

[74] Z. Hong and B. L. Hughes, "Robust space-time codes for time-selective fading," in *Proc. Information Theory Workshop*, Sept. 2001, pp. 112–114.

[75] W. Su, Z. Safar, and K. J. R. Liu, "Space-time signal design for time-correlated Rayleigh fading channels," in *Proc. IEEE International Conf. Commun.*, May 2003, pp. 3175–3179.

[76] B. M. Hochwald and T. L. Marzetta, "Unitary space-time modulation for multiple-antenna communications in Rayleigh flat fading," *IEEE Trans. Inform. Theory*, vol. 46, pp. 543–564, Mar. 2000.

[77] B. H. Hochwald, T. L. Marzetta, and T. J. Richardson, "Systematic design of unitary space-time constellations," *IEEE Trans. Inform. Theory*, vol. 46, pp. 1962–1973, Sept. 2000.

[78] V. Tarokh and H. Jafarkhani, "A differential detection scheme for transmit diversity," *IEEE J. Select. Areas Commun.*, vol. 47, pp. 1169–1174, July 2000.

[79] B. L. Hughes, "Differential space-time modulation," *IEEE Trans. Inform. Theory*, vol. 46, pp. 2567–2578, Nov. 2000.

[80] B. M. Hochwald and W. Sweldens, "Differential unitary space-time modulation," *IEEE Trans. Commun.*, vol. 48, pp. 2041–2052, Dec. 2000.

[81] D. Gu and C. Leung, "Performance analysis of transmit diversity schemes with imperfect channel estimation," vol. 39, Feb. 2003, pp. 402–403.

[82] X. Wang and H. V. Poor, "Space-time multiuser detection in multipath CDMA channels," *IEEE Trans. Signal Processing*, vol. 47, pp. 2356–2374, Sept. 1999.

[83] A. Dua, U. B. Desai, and R. K. Mallik, "Minimum probability of error-based methods for adaptive multiuser detection in multipath ds-cdma channels," *IEEE Trans. Wireless Commun.*, vol. 3, pp. 939–948, May 2004.

[84] E. A. Fain and M. K. Varanasi, "Diveristy order gain for narrow-band multiuser communication with pre-combining group detection," *IEEE Trans. Commun.*, vol. 48, pp. 533–536, Apr. 2000.

[85] A. M. Tehrani, R. Negi, and J. Cioffi, "Space-time coding over a code division multiple access system," in *Proc. IEEE WCNC*, Sept. 1999, pp. 134–138.

[86] J. Geng, U. Mitra, and M. Fitz, "Optimal space-time block codes for CDMA systems," in *Proc. MILCOM*, Oct. 2000, pp. 387–391.

[87] G. C. Briones and C. Rodriguez, "On multiuser receiver performance analysis and code design for space-time coded DS-CDMA systems," in *The 5th International Symposium on Wireless Personal Multimedia Communications*, Oct. 2002, pp. 701–705.

[88] B. Hochwald, T. L. Marzetta, and C. B. Papadias, "A transmitter diversity scheme for wideband CDMA systems based on space-time spreading," *IEEE J. Select. Areas Commun.*, vol. 19, Jan. 2001.

[89] V. DaSilva and E. Sousa, "Fading-resistant modulation using serveral transmitter antennas," *IEEE Trans. Commun.*, vol. 45, pp. 1236–1244, Oct. 1997.

[90] G. J. Foschini, G. D. Golden, R. A. Valenzuela, and P. W. Wolnianski, "Simplified processing for high spectral efficiency wireless communication

employing multi-element arrays," *IEEE J. Select. Areas Commun.*, vol. 17, pp. 1841–1852, Nov. 1999.

[91] H. H. X. Li, G. J. Foschini, and R. A. Valenzuela, "Effects of iterative detection and decoding on the performance of blast," in *Proc. IEEE Globecom*, Dec. 2000, pp. 1061–1066.

[92] E. Biglieri, G. Taricco, and A. Tulino, "Decoding space-time codes with blast architectures," *IEEE Trans. Signal Processing*, vol. 50, pp. 2547–2552, Oct. 2002.

[93] D. Wubben, J. Rinas, R. Bohnke, V. Kuhn, and K. D. Kammeyer, "Efficient algorithm for decoding layered space-time codes," *IEE Electronic Letters*, vol. 37, pp. 1348–1350, Oct. 2001.

[94] H. E. Gammal and E. Geraniotis, "A new approach to layered space-time coding and signal processing," *IEEE Trans. Inform. Theory*, vol. 47, pp. 2321–2334, Sept. 2001.

[95] P. Alexander, M. Reed, J. Asenstorfer, and C. Schlegel, "Iterative multiuser interference reduction: turbo CDMA," *IEEE Trans. Commun.*, vol. 47, pp. 1008–1014, July 1999.

[96] S. Marinkovic, B. Vucetic, and A. Ushirokawa, "Space-time iterative and multi-stage receiver stuctures for CDMA mobile communication systems,," *IEEE J. Select. Areas Commun.*, vol. 19, pp. 1594–1604, Aug. 2001.

[97] F. R. Farokhi, G. J. Foschini, and R. A. Valenzuela, "Link-optimal space-time processing with multiple transmit and recive antennas," *IEEE Commun. Lett.*, vol. 5, pp. 241–267, 2001.

[98] X. Lin and R. S. Blum, "Improved space-time codes using serial concatenation," *IEEE Commun. Lett.*, vol. 4, pp. 221–223, July 2000.

[99] G. Bauch, "Concatenation of space-time block codes and turbo-TCM," in *Proc. IEEE International Conf. Commun.*, 1999, pp. 1202–1206.

[100] A. Abdi and M. Kaveh, "A space-time model for multielement antenna systems in mobile fading channels," *IEEE J. Select. Areas Commun.*, vol. 20, pp. 550–560, Apr. 2002.

[101] Z. Safar and K. J. R. Liu, "Space-time correlation of MIMO flat Rayleigh fading channels," *EUSIPCO*, 2002.

[102] B. Abdool-Rassool, M. R. Nakhai, F. Heliot, L. Revelly, and H. Aghvami, "Search for space-time trellis codes: novel codes for rayleigh fading channels," *IEE Proceedings on Communications*, vol. 151, pp. 25–31, Feb. 2004.

[103] K. L. Lo, S. Marinkovic, Z. Chen, and B. Vucetic, "Performance comparison of layered space-time codes," in *Proc. IEEE International Conf. Commun.*, Apr. 2002, pp. 1382–1386.

[104] C. D. Mayer, *Matrix Analysis and Applied Linear Algebra.*

[105] Z. Safar and K. J. R. Liu, "Performance analysis of space-time codes over correlated Rayleigh fading channels," in *Proc. IEEE International Conf. Commun.*, May 2003, pp. 3185–3189.

[106] H. S. A. Hedayat and A. Nosratinia, "Analysis of space-time coding in correlated fading channels," *IEEE Trans. Commun.*, vol. 4, pp. 2882–2891, 2005.

[107] R. A. Horn and C. R. Johnson, *Topics in matrix analysis.* Cambridge University Press, 1991.

[108] R. A. Horn, *Matrix analysis.* Cambridge University Press, 1985.

[109] Q. Yan and R. S. Blum, "Optimum space-time convolutional codes for quasi-static slow fading channels," in *Proc. IEEE WCNC*, 2000.

[110] R. Muirhead, *Aspects of Multivariate Statistical Theory.* John Wiley & Sons, 1982.

[111] A. Papoulis, *Probability, Random Variables and Stochastic Process.* McGraw-Hill, 1991.

[112] A. Matache and R. D. Wesel, "Universal trellis codes for diagonally layered space-time systems," *IEEE TRANSACTIONS ON SIGNAL PROCESSING*, vol. 51, pp. 2773–2783, Nov. 2003.

[113] D. Gu and C. Leung, "Performance analysis of transmit diversity schemes with imperfect channel estimation," *IEE Electronic Letters*, vol. 39, pp. 402–403, Feb. 2003.

Author's Publications

Journal Papers

1. Tianyu Mao and Mehul Motani, "STBC-VBLAST for Wireless MIMO Systems", submitted for review, 2007.

2. Tianyu Mao and Mehul Motani,"Space-time Coding for Narrowband Multiuser Correlated Fading Systems", submitted for review, 2007.

Conference Papers

1. C.C. Ko and Tianyu Mao, "New Method for Calculating Pair-wise Error Probability of Space-time Signals", *IASTED International Conference on Wireless and Optical Communications (WOC)*, Canada, 2002.

2. Tianyu Mao, Mehul Motani and C. C. Ko,"Space-time Coding for Narrowband Multiuser Composite Fading Systems", in *Proc. IEEE Vehicular Technology Conf.*, 2004 spring, pp.789-793.

3. Tianyu Mao and Mehul Motani, "STBC-VBLAST for MIMO Wireless Communication Systems", in *Proc. IEEE International Conf. Commun.*, May 2005, pp. 2266-2270.